POLITECNICO
MILANO 1863

TÉCNICO
LISBOA

Assessing electrically conductive polymers for the manufacture of substrates for neural stem cells culture

Laura Sordini

Thesis to obtain the Master of Science Degree in

Biomedical Engineering

Supervisors

Professoressa Sara Mantero

Professor Frederico Castelo Alves Ferreira

Co-supervisors

Professor Jorge Manuel Ferreira Morgado

Doctor Carlos Vitorino Rodrigues

July 2018

“Ubi fracassorium, ibi fuggitorium”

Pulcinella

Acknowledgements

The merit of this thesis work goes to the perfect combination of smart supervisors, amazing colleagues, and great friends.

First of all, I would like to thank my Italian supervisor, Professor Sara Mantero, who gave me the possibility to live this unique opportunity.

Second, I need to thank my Portuguese supervisor, Professor Frederico Ferreira, who thought me that there is no limit to the ideas a scientist can have, and to the experiments he can try.

Special mention goes also to my co-supervisors, Professor Jorge Morgado, from whom I learned that for every problem, there must be a solution, and Carlos Rodrigues, who was the one actually looking for the solution!

Impossible not to thank all my colleagues from SCERG team, for all the support that they gave to me, from teaching me how to turn on a microscope, to driving me back home by night. For all the weekends they saved me from going to Taguspark, for all the contribute that they gave to my experiments; for all the laughs we shared together, and for speaking English with me until the end, I need to thank Carlos, Diogo, Ana Rita, Sara, Silvia, Carina, Margarida, Teresa, Mariana, Marilia, Rodrigo, André, Sara, Miguel, Claudia, Ana, Joao, Joao, Joao…

Finally, I need to thank my beloved italian friends, that helped me feeling at home, always. Dear Silvia, Sara, Andrea, Francesca, Edoardo, Tommaso, Giulia, Alan…it is true that if you laughed a lot, you will cry a lot!

Last but not least, to the gorgeous city of Lisbon, that made my stay abroad more magic than I have ever imagined.

Muito obrigada a todos, vou-vos manter no meu coração!

Abstract

The ability to culture and differentiate neural stem cells (NSCs) to generate functional neural populations is attracting increasing attention for its potential to enable cell-therapies to treat neurodegenerative disorders, such as Parkinson desease. Recent studies proved that the electrical stimulation improves neuronal differentiation in stem cells populations; to develop electroconductive biocompatible materials is a cue of increasing importance in the areas of tissue engineering and regenerative medicine.

In this thesis work, we have been studying the use of conjugated polymer poly (3,4-ethylenedioxythiophene) doped with polystyrene sulfonate (PEDOT:PSS) for the manufacture of conductive substrates to cultivate and/or differentiate NSCs using electrical stimulation. To better reproduce the natural 3D environment, polybenzilimidazole (PBI) was electrospun to provide a electrically conductive, thermal stable and biocompatible mesh of nanometric fibers, that was then coated with PEDOT:PSS to enhance the electrical conductivity.

Our findings suggest that the assessed polymeric substrates exhibit adequate physicochemical properties and a good biocompatibility that promote cell attachment and proliferation. Moreover, our results indicate that, the application of pulsed DC electric field (EF) of 1 V/cm for 12 days consent to obtain functional early differentiated neurons.

Keywords: Neural stem cells, PEDOT:PSS, PBI, electrical stimulation, electrospinning, differentiation

Sommario

La capacità di coltivare e differenziare cellule staminali neuronali (NSCs) per generare popolazioni di neuroni funzionali sta attraendo crescente attenzione per il suo potenziale nel consentire terapie cellulari al fine di trattare malattie neurodegenerative, come il morbo di Parkinson. Recenti studi hanno provato che la stimulazione elettrica aumenta la differenziazione neuronale in popolazioni di cellule staminali; sviluppare materiali elettroconduttivi biocompatibili è una strategia che sta acquisendo crescente importanza nelle aree dell'Ingegneria dei Tessuti e della Medicina Rigenerativa.

In questo progetto di tesi, abbiamo studiato l'ultilizzo del polimero coniugato poli(3,4-etilendiossitiofene) dopato con polistirensulfonato (PEDOT:PSS) per realizzare substrati conduttivi per coltivare e/o differenziare NSCs usando una stimolazione elettrica. Al fine di riprodurre meglio l'ambiente 3D naturale, il polimero polybenzilimidazolo (PBI) è stato elettrofilato per ottenere una mesh di fibre nanometriche, elettricamente conduttive, termicamente stabili e biocompatibili, su cui è stato poi effettuato un coating di PEDOT:PSS per aumentarne la conduttività elettrica.

I nostri risultati suggeriscono che i substrati realizzati esibiscano adeguate caratteristiche chimico-fisiche e una buona biocompatibilità per promuovere l'adesione cellulare e la proliferazione. Inoltre, i nostri risultati indicano che l'applicazione di un campo elettrico pulsante in corrente cotinua (DC) dell'intensità di 1V/cm per 12 giorni consenta di ottenere popolazioni di neuroni funzionali ai primi stadi di differenziazione.

Table of contents

List of Abbreviations

ALS – amyotrophic lateral sclerosis
APC – adenomatous polyposis coli
APES – aminopropyltriethoxysilane
BPs – basal progenitors
CAMs – cell adhesion molecules
CNS – central nervous system
CP – conjugated polymers
CSF – cerebrospinal fluid
CSPG – chondroitin sulfate proteoglycans
DAPI – 4´,6-diamino-2-phenylindole
DBSA – dodecylbenzenesulfonic acid
DC – direct current
DMEM – Dulbecco´s modified Eagle´s medium
DMSO – dimethylsulfoxide
DRG – dorsal root ganglia
EBs – embryonic bodies
DVS - divinylsulfone
ECM – extracellular matrix
EF – electrical field
EG – ethylene glycol
EGF – epidermal grow factor
ESCs – embryonic stem cells
FBS – fetal bovine serum
FGF-2 – basic fibroblast growth factor
GFAP- glial fribrillary acidic protein
GOPS – 3-glycidoxypropyltrimethoxysilane
hESCs – human embryonic stem cells
IKVAV – isoleucine-lysine-valine-alanine-valine
IMDM – Iscove´s modified Dulbecco´s medium
iPSCs – induced pluripotent stem cells
ITO – indium-tin oxide
LN – laminin
MAP2 – microtube-associated protein 2
MAPK – mitogen-activated protein kinases
MSCs – mesenchymal stem cells
MTT – 3-(4,5-dimethylthiazol-2-yl)-2,5-diphenyltetrazolium bromide
ND – neurodegenerative disorders
NEPs- neuroepithelial progenitors
NGF – nerve growth factor
NGS – normal goat serum
NS – neural stem cell line
NSCs – neural stem cells
P19 EC – P19 pluripotent embryonal cell

PBS – phosphate buffered saline
PD – polydopamine
PDMS – polydimethylsiloxane
PEDOT – poly (3,4-ethylene dioxythiophene)
PEG – poly(ethylene glycol)
PEI – polyethyleneimine
PFA – paraformaldehyde
PLA – poly(D,L-lactide)
PolyA – polyacrylamide
PSS – polystyrenesulfonate
RG – radial glia
RGD – arginine-glycine-aspartic acid
RT – room temperature
SGZ – subgranular zone
SVZ – subventricular zone
TIC – Transient ionic current
TnC – tenascin C
Tuj1 – β-tubulin
VEGF – vascular endothelial growth factor
VSCC – voltage sensitive calcium channels
YIGSR – tyrosine-isoleucine-glycine-serine-arginine

List of Figures

Chapter I: Introduction

I.1 Stem cells

Stem cells, scaffolds and growth-stimulating signals are the key components of the tissue engineering, whose principal aim is to develop biological substitutes to restore, replace or regenerate defective tissues [Chan, B. & Leong, K., 2008]. Stem cells are distinguished from the other cells because they have the ability to divide producing copies of themselves (self-renewal) and/or to differentiate into mature cells that have characteristic shapes and specialized functions [Winslow, T. & Kibluk, L. ,2001]. Cells from the mammalian embryo have the capacity to develop in every type of cell, and are so defined totipotent [Odorico, J.S., 2001]; stem cells are also present in adult tissues, even if with a limited cellular regeneration or turnover, and form only a limited number of cell types, so they are defined multipotent. In adult organisms, stem cells and progenitor cells are responsible for tissue homeostasis and repair; different stem cell types can be recognized and isolated, like hematopoietic stem cells (HPCs), mesenchymal stem cells (MSCs), neural stem cells (NSCs). In the current work the human adult neural stem cells (NSCs) will be studied. These are interesting cell sources for cell therapies, providing models for drug screening and offering hope for the treatment of several diseases, namely in the case of a stroke, Alzheimer´s disease, amyotrophic lateral sclerosis and other neurodegenerative diseases [Rodrigues, C.A., 2011].

I.2 Neural Stem cells

NSCs are multipotent cells present in the central nervous system (CNS), that are able to self-renew and generate neurons, astrocytes, and oligodendrocytes [McKay, R. 1997]. During and after gastrulation, mammalian neurogenesis starts with the process of neural induction that allows the formation of neuroectoderm [Casarosa, S., 2013]. Neuroectoderm forms the neural plate and, after neurulation, occurs the formation of the neural tube [Conti, L. & Cattaneo, E., 2010]. These structures have a heterogeneous and complex population of cells called neuroepithelial progenitors (NEPs) [Casarosa, S., Zasso, J. & Conti, 2013.] NEPs, radial glia (RG), basal progenitors (BPs) and adult progenitors are the main types of cells that can be distinguished in the brain. NEPs undergo symmetric division that gives rise to new neuroepithelial cells and, at a later stage of brain development, they give rise to RG and BP by undergoing asymmetric division [Conti, L. & Cattaneo, E., 2010]. RG serve as scaffolds for migrating newborn neurons and undergo symmetrical proliferative and asymmetric neurogenic divisions. In addition, RG cells are able to generate glial, neuronal and oligodendroglial lineages [Conti, L. & Cattaneo, E., 2010]. BPs are considered neurogenic transit-amplifying progenitors once they increase the production of neurons [Conti, L. & Cattaneo, E., 2010]. Adult progenitors are cells present in neurogenic region (SVZ, SGZ) and in non-neurogenic regions (spinal cord), which maintain the neurogenesis and gliogenesis throughout adult life [Garzón-Muvdi, T. & Quiñones-Hinojosa, A., 2010].

Adult neural stem cells (NSCs) continuously generate neurons throughout life in two brain regions: the subgranular zone (SGZ) of the hippocampus and the ventricular-subventricular zone (V-SVZ), adjacent to the lateral ventricles. In these regions, they reside in stem cell niches that provide microenvironmental cues essential to the balance between stem cell quiescence and proliferation and to direct neurogenesis versus gliogenesis lineage decisions [Conover, J.C. & Notti, R.Q., 2008]. In addition to the restraints imposed by niche cytoarchitecture, cells within the neurogenic niche rely on growth factor signaling, cell to cell contact and cell to ECM interactions for homeostatic cell turnover and increased cell production in response to stimulation. The ECM gives structural support for cells to attach, grow, migrate and respond to signals, contributes to the mechanical properties (elasticity and rigidity) of tissues, provides bioactive cues to regulate the activities of residing cells, is a reservoir of growth factors and provides a flexible physical environment to allow neovascularization and remodeling in response to tissue dynamic processes such as homeostasis and morphogenesis [Chan, B. & Leong, K. 2008]. NSCs have cell adhesion molecules (CAMs) located on their surface through which they interact with other cells and the ECM components surrounding them [Bian, S., 2013]. Integrins, immunoglobulins, selectins and cadherins are families of CAMS that interact with the glycoprotein tenascin C (TnC), chondroitin sulfate proteoglycans (CSPG), heparin sulfate proteoglycans, collagen IV, fibronectin, laminin and thrombospondin (ECM components) [Kazanis, I., 2011],[Little, L., 2008] and that play a key role in maintenance of the architecture and shape of NSC niche and that are involved on signaling transduction that regulate cell survival, proliferation, differentiation and migration [Bian, S., 2013].

The NSCs populations can be isolated from in vivo sources, the fetal and adult nervous systems, or in vitro derived from ESCs (- derived from blastocyst stage) or from iPSCs (- derived from reprogrammed cells)[Garzón-Muvdi, T. & Quiñones-Hinojosa, A., 2010],[Casarosa, S., Zasso, J. & Conti, L. 2013],[Conti, L. & Cattaneo, E., 2010]. The limited supply of human fetal tissue and ethical concerns about deriving neural progenitors from aborted fetuses, have limited the use of fetal neurons in clinical applications thus making ESCs and iPSCs attractive alternatives.

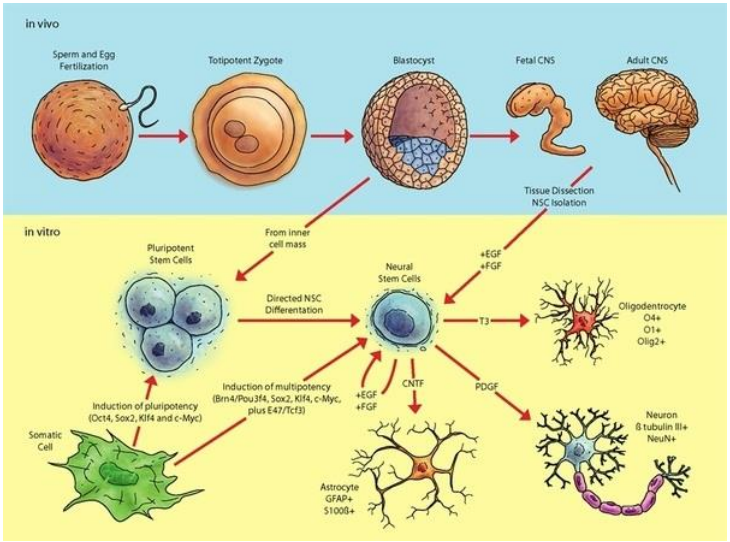

***Figure 1*. Pathway of pluripotent stem cells to neural cell populations**. *Fertilization and subsequent cellular divisions create the embryonic blastocyst, where pluripotent ESCs are derived (from the inner cell mass; ICM). Additionally, pluripotent and multipotent-like cells can be created via transduction of various factors into differentiated tissue, such as fibroblasts. In vitro analyses of*

pluripotent and multipotent neural stem cells are integral for understanding aspects of neural differentiation. The in vivo niche of stem cells contains a considerable diversity of biomolecules whose roles still need be deciphered. Exposure of ESC in vitro to various growth factors in serum free media such as fibroblast growth factor 2 (FGF2) and epithelial growth factor (EGF) allows selection of cell lines possessing a neural fate. Neural stem cells can also be acquired from adult tissue and expanded in vitro. [Brendan M. Olynik, The Genetic and Epigenetic Journey of Embryonic Stem Cells into Mature Neural Cells*, Frontiers in Genetics, 2010].*

Protocols based on in vivo neurogenesis have been performed in vitro to differentiate ESC into NSC, enabling the generation of a range of distinct neural precursor populations that are similar to the populations from stage-specific transitions (blastocyst, neural plate, neural tube, fetal and adult brain) [Casarosa, S., Zasso, J. & Conti, L., 2013]. The developmental stages of NSC populations isolated or generated in vitro and in vivo are illustrated in Fig.2. In order to allow stable in vitro maintenance, cells need to be immortalized, a procedure that blocks the progression of developmental programs by pushing the cells to remain in enduring proliferation [Casarosa, S., Zasso, J. & Conti, L., 2013].

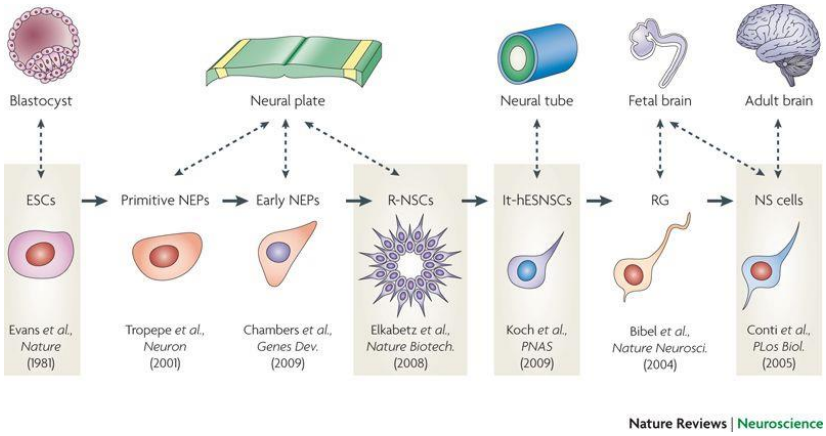

Figure 2 The different NSC populations that can be obtained in vitro correspond to stage specific neural progenitors present at defined in vivo developmental stages . *[Conti, L. & Cattaneo, E. Neural stem cell systems: physiological players or in vitro entities? Nature Reviews Neuroscience 11, 176-187 (2010).]*

In the present work, the human neural progenitor cell line ReNcell VM, derived from 10-week-old fetal ventral mesencephalon and immortalized by retroviral transduction with the v-myc oncogene was used.

I.3 ReNcell VM line

The ReNcell VM line is an immortalized hNSCs line derived from the ventral mesencephalon of ten-week gestation fetal neural tissue. The immortalization using the myc transcription factor serves to extend the normal life span of fetal-derived hNSCs since their major limitation is the high rate of mortality when they grow in culture. ReNcell VM line has a normal karyotype and proliferates indefinitely, showing a positive signal for the NSCs marker nestin. When the growth factors are omitted from the medium, these cells undergo differentiation in neuronal and glial direction, showing a strong labeling for the neuronal marker Tuj1 and for the dopaminergic marker tyrosine hydrolase (TH). ReNcell VM can be differentiated in vitro to a high level of human dopaminergic neurons. Neurons differentiated from ReNcell VM have furthermore been shown to be electrophysiologically active. ReNcell VM may be used for a variety of research applications such as studies of

neurotoxicity, neurogenesis, electrophysiology, neurotransmitter and receptor functions. However, this cell line is purely used for research and cannot be used in human therapy. This line can be used for the understanding of stem cells and might ultimately lead to the design and selection of future cell lines for the treatment of neurodegenerative diseases [Donato, R. et al., 2007].

I.4 Neural stem cells therapies: state of the art

In neurodegenerative disorders (ND) such as Alzheimer´s disease, Huntington´s disease, amyotrophic lateral sclerosis (ALS) and Parkinson's disease, there is a massive loss of one or several types of neurons that promotes chronic or progressive decline in cognitive function affecting the memory, behavior, language, learning and emotion [Kim, S.U., Lee, H.J. & Kim, Y.B. 2013],[Dantuma, E., Merchant, S. & Sugaya, K., 2010]. According to the DEMENTIA - A Public Health Priority report, annual, is estimated that the number of new cases of people with dementia is about 7.7 million, that is, a new case every 4 second. Current therapies for ND alleviate only poorly the symptoms once they are inefficient to rescue or regenerate cellular function or even halt the neuronal death process. Stem-cell transplantation provides a novel and attractive strategy for these diseases that remain without effective therapy. The intravenous injection or the local transplantation of NSCs isolated from different sources have been used as strategies to treat severe injuries in CNS once, in these situations, the endogenous repair is not enough for functional recovery. The administration of growth factors, drugs and antioxidants is another strategy used to modulate the proliferation, migration and differentiation of endogenous NSCs to increase their efficacy in neurogenic areas of the brain. The transplanted NSCs can cooperate with other cells in the brain to activate endogenous NSCs of niche and also secrete trophic factors and modulate the immune system providing neuroprotection [Kokaia, Z., Martino, G., Schwartz, M. & Lindvall, O., 2012]. NSC have been used in pre-clinical and clinical trials in order to promote the neural regeneration. In 2009, the first pre-clinical trial was authorized in rats that used spinal cord grafts of oligodendrocyte precursors derived from hESCs to restore function [Keirstead, H.S. et al. 2005]. The NSCs can be used as in vitro models to screen possible drug candidates to treat some diseases, to study disease mechanisms and test drug toxicity in way to avoid toxic and side effects due to high dosages [Aboody, K., 2011]. The challenges for regenerative medicine future are the determination of ways to promote survival and integration of neural precursor transplants in the adult brain and the study of the mechanisms to reverse behavioral and cognitive deficits in ND [Feng, Z. & Gao, F. 2012].

I.5 Biomaterials for NSCs culture: state of the art

Biomaterial scaffolds combined with bioactive factors and multipotent cells have been used in tissue engineering strategies to, after transplantation into damaged tissue, promote tissue development and function improvement. This strategy for neural repair and regeneration is illustrated in Fig.3. A biomaterial is defined as material which is used in body and that by contacting with biological components of proteins, cells and due to their physicochemical properties, such as wettability, electric charge, roughness and surface modification with

chemical immobilization of CAMs, is able to affect the adhesion, proliferation and differentiation of cells [Cui, F.-Z., 2011], [Wang, Y. et al., 2010].

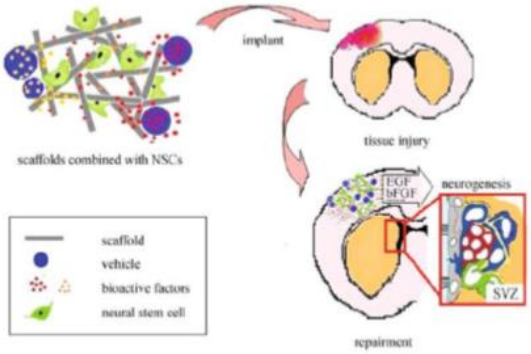

Figure 3 Neural repair and regeneration strategy based on immobilization of growth factors on a biomaterial scaffold *The NSC are seeded on the scaffold and transplanted to injury tissue to promote neurogenesis. [Wang, Y. et al. Interactions between neural stem cells and biomaterials combined with biomolecules. Frontiers of Materials Science in China 4, 325-331 (2010)]*

Materials of natural and synthetic origin have been shown to promote adhesion, proliferation and neuronal differentiation of neural cells in vitro and in vivo. Synthetic materials, like carbon nanotubes, have been investigated as conductive scaffolds [Ning Li, 2013], but several issues relate to their biocompatibility for long terms applications: synthetic particles recognized by the immune system, such as CNTs, are not generally susceptible to digestion inside macrophages, or to cell-killing mechanisms, but nevertheless can activate such mechanisms, and this can result in inflammation and tissue damage to the host [M.V. Carroll, R.B. Sim, 2011]. Metals, such as platinum and gold, have good conductivity but their implantation is limited by their ions release and their non-biodegradability; they are currently studied as electrodes for brain stimulation [M. Leber, 2017]. Natural biomaterials such as collagen, chitosan, fibrin, cellulose, hyaluronic acid and gelatin possess desired cell recognition sites to control cell behavior, provide cues for stem cells and tend to be biocompatible, biodegradable and inflammation resistant [Subramanian, A., 2009]. Limitations of these proteins and polysaccharides include the immunogenic response, since the body recognizes the foreign material and attempts to destroy it and the possible loss of biological activity during their processing. Furthermore, they have low mechanical properties and also have problems with purity and the availability of large-scale sources [Little, L., 2008], [Cui, F.-Z., 2011], [Marklein, R.A. & Burdick, J.A., 2010], [Willerth, S.M. & Sakiyama-Elbert, S.E., 2008]. Lu et al. (2012) developed a chitin-alginate microfibrous culture system that controls the neuronal differentiation and maturation of human pluripotent stem cells due to the manipulation of medium components [Lu, H.F. et al. 2012]. Synthetic polymer-based biomaterials have a defined chemical composition and have the advantage of controlling the mechanical properties, shape and degradation rate allowing the release or display of neurotrophic factors [Cui, F.-Z., 2011], [Marklein, R.A. & Burdick, J.A., 2010], [Cherry, J.F. et al., 2012]. However, the byproducts of these materials, that are chemically modified to sustain cell adhesion, are inflammation-active and change the environmental pH to a lower level than normal which is harmful to seeded cells and surrounding tissues [Cui, F.-Z., 2011], [Marklein, R.A. & Burdick,

J.A. 2010], [Willerth, S.M. & Sakiyama-Elbert, S.E., 2008]. Synthetic substrates such as polydimethylsiloxane (PDMS), polystyrene, polyacrylamide (PolyA), poly(D,L-lactide) (PLA), polydopamine (PD), poly(ethylene glycol) (PEG), hydrogels and selfassembled protein constructs have been used to culture and differentiate NSCs [Yang, K. et al. 2012], [Lim, T.C., 2012], [Palchesko, R.N., 2012], [Prabhakaran, M.P., 2011]. The ideal neural scaffold should be biocompatible, biodegradable, resistant to structural collapse during implantation and should have a porous connectivity to allow tissue vascularization and cell migration, and also a three-dimensional shape with mechanical, electrical, biochemical and topographical properties to mimic the ECM [Subramanian, A., 2009].

I.6 Conductive scaffolds

Several tissues are responsive to electrical fields and stimuli which has made electrically conductive materials an attractive approach to control cell state and fate via regulation of conductivity, mechanical properties, volume and oxidation states [Ostrakhovitch, E., 2012]. Electrical stimulation is demonstrated to improve and maintain cell function in several tissues, like bone, skin, heart and brain. Conductive scaffolds can be potential candidates for biosensors, peripheral nerve guides and neural stimulation, used in the cochlear implant, bionic eye, and deep brain stimulation, which involves implantation of an array of electrodes into a patient's brain [Harris AR , 2015]. The current passed through the electrodes is used to provide sensory queues or reduce symptoms associated with movement disorders and for psychological and pain therapies. Another interesting biomedical application for conductive materials, is the connection of prosthetic implants to the residual muscles or the nerves, thus creating an electrically conductive interface for limb prosthesis or neuroprosthesis to mechanically control their contraction, or to introduce a sensitive function [Rylie A. Green, 2008].

Conjugated polymers (CP) are molecular materials whose backbone is made of alternating double- and single- bonds. These result from the bonding between sp2 hybridized atoms (mostly carbon), so that the overlap of pure p-orbitals of neighboring atoms leads to the formation of π molecular orbitals [Guimard, N.K., 2007]. It is this special conjugation that enables electron delocalization along the polymer chains and is at the origin of their conductive properties [Harun, M.H., 2007] in contrary to the traditional polymers that are made up of essentially σ-bonds and hence a charge once created on any given atom on the polymer chain is not mobile. When in the pure state, CP behave very much like inorganic semiconductors as there is an energy gap separating the bonding π orbitals from the anti-bonding π* molecular orbitals. Only upon doping, that corresponds to an oxidation or a reduction of the polymer chains, their conductivity can be changed from insulating to conducting, with the conductivity increasing as the doping level increases. In some special cases, conductivity values that approach those of the metals can be obtained. CPs are easy to synthesize, by chemical or electrochemical polymerization reactions, and to process and are inexpensive. Various methods such as electropolymerization, spin coating and inkjet printing, have been used to deposit and pattern this type of polymers. In this study the spin coating method was selected to deposit polymers on substrates. These polymers have attractive properties for biological applications. Namely, they are usually biocompatible, allow the control over the level and duration of electrical stimulation for tissue engineering

applications and possess the ability to entrap and controllably release biological molecules [Guimard, N.K., 2007]. The ability to modify their chemical structure, namely by adding functional groups to the CPs backbone, and/or their ability to be combined with various organic compounds, opens the possibility to easily control and modulate their electrical, physical, chemical and other properties in order to better suit the nature of the specific applications [Guimard, N.K., 2007].

I.6.1 PEDOT:PSS

Poly(3,4-ethylenedioxythiophene):poly(styrene sulfonate) (PEDOT:PSS) chemical structure is shown in Fig. 1; it is a polymer electrolyte consisting of positively charged conjugated PEDOT and negatively charged saturated PSS. PSS is a polymer surfactant, which helps disperse and stabilize PEDOT in water and other solvents. PEDOT is known to possess both ionic and electronic conduction and it has been the subject of extensive research in different fields and proposed applications, including microelectronics, sensing, actuation, as a bio-compatible material for neural implants, biological scaffolds, optoelectronic applications, *etc.* [E. Smela, 2003]. Key features for the success of PEDOT as an attractive conductive polymer material are good conductivity and chemical stability; in addition, a very important and interesting feature for many applications is the market availability of PEDOT/PSS, the macromolecular complex of PEDOT with poly(styrenesulfonate) (PSS), as a ready-to-use waterborne dispersion of PEDOT/PSS gel particles. Conductive films in which the gel particles merge to form a continuous film under water evaporation are obtained by spin coating onto different substrates (Si, glass, ITO, *etc.*). PEDOT/PSS has already been proposed and successfully employed in organic electronics as conductive coating (*e.g.* antistatic protective coating), as conductive layer in multilayer structures (*e.g.* charge injection in OLED) or also as active material in the development of a number of sensing and actuating devices, based on its stimuli-responsive properties. [F. Greco, 2011]. PEDOT, whose biocompatibility has been proved in very recent works, has been successfully applied in the development of microelectrodes for neural interfaces as well as in scaffolds for epithelial cell adhesion and proliferation controlled by electrochemical modulation of surface properties [Maria H.Bolin, 2009] [K. Svennersten, 2009].

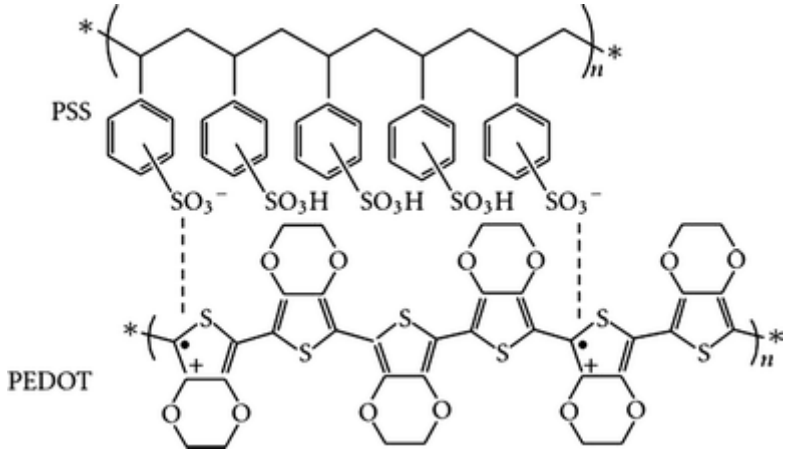

Figure 4 Chemical structure of PEDOT:PSS. *[Abdulkadir Sanli*, Investigation of physical aging of carbon nanotube/PEDOT:PSS nanocomposites by electrochemical impedance spectroscopy, *2015]*

I.6.2 PEDOT:PSS crosslink

The commercially available PEDOT:PSS aqueous dispersion is a deep-blue opaque solution. PEDOT:PSS exhibits a wide range of electrical conductivities from 10^{-2} to 10^{3} S cm^{-1}, influenced by synthetic conditions, processing additives or post-treatment [K. Sun, 2015].
It is well known that addition of solvents, such as ethylene glycol (EG), glycerol, dimethyl sulfoxide (DMSO), and sorbitol significantly improves the conductivity of PEDOT:PSS by up to 2 or 3 orders of magnitude [Yong Hyun Kim , 2011].
One of the most important advantages of PEDOT:PSS is its water-solubility, which enables simple and environmental friendly manufacturing processes. Unfortunately, this also implies that pristine PEDOT:PSS films are unsuitable for applications in aqueous environments [O. Berezhetska, 2015]. An usual strategy to obtain water-stable films has been to crosslink the active layer with methoxysilane-based molecules such as (3-glycidyloxypropyl)trimethoxysilane (GOPS), which have been proven useful in successfully preventing both dissolution and delamination of PEDOT:PSS films in aqueous solutions. Unfortunately, however, addition of GOPS also reduces the electronic as well as the ionic conductivity [E. Stavrinidou, 2013] [A. Håkansson, 2017].

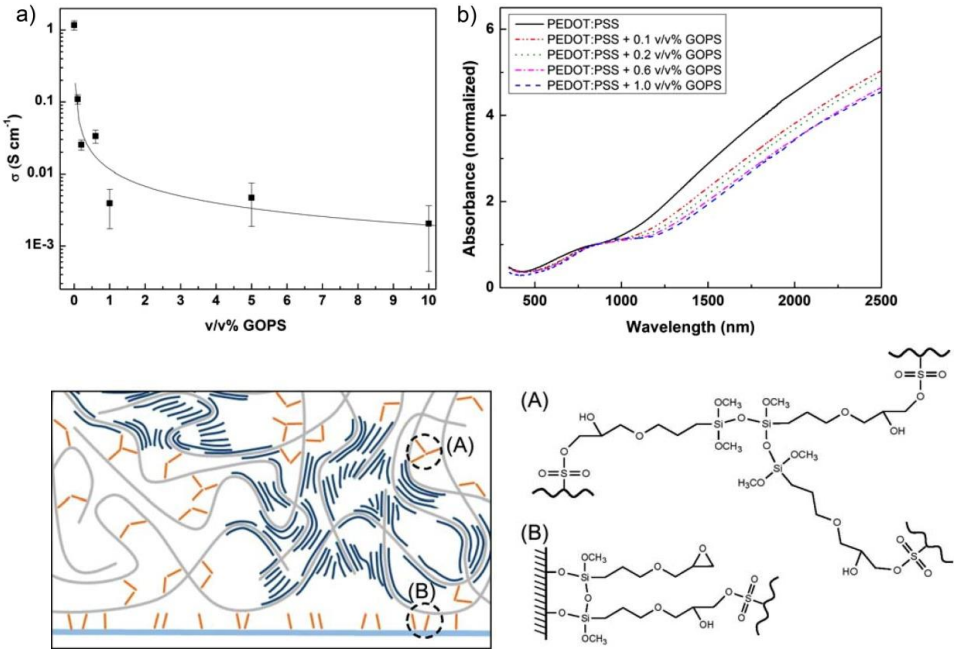

Figure 5 Mechanism of GOPS crosslink and trend of conductivity in response to GOPS content. *[Anna Håkansson et al., Effect of (3-Glycidyloxypropyl)Trimethoxysilane (GOPS) on the Electrical Properties of PEDOT:PSS Film, 2017]*

Combined approach has been successfully realized, crosslinking PEDOT:PSS with GOPS and performing a primary doping with EG and a secondary doping with dodecylbenzensulphonic acid (DBSA) [F.Soares, 2015]; spin-coated films have been realized with a conductivity of 4.3 S/m and used to electrically stimulate NSCs.
Another crosslinking agent that was successfully used to obtain electrically conductive, spin-coated, water-stable PEDOT:PSS films is divinylsulfone (DVS) [D.Mantione,

2017]. DVS does not reduce electronic conductivity of PEDOT:PSS but increases it acting as another secondary dopant; substrates with a conductivity of $75x10^3$ S/m were used to stimulate NSCs.
Both crosslinking strategies have been tested in this work.

I.6.3 PBI

Polybenzimidazoles (PBI) cover a large family of polymers containing benzimidazole units.

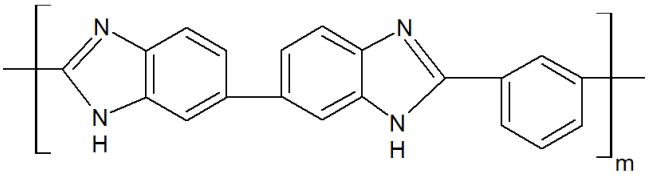

***Figure 6 Scheme of Polybenzilimidazole structure**. [Q. Li, PBI-Based Polymer Membranes for High Temperature Fuel Cells - Preparation, Characterization and Fuel Cell Demonstration, Fuel cells 2004, 4, No. 3].*

The PBI referred to in this work is poly 2,2'-m-(phenylene)-5,5'-bibenzimidazole as shown in Figure 6. It is a fully aromatic heterocylic polymer. The presence of three benzene rings with side groups in the repeating unit contributes to the polymer's superior properties such as thermal stability (Tg= 425±436 ° C), retention of stiffness and toughness. Polybenzilimidazole has been used as a powerful candidate for fuel cells due to the high proton conductivity above 100 °C under non-humid conditions [Fujigaya T., 2013]. As an amorphous thermoplastic polymer, PBI has a good chemical resistance and excellent textile fiber properties [Tai Shung Chung, 1997]. PBI in the form of fibers, films and membranes, has been studied for blood dialysis and reverse osmosis at high temperatures and in harsh environments [Tai Shung Chung, 1997]. Among the organic solvents that dissolve PBI, N,N-dimethylacetamide (DMAc) is the most widely used. It is well known that PBI has a high affinity for moisture and is hydrophilic. Immersed in distilled water or exposed to a moist atmosphere, PBI membranes can absorb up to 19 wt% of water, corresponding to about 3.2 water molecules per repeat unit of PBI [Q. Li, 2004]. Biocompatibility of PBI has not been widely studied yet, so was taken in particular account during this work.

I.7 2D vs 3D substrates

Conventional two-dimensional (2D) cell culture systems have been an extremely valuable tool that have provided important knowledge for more than 100 years, offering simplified and low-cost methods for modelling CNS diseases [M. Blain, 2010], [A.M. Hopkins, 2015]. However, scientists argue that 2D models do not mimic tissues complexity, creating a need for more physiologically relevant models [Eduarda G Z Centeno, 2018]. Since almost all cells in the *in vivo* environment are surrounded by other cells and extracellular matrix (ECM) in a three-dimensional (3D) fashion, 2D cell culture does not adequately take into account the natural 3D environment of cells. As a result, 2D cell culture tests sometimes provide

misleading and nonpredictive data for *in vivo* responses [A. Birgersdotter, 2005][V.M. Weaver, 1997][K. Bhadriraju, 2002]. In fact, research has found that cells in the 3D culture environment differ morphologically and physiologically from cells in the 2D culture environment [H. Baharvand H*,* 2006], [P.D. Benya, 1982], [C.M. Nelson, 2005]. It is the additional dimensionality of 3D cultures that is the crucial feature leading to the differences in cellular responses because not only does it influence the spatial organization of the cell surface receptors engaged in interactions with surrounding cells, but it also induces physical constraints to cells. These spatial and physical aspects in 3D cultures affect the signal transduction from the outside to the inside of cells, and ultimately influence gene expression and cellular behavior. It has been demonstrated that cell responses in 3D cultures are more similar to in vivo behavior compared to 2D culture. [K. Shield, 2009], [M. Zietarska, 2007], [J. Lee, 2008]. In the past several years, tremendous effort has been put into the development of a variety of 3D culture systems, as well as the adoption of 3D cell culture systems in drug discovery, cancer cell biology, stem cell study, engineered functional tissues for implantation, and other cell-based analysis. Such 3D culture systems provide excellent in vitro models, allowing the study of cellular responses in a setting that resembles in vivo environments [A. Birgersdotter, 2005], [B. A. Justice, 2009], [A. Reininger-Mack, 2002], [T. Sun, 2006], [Rasheena Edmondson, 2014].

I.8 Surface strategies to control cell response

The classic cell culture conditions provide a homogenous adhesion substrate which is flat and rigid having little in common with the *in situ* microenvironment in which cells reside [Théry, M., 2010]. Researchers have modeled topography, surface chemistry, electricity and stiffness of the material in order to get a substrate with properties similar to those of ECM. Recent studies have indicated that cells not only detect the composition and stiffness of their substrates but can also detect their topography. This is also true of artificial substrates: pore sizes in engineered trabecular bone, for example, depend on the initial scaffold geometry [Hofmann et al., 2007]. Because it is clear that the ECM can affect cell fate and differentiation, the field is looking towards cell and developmental biology for guidance in the design of such scaffolds. Many successful artificial substrates are biomimetic: they mimic in vivo structures. Nanotechnology has made it possible to produce biomimetic synthetic nanofibers, the diameters of which are within the sub-micrometer range [Ashammakhi et al., 2007; Griffith and Swartz, 2006]. Recent studies indicate that cells sense and respond differently to such nanofibers. For example, Li et al. showed that chondrocytes secrete increased amounts of ECM when seeded on a nanofiber compared with a microfiber matrix [Li et al., 2006]. Studies using another culture system have demonstrated that nanotopography strongly influences stem cell differentiation; seeding cells on a nanograting that has a diameter one order of magnitude less than the width of the cell more effectively promotes neuronal differentiation of human MSCs than do other configurations of the same material or retinoic acid [Yim et al., 2007]. These studies and others [Griffith and Swartz, 2006] indicate the need for scaffold designs that provide the appropriate mechanical signals.

I.9 Electrospinning

Electrospinning has gained popularity in the last 10 years due in large part to an increased interest in nanoscale properties and technologies. This technique allows for the production of polymer fibers with diameters varying from 3 nm to greater than 5 µm [T. Subbiah, 2005]. Potential applications of electrospinning include filtration membranes, catalytic nanofibers, fiber-based sensors, and tissue engineering scaffolds [Z. M. Huang, 2003], [A. Frenot, 2003] One attractive feature of electrospinning is the simplicity and inexpensive nature of the setup; the typical electrospinning setup consists of a syringe pump, a high voltage source, and a collector (Fig.7).

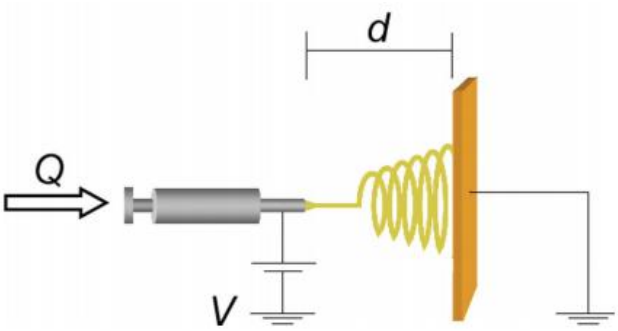

***Figure 7. Typical electrospinning setup**. Q, flow rate; d, distance between plate and needle; V, applied voltage. [P. P. Quynh, Electrospinning of Polymeric Nanofibers for Tissue Engineering Applications: A Review, Tissue Engineering Volume 12, Number 5, 2006].*

During the electrospinning process, a polymer solution is held at a needle tip by surface tension. The application of an electric field using the high-voltage source causes charge to be induced within the polymer, resulting in charge repulsion within the solution. This electrostatic force opposes the surface tension; eventually, the charge repulsion overcomes the surface tension, causing the initiation of a jet. As this jet travels, the solvent evaporates and an appropriate collector can be used to capture the polymer fiber. From the previous description of theory, it is clear that the electrospinning process can be manipulated by a number of variables. Doshi and Reneker classified the parameters that control the process in terms of solution properties, controlled variables, and ambient parameters [J. Doshi, 1995]. Solution properties include the viscosity, conductivity, surface tension, polymer molecular weight, dipole moment, and dielectric constant. The effects of the solution properties can be difficult to isolate since varying one parameter can generally affect other solution properties (e.g., changing the conductivity can also change the viscosity). Controlled variables include the flow rate, electric field strength, distance between tip and collector, needle tip design, and collector composition and geometry. Ambient parameters include

temperature and humidity [P. P. Quynh, 2006]. SEM picture of electrospun mesh of fibers is showed in Figure 8.

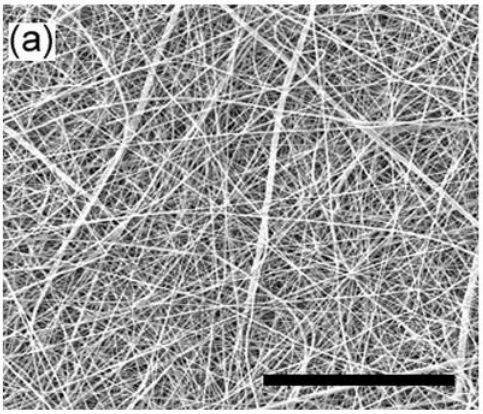

Figure 8 . (a) A random polymer fiber mesh produced by electrospinning a 9% PCL solution*. Scale bars, 100nm; spinning conditions: solvent chloroform/methanol (3:1 by vol), voltage 25 kV, distance to collector 15 cm, flow rate 6 mL/h. [P. P. Quynh, Electrospinning of Polymeric Nanofibers for Tissue Engineering Applications: A Review, Tissue Engineering Volume 12, Number 5, 2006].*

I.10 Surface functionalization

Several strategies such as adsorption, entrapment and covalent attachment of desired biomolecules have been used by the researchers in order to improve the biological properties of a CP to enhance the adhesion and growth of cells. One of the key adhesion ligands for NSC growth and survival is the laminin (LN). LN is a protein that is part of the ECM and that has "arms" that, upon association with other LN molecules, form sheets and bind cells. The LN protein is constituted by specific amino acid sequences such as arginine-glycine-aspartic acid (RGD), isoleucine-lysine-valine-alanine-valine (IKVAV) and tyrosine-isoleucine-glycine-serine-arginine (YIGSR) that are responsible to guide cell adhesion and neurite outgrowth [Little, L., 2008], [K. Venstrom, 1993], [L. Luckenbill-Edds, 1997]. Integrins are transmembrane αβ heterodimers that, after LN bind on their receptors, suffer a change of conformation which in turn, triggers intracellular signals that synergistically act with growth factors in order to regulate self-renewal and maintenance of NSCs through mitogen-activated protein kinases (MAPK) signaling pathway [L. A. Flanagan, 2006], [P. Hall, 2008], [L. S. Campos, 2004]. The growth factors added to culture medium or secreted by NSCs are chemical messengers that mediate intracellular communication that, as referred before, affect cell fate [D. E. Discher, 2009]. The EGF and FGF2 are examples of these growth factors that act on regulation of the several genes required to sustain self-renewal and differentiate potential of NSCs in vitro [L. Conti, E. Cattaneo, 2010]. However, their action on cell fate is dependent on the cell origin, the stage of differentiation and on the concentration, time and duration of exposure used [Dhara, S.K. & Stice, S.L., 2008], [Tarasenko, Y.I., 2004]. The withdrawal of EGF and FGF2 or the addition of differentiation factors to the medium induces the NSCs to spontaneously acquire a neuronal or glial phenotype [Discher, D.E., 2009], [Dhara, S.K. & Stice, S.L. 2008] [Tarasenko, Y.I., 2004], [Johe, K.K., 1996]. Fibronectin, heparin, retinoic acid, hyaluronic acid and nerve growth factor (NGF) are examples of other proteins used to functionalize polymeric substrates. However, their adsorption is influenced

by chemical structure, surface energy, surface topography, roughness and hydrophobicity of polymer surface.

I.11 Electrical stimulus

All cells of human body respond to electrical fields (EF) but nerve cells are specifically designed to transmit electrical impulses from one site of the body to another and to receive and process information implying that an ideal neural scaffold should possess electrical conductivity to promote neurite outgrowth and enhance nerve regeneration in culture. The ion influx across membrane, the membrane potential and the intracellular signal transduction pathways are affected by the unequal distribution of ions between the intra- and extracellular compartments which, subsequently, affects cell behavior. The standing voltage gradients of the extracellular milieu are crucial to cell adhesion, migration and differentiation [Yao, L., 2011]. Modalities such as micro electrode arrays, conductive polymers, static and continuous direct current (DC) EF and electromagnetic fields have been used to electrically stimulate cells [Ariza, C.A. et al. 2010]. Several studies have reported that extracellularly applied EF, on the order of 1 V/cm, promotes neurite outgrowth cathodically [Yao, L., 2011], [Jaffe, L.F. & Poo, M.M. 1979], [Hinkle, L., 1981], [Patel, N. & Poo, 1982], [Valentini, R.F., 1992], [Li, S., 2010], [Chang, Y.-J., 2013]. Wood et al. showed that different surface coatings, cell culture mediums, growth supplements and EF magnitude and application time, influence the growth of chick embryonic dorsal root ganglia (DRG) neurites [Wood, M. & Willits, R.K. 2006]. Yamada et al. reported that colonies of embryonic bodies (EBs) that received 10 V stimulation assume specifically a neuronal fate compared to controls (no electrical stimulation received) that have a low differentiation efficiency. The resulting neural cells have potential to differentiate into various types of neurons in vivo and, when injected in blastocysts of adult mice, they contribute to the injured spinal cord as neuronal cells [Yamada, M. et al., 2007]. The influence of pulse EF and alternating current fields on neural stem cells behavior has been studied. Kimura et al. planted PC12 cells on ITO electrodes and subjected them to a rectangular peak-to-peak pulse wave potential of 100 mV, with frequency of 100 Hz, for different times. These authors showed that a potential application for more than 60 min is harmful to cells, but a good rate of differentiation was obtained when an electric potential was applied for 30 min every 24h, repeated 3 times [Kimura, K., 1998]. Park et al. cultured PC12 cells on gold nanoparticles deposited on polyethyleneimine (PEI) - precoated surfaces and evaluated its response to a pulsed and constant electrical stimulation of 250 mV for 1 h once every 3 days, concluding that alternating current stimulation promotes a better viability of cells (~ 90% viable cells) comparatively to the constant current stimulation (~70% viable cells) [Park, J.S. et al. 2008]. Chang et al. used a biphasic electrical current stimulator chip to stimulate fetal NSCs at 100 Hz with a magnitude of 4,8,16 or 32 $\mu A/cm^2$ and duration of 50 or 200 µs for 4 days. The rate of proliferation increased when a current density of 4 or 8 $\mu A/cm^2$ was applied for 200 µs, at 100 Hz, not being affected by an electrical stimulation with relatively higher amplitudes or lower pulse durations. The current density of 4 µA/cm2 for 200 µs increases neural differentiation of fetal NSCs [Chang, K.-A. et al. 2011]. New therapeutic strategies based on nanotechnology and functional biomaterials having the ability to induce EF must be

developed in order to control proliferation, differentiation and guidance of regenerating neurons and implanted neural stem cells.

Chapter II: Materials and Methods

II.1 Manufacture of 2D PEDOT:PSS films

II.1.1 Samples preparation

Glass coverslips with 4.84 cm^2 surface area were cleaned before being used for the film deposition. Every coverslip was rinsed several times in MilliQ water with detergents, then cleaned with isopropanol and acetone in ultrasounds. Nitrogen stream was used to dry the samples. Then, the surface was exposed to Plasma oxygen treatment (PlasmaPrep2, GaLa Instrument), to remove organic compounds from the sample and to increase the hydrophilicity of the surface.

II.1.2 Crosslinked PEDOT:PSS solutions

Different PEDOT:PSS crosslinking methods were used to prepare the solutions to make thin conductive films by spin coating.

- Crosslinking 1: The ethylene glycol (Sigma-Aldrich) was added in a volume ratio of 1:4 to filtrated PEDOT:PSS (Heraeus, CLEVIOS P AI 4083, solids content 1.3-1.7%). Dodecylbenzenesulfonic acid (DBSA) (0.5µL/mL) and 3-glycidoxypropyltrimethoxysilane (GOPS) (10 mg/mL) were added to the solution to improve film formation and stability, as described by Soares et al.
- Crosslinking 2: The ethylene glycol was added in a volume ratio of 1:8 to filtrated PEDOT:PSS. Then, the DBSA (1 µL/mL) and the crosslinker divinylsulfone (DVS) (50 mg/mL) were added to the solution to improve film formation and stability, as described by Mantione et al.

II.1.3 Spin coating

Spin coating is a procedure used to prepare uniform thin films on flat substrates. In this process, as illustrated in Fig.9, a small amount of a solution is placed on the center of the substrate, which is either spinning at low speed or not spinning at all. The substrate is then rotated at high speed in order to spread the coating material by centrifugal force. The film thickness is controlled by adjusting the polymer solution concentration and the spinning speed. In general, higher spinning speeds lead to thinner films.

The aqueous dispersion crosslinked with GOPS was spin coated (Spin-Coater KW-4A, Chemat Technology) on previously prepared glass coverslips at a velocity of 1800 rpm for 60s, as described by Soares et al.

The aqueous dispersion crosslinked with DVS was spin coated onto cleaned glass coverslips at a velocity of 1000 rpm for 40s, as described by Mantione et al.

The commercial aqueous dispersion of PEDOT:PSS only, used as control for conductivity measurements, was spin coated at 1800 rpm for 50 s.

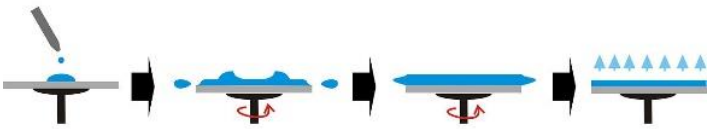

***Figure 9**. **Spin coating process**. In this process an excess of solution is placed onto the center of substrate, which is spinner at high speed in order to spread the fluid. [Spincoater.com, Laurell Technologies2018)]*

II.1.4 Annealing

The annealing process consists in heating a polymer to elevated temperatures far below the melting point. After this treatment, semicrystalline polymers usually change their physical properties: the heat treatment results in a reorganization of the structure leading to a state of order with a lower free energy. [E. W. Fischer, 2009]. This allow the clearance of residual traces of solvents (water) improving the performances of the films and also enhances the morphology of polymeric film. The selected annealing temperature and process duration were the following:

- PEDOT:PSS solution crosslinked with GOPS: 150°C, 2 min
- PEDOT:PSS solution crosslinked with DVS: 50°C, 1 h
- PEDOT:PSS solution not crosslinked: 120°C, 10 min

Different conditions were used: in the case of the GOPS and DVS crosslinked films, these were the softer conditions that were shown to ensure complete crosslinking of the PEDOT:PSS film, while in the case of the non-crosslinked PEDOT:PSS, this is the minimum time to ensure complete drying of the film.

II.1.5 Film thickness

The thickness of the spin coated films was measured trough profilometry analysis (Dektak 3.21 Profilometer). First, a thin cut on the polymeric layer is done with a scalpel, paying attention not to carve the glass too. Then, profilometric analysis in conducted perpendicularly to the cut in order to define the depth of the incision.

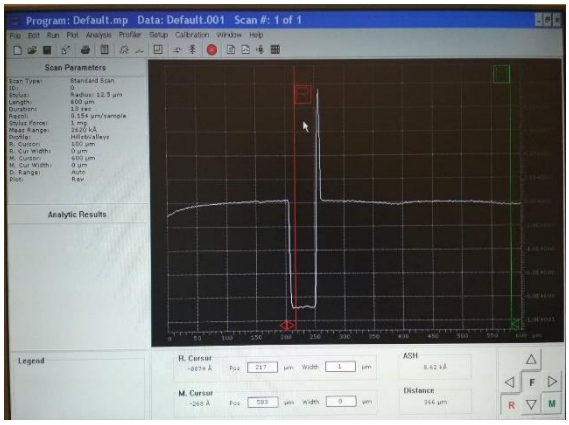

Figure 10 . Profilometer analysis of the film thickness. *A thin cut is done on the polymeric film with a scalpel, then profilometric analysis is conducted perpendicularly. Positioning the red cursor inside the incision and the green one outside, it is possible to know the depth of the cut, calculated automatically by the software, that corresponds to the film thickness.*

II.2 Manufacture of 3D scaffolds

II.2.1 Preparation of glass coverslips

Squared glass coverslips with a surface area of 4.84 cm^2 were cleaned with detergents in MilliQ water. A biological glue (Silastic type A adhesive) was applied only at the edges of the coverslip, to preserve the quality of the microscopy imaging.

II.2.2 Electrospinning technique

Electrospinning process was carried out using a system developed in our laboratories. A schematic sketch of the system is shown in Fig. 11. Two different types of collectors were used: a flat one, wrapped into aluminum foil, to obtain random fibers, and a parallel plate one, to obtain aligned fibers.

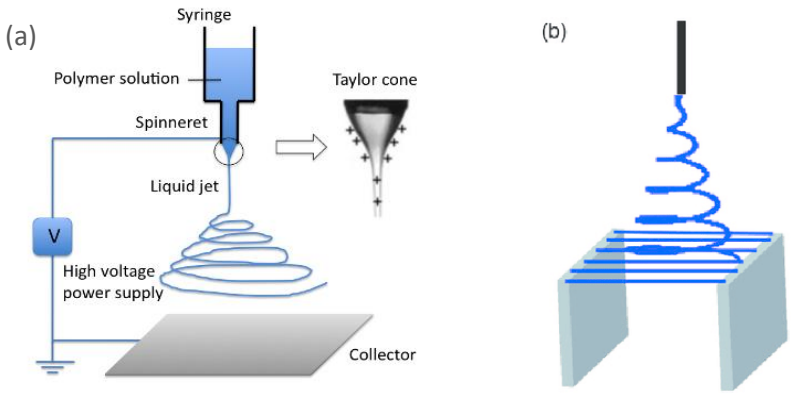

Figure 11 . A schematic diagram showing electrospinning set up with flat collector (a) and parallel plate collector (b)*. [Athira K. S , Fabrication of Poly(Caprolactone) Nanofibers by Electrospinning, Journal of Polymer and Biopolymer Physics Chemistry. 2014],[Hao-Yang Mi, Fabrication of porous synthetic polymer scaffolds for tissue engineering, Journal of Cellular Plastics, 2014]*

II.1.3 Electrospinning of PEDOT:PSS fibers

Several issues are related with the electrospinnability of PEDOT:PSS. First, the viscosity of the commercial aqueous dispersion is very low (11 cP), while for the electrospinning high viscosities are requested from the solution (≈ 3000 cP). Second, the PEDOT:PSS fibers need to become water insoluble and stable in the long term to be used for cell culture and differentiation. Third, the conductivity of the material needs to remain high after the electrospinning process, so no insulating agents can be added to the solution, or they must be removed after the process. Moreover, as the content of PEDOT:PSS in the commercial aqueous dispersion is very low (1.3% w/w), only small amounts of other materials can be added to obtain conductive fibers with PEDOT:PSS as main component.

A first attempt of fibers realization was made adding polyvinylpyrrolidone (PVP), a slightly conductive polymer. To prepare the solution, 1.4g of PVP were dissolved in 6.5mL of PEDOT:PSS aqueous dispersion, then 3.5mL of dimethylformamide (DMF) were added; the solution was left stirring overnight. The electrospinning process was carried on with a flow rate of 0.3mL/h, a voltage of 30kV, and a distance between the spinneret and the flat collector of 14cm.

Then, several strategies were tried to increase the viscosity in the solution, both chemically and physically; a Brookfield Digital Viscometer DV-II was used to perform the measurements (parallel-plate). First, the use of crosslinking agents was investigated, in order to improve the fibers stability in water too: the same two solutions prepared for films manufacture were tested, with GOPS and DVS as crosslinkers (see section 1.2). Another strategy was to add Sorbitol to the commercial PEDOT:PSS solution: as water soluble component, we checked the possibility to use it as viscosity increaser and to remove it after fibers formation. Finally, we tried to increase the viscosity through the evaporation of the water content: Rotavapor and Rapidvap process were assessed to concentrate the PEDOT:PSS solution, while lyophilization technique, performed with Liophilizer (reference), was used to obtain a material powder, resuspendable in a smaller amount of solvent. The post-addition of polyethylenglycole (PEG300 Da) was also tested to increase the viscosity.

Electrospinning parameters were: flow rate ranging from 0.1 to 0.3mL/h, voltage range of 10-30kV, distance spinneret-collector of 7-14 cm.

Electrospinning parameters	
Set-up	Vertical
Collector	Flat or parallel plate

Flow rate	0.1-0.3 mL/h
Voltage	10-30kV
Distance	7-14 cm

Table 1. Parameters for PEDOT:PSS fibers electrospinning

II.1.4 PEDOT:PSS coating onto electrospun fibers

A combined approach was also tried in order to have a 3D conductive scaffolds. Different materials were used to obtain fibers with electrospinning technique:

- Polybenzilimidazole (PBI): a solution of PBI (Performance products, USA)13% w/w in DMAc (Panrec, Spain) was prepared in the laboratories. Fibers were electrospun under these conditions: flow rate of 0.3mL/h, applied voltage of 20kV, distance spinneret-collector of 13cm, humidity between 50-60%;
- Polycaprolactone (PCL)(Sigma Aldrich): a 10% solution in hexafluoro-2-propanol (HFP)(Sigma Aldrich) was electrospun at 12kV, both on a flat collector covered with alluminium foil and on a parallel plate collector, with a flow rate of 0.3mL/h and a spinneret-collector distance of 8 cm;
- Polyvinylalcohol (PVA)(Sigma Aldrich): a 8% solution in water was electrospun at 10kV, on a flat or parallel plate collector, with a flow rate of 0.1mL/h and a spinneret-collector distance of 13 cm.

Electrospinning parameters	PBI (13% in DMAc)	PCL (10% in HFP)	PVA (8% in H_2O)
Set-up	Vertical	Vertical	Vertical
Collector	Flat or parallel plate	Flat or parallel plate	Flat or parallel plate
Flow rate	0.3 mL/h	0.3 mL/h	0.1 mL/h
Voltage	20 kV	12 kV	10 kV
Distance	13 cm	8 cm	13 cm
Humidity	50-60%	(Not critical)	(Not critical)
Needle diameter	purple	green	purple

Table 2. Electrospinning parameters for PBI, PCL,PVA

Then, the same PEDOT:PSS solutions utilized for the films were prepared as described at section II.1.2. Three different coating methods were tested:

- Spin coating of the PEDOT:PSS crosslinked solution on fibers samples (1000rpm, 40s);
- Dipping of fibers for several times in the solutions;
- Immersion of the fibers for 24h in the two different solutions.

After the coating, an annealing treatment was carried on the samples with the same conditions described at point 1.4 (150°C, 2 minutes for the solution crosslinked with GOPS, 50°C, 1 h for the solution crosslinked with DVS).

Fibers were observed both with optical microscope and SEM before and after the coating. EDS analysis was carried on the samples to understand which coating system was the best: the peak of sulfur was used to identify on which samples the PEDOT:PSS content was higher.

Material	Coating solution	Annealing	Coating method
PBI	Solution 1	150°C, 2min	Spin coating
PBI	Solution 1	150°C, 2min	Dipping several times
PBI	Solution 1	150°C, 2min	Immersion for 24h
PBI	Solution 2	50°C, 1h	Immersion for 24h
PCL	Solution 1	150°C, 2min	Immersion for 24h
PCL	Solution 2	50°C, 1h	Immersion for 24h
PVA	Solution 1	150°C, 2min	Immersion for 24h
PVA	Solution 2	50°C, 1h	Immersion for 24h

Table 3. Materials, solutions and process parameters to obtain a PEDOT:PSS coating onto polymeric electrospun fibers

.

II.1.5 Additional tests on PBI fibers

PBI was poorly used before for biomedical applications; a particular attention was reserved to this material in order to fully characterize its biological response. Different physical treatments were applied to be sure that the organic solvent (DMAc), used to electrospin it, was totally removed from the fibers. The first treatment was performed leaving the PBI electrospun fibers in vacuum for 3 hours, with a desiccator, to help the evaporation of the solvent. Then, some fibers were washed with MilliQ water, as the DMAc is water soluble while PBI is not; the water was kept apart to perform absorbance analysis. Additionally, some of the fibers that were previously left in vacuum and washed, were also treated with high temperature

on a hot plate: DMAc has an evaporation temperature of 160°C, so the material was heated up to these values. PBI's melting temperature is around 400°C, so there was no risk to damage the fibers; however, fibers after temperature treatment were observed with SEM microscope to assure the absence of negative effects. Finally, some fibers were washed again after the heat treatment and the water was again analyzed with absorbance on the full spectrum. Results were compared with normal MilliQ water. Fibers after every performed test were sterilized and used for cytotoxicity assays to evaluate which one was guaranteeing the best biocompatibility results.

II.3 3D-printing of a set-up for cell culture and electrical stimulation

II.3.1 Design of frame and container

Electrical stimulation has to be provided to the material through the use of electrodes; these electrodes should not be immersed in the cells culture medium, to avoid the generation of ionic currents that can alter the pH and the condition to which the NSCs are exposed. In order to reach this goal, a customized set-up was design with the software Onshape®. The first part of the design is a "frame", where fibers can directly electrospun; the hole in the middle, as shown in Fig. 12, is the area where cells should be seeded and was designed to avoid the presence of the glass coverslip and to improve the quality of the microscopy imaging.

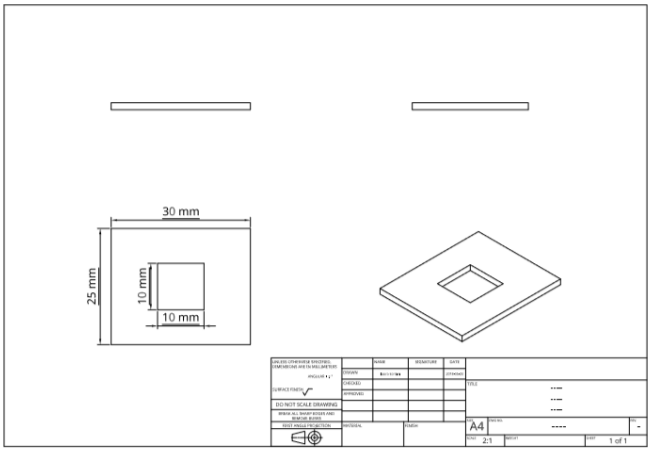

Figure 12. Onshape CAD design of "frame"

The second piece (Fig.13) is a "container" for culture medium; when this element is attached on the frame, it creates an isolated chamber for cells culture, leaving a part

of the frame with the fibers outside where electrodes can be glued to apply the electrical stimulation.

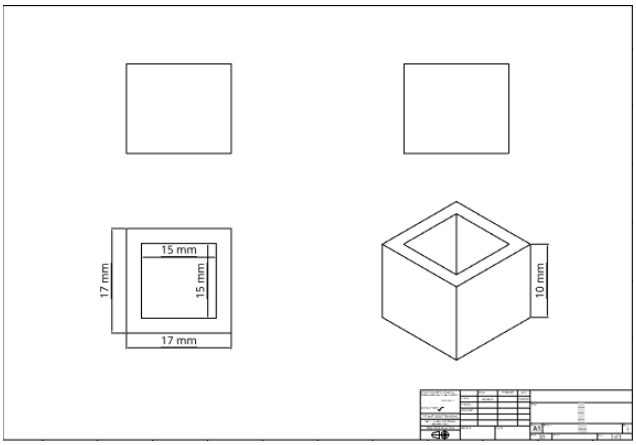

Figure 13. Onshape CAD design of "squared container"

Another element was also designed, for the electrical stimulation of the cells seeded onto spin coated films: a cylindric container, with two lateral parts for the insert of the electrodes, that can be glued directly in the surface of the film, as shown in Fig.14.

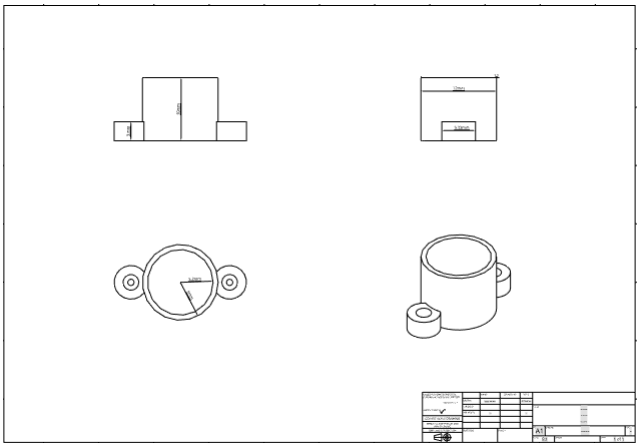

Figure 14. Onshape CAD design of "cylindric container"

II.3.2 3D-printing

The whole set-up was realized with a 3D printer (Makerbot Replicator 2x) through the fuse deposition modeling technique (FDM). This technique consents to melt a filament of polymeric material at the proper melting temperature and to create a 3D object according to the CAD file with the design obtained with Onshape software: every time the printer deposits a layer of melted material on the x-y plane, a platform lowers on the z axis proportionally to the height of the material layer, in order to sub sequentially deposit another layer of material on the previous one, creating the 3D design. The chosen material for the two pieces was polylactic acid (PLA), because of its biocompatibility.

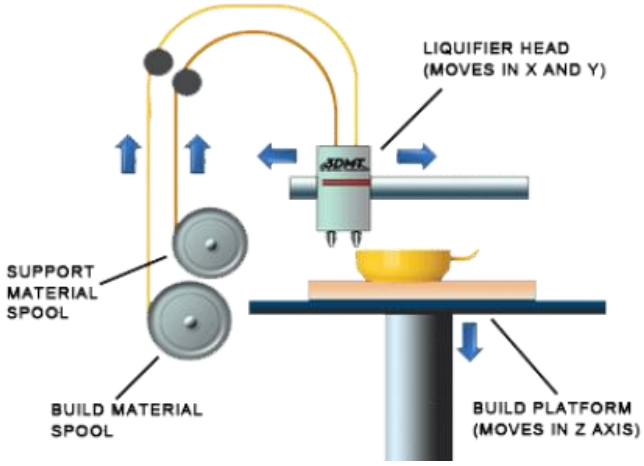

Figure 15. Schematic diagram of 3D printing process

II.3.3 Set-up assembly

The two pieces were separately realized and successively joined with a biological glue or with Sylgard® silicon elastomer (PDMS)(Dow Corning), as shown in Fig. 16; the two silver stripes in figure represent the space where to put silver glue to connect the electrodes for the electrical stimulation.

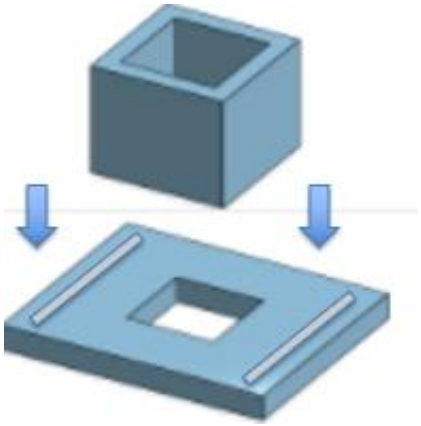

Figure 16. Schematic diagram of 3D-printed set-up assembly.

PDMS was prepared in the laboratories from a kit: 10% curing agent was added to the base; after mixing, many air bubbles are forming, so it is necessary to leave the mixture in vacuum for 1h in order to remove them. Than, the liquid silicon was applied on the edges of the container with a spatula, placed on the frame and left into the heater at 70°C for 1h to let it crosslink.

II.4 Conductivity measurements

II.4.1 Four Probe-Method

The key analysis carried on the samples was concerned on the electrical conductivity. Four probe apparatus is one of the standard and most widely used apparatus for the measurement of resistivity of semiconductors. This method is employed when the sample is in the form of a thin wafer, such as a thin semiconductor material deposited on a substrate. The sample is millimeter in size and having a thickness w. It consists of four probes arranged linearly in a straight line at equal distance S from each other. A constant current is passed through the two probes and the potential drop V across the middle two probes is measured (Fig. 17).

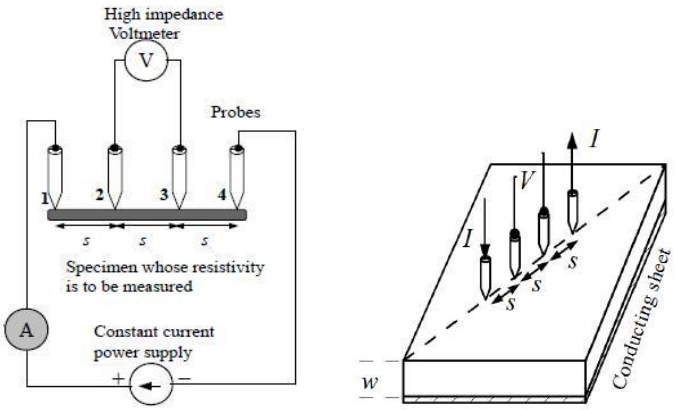

Figure 17 The figure shows the arrangements of four probes that measure voltage (V) and supply current (A) to the surface of the material. *[Resistivity by Four Probe Method , vlab.amrita.edu,.2013]*

In this thesis work, a variation of the apparatus was used: four electrodes were connected to four gold stripes deposited on the material, crossing the entire transversal section. Recording the potential drop for every value of applied current, it is possible to the derive the slope of the straight line according to Ohm's law:

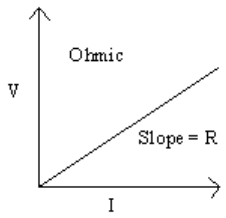

Figure 18 V-I graph of an ohmic conductor

At a constant temperature, the resistance, R of a conductor is proportional to its length L and inversely proportional to its area of cross section A (product of the sample thickness per sample width):

$$R = \rho \frac{L}{A} \quad (1)$$

Where ρ is the resistivity of the conductor and its unit is ohmmeter.
From this step it is possible to evaluate the conductivity, as it is the opposite of the resistivity:

$$\sigma = \frac{1}{\rho} \quad (2)$$

The four-point probe method relies on the application of a constant current (I) across two outer electrodes at the surface material and on measurement of the potential between the inner pair of electrodes.
Silver glue (HAZ Electrodrag 1415, Agar) was used to connect the probes to the sample.
Sample thickness was measured with Dektak 3.21 Profilometer as already described at point II.1.5 of this chapter.

II.4.2 Edwards vacuum coating system

For the deposition of the four straight conductive stripes, a physical vapour deposition (PVD) was made with Edwards vacuum coating system (instrument characteristics). With this system, it is possible to melt and evaporate gold from an incandescent tungsten filament under high vacuum, being the Au atoms deposited on the surface of the sample:

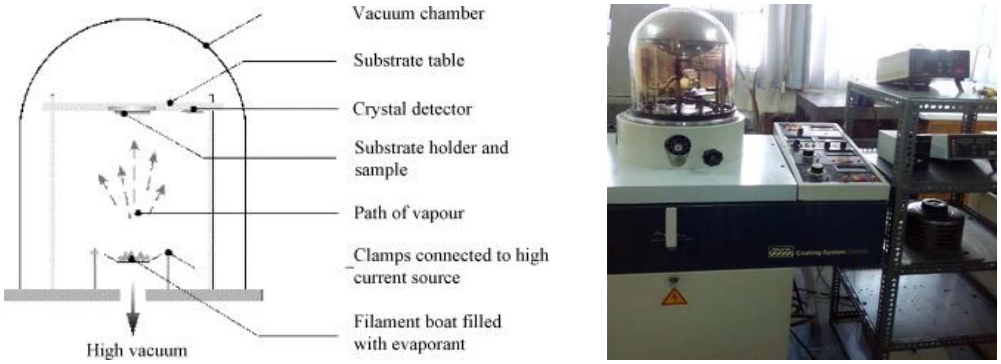

Figure 19 Left: Schematic diagram of a resistive thermal evaporation system**. ["Study of Indium Tin Oxide (ITO) for Novel Optoelectronic Devices", Ph.D. thesis by Shabbir A Bashar]. **Right: Edward's vacuum coating system.

A PET shadow mask with four channels shape was used to cover the areas of the samples where no gold was requested.

II.5 Stability test on the materials

The first test that was conducted on the samples was concerned on the materials stability in a wet environment for sufficiently long periods of time, to check the suitability of the substrates for cell culture conditions.
Samples were placed in MilliQ water for 2 weeks. Then, triplicates of 200 µL aliquotes were taken from the water that stayed in contact with the materials and compared to a blank (simple MilliQ water) with an absorbance analysis (Tecan Infinite 2000 Pro). Samples' surface was also observed with optical microscope to evaluate the presence of any defect.
The test was then repeated with samples placed in culture medium for 2 weeks in the incubator (37°C).

II.6 Sterilization of the samples

To preserve the sterility of the cell culture, samples were sterilized with a solution of PBS + 1% Antibiotic-Antimitotic (Gibco®); samples were first washed three times with PBS and then left in the solution for 2 days, after which they were washed three times again with PBS. Another sterilization method, with UV light for 1hour and 30 minutes, was also tested.

II.7 Biocompatibility tests with fibroblasts

Mouse fibroblasts L929 cell line was used to assess the biocompatibility of the materials. Culture medium used for fibroblasts is DMEM/F-12 (Life Technologies) supplemented with 10% FBS (Termofisher).
Indirect and direct cytotoxic tests were performed following the ISO 10993-5 guidelines for medical devices in order to assess the cytotoxicity of each polymer.
Direct culture of cells on the surface of the materials was carried on for 10 days, performing qualitative viability analysis and cell fluorescence staining at different time points. Cells were also imaged with SEM microscopy to better evaluate their morphological response in contact with the substrates.

II.7.1 Cells thawing

The cells were thawed from liquid nitrogen; frozen vials were submerged in water bath at 37°C and resuspended in DMEM + 10% FBS. The suspension was centrifuged at 1000 rpm for 3 minutes, then the supernatant was discarded. Fibroblasts pellet was resuspended in fresh culture medium and then the Trypan Blue (Gibco®) exclusion method (Neubauer® hemocytometer) was used to determine cells number and viability. This process was carried out fast to avoid losing cell viability.

II.7.2 Cell expansion

In order to expand cells, L929 were plated on T-flasks (Falcon®, BD Biosciences) and incubated at 37ºC and 5% CO2 in a humidified atmosphere using DMEM + 10% FBS medium. The medium was changed every 2 days until cells reached an 80-90% confluence. They were then harvested using trypsin/EDTA (reference) 0.025% in PBS by incubation at 37ºC and 5% CO2-humidified atmosphere for 5 min. Then, culture medium was added to block the action of the enzyme and the cell suspension was centrifuged at 1000 rpm for 3 minutes. After wasting the supernatant, the pellet was resuspended in fresh DMEM + 10% FBS and cells number and viability was determined through Trypan Blue exclusion method using a hemocytometer under an optical microscope (Olympus).

II.7.3 Cell cryopreservation

After expansion, the remaining cells were harvested using trypsin, centrifuged for 3 minutes at 1000 rpm and resuspended in culture medium with 10% (v/v) dimethyl sulfoxide (DMSO). Then, they were transferred to cryogenic vials for storage at - 80ºC. The freezing in liquid nitrogen at -196 ºC is used for cryopreserving cells for long time.

II.7.4 Indirect cytotoxicity assay

For indirect contact assays, triplicates for each material were placed on 6-well plates (Falcon®, BD Biosciences) containing 2 mL of DMEM + 10% FBS (Termofisher) and kept in an incubator (37 °C, 5 /% CO2, fully humidified) for 24 hours. Media incubated with sterile glass coverslips were used as a negative control, and a piece of latex glove (toxic) was used as positive control. L929 fibroblasts, seeded in 24-well plate (Falcon®, BD Biosciences) at an initial density of 8×10^4 cells/cm^2, were kept in the incubator for 24 hours and then cultivated with the liquid extracts from the materials. Cell metabolic activity was quantified after 24 hours cultures using MTT, i.e. (3-(4,5-Dimethylthiazol-2-yl)-2,5-Diphenyltetrazolium Bromide) and measuring absorbance of at 570 nm using the MTT Assay (procedure described in a later section). Absorbance for the negative control was reported at 100% and all other values were calculated respectively.

II.7.5 MTT Assay

MTT solution was prepared from a powder (reference) with a concentration of 5mg/mL in PBS, agitated vigorously and then diluted again in PBS to a final concentration of 1mg/mL. To perform the assay, culture medium was removed from the plate and the working solution was added in each well and kept in the incubator at 37°C for 2 hours. MTT solvent was prepared with 2mL of 37% HCl in 198 mL of isopropanol. After 2 hours, MTT solution was replaced with MTT solvent and left in the plate while agitating for 5 minutes. From each well, triplicates of 200 µL aliquots were transferred to a 96-well transparent plate. Absorbance was measured with Tecan Infinite 2000 Pro and quantified at 570 nm wavelength. Negative control was used as reference to calculate total cell viability.

II.7.6 Direct cytotoxicity assay

L929 fibroblasts were seeded in a 6-well plate at an initial density of $1.5x10^5$ per cm^2 and kept in an incubator (37 °C, 5 /% CO2, fully humidified) for 24 hours. After the incubation period, materials were placed on the top of the culture. After 24 hours in contact with the materials, cells were observed under an inverted optical microscope (Leica DMI 3000B, Germany) in order to qualitatively evaluate whether cells were confluent or a halo of inhibition at cell material interface was formed.

II.7.7 Adhesion tests

A 6-well plate was prepared with one sterile sample per well. Fibroblasts were harvested from a confluent T-flask, counted with Trypan blue and resuspended in fresh culture medium. Cells were then seeded onto the samples' surface with a density of 10^5 cells/cm^2: the maximum volume containing the cells should be calculated to pipette the cells on the samples in just one drop, not to seed the cells on the well. Then, the plate was left in the incubator at 37°C for 1 hours to let cells adhere. After one hour, 2mL of culture medium were added in each well. As the observation of the cells on the fibers is not always clear with optical microscope, a blank with cells on a glass coverslip was always prepared to monitor the culture.

II.7.7.1 Calcein staining

Calcein (BD Pharmingen) was taken from the 20°C refrigerator and diluted in order to have a concentration of 2 µM in DMEM + 10% FBS. Culture medium was removed from the wells and the samples were washed with PBS. Then diluted calcein was added to every well and the plate was incubated for 20-40 minutes at 37°C in the incubator. Cells were then observed with fluorescence optical microscope (DMI 3000B, Leica) under blue light.

II.7.7.2 DAPI and Phalloidin staining

For DAPI and Phalloidin staining, cells need first to be fixed. After removing culture medium, samples were washed two times with PBS and incubated for 15-20 minutes at room temperature with a solution of paraformaldehyde (PFA) 2% in PBS. Then, PFA was removed and samples were incubated with blocking solution (reference) for 15-30 minutes at room temperature. After removing the solution, a dilution of Phalloidin 1:100 in PBS was pipetted on the surface of the samples and the plate was left in the dark for 20-30 minutes at room temperature. Successively, samples were washed again two times with PBS and incubated with a solution of DAPI 15 µL/ 10 mL of PBS, for 3-5 minutes in the dark. Finally, samples were washed with PBS to remove residual crystals and observed with a fluorescence optical microscope (DMI 3000B, Leica) under UV and green light. Two different pictures were acquired with a digital camera (DXM 1200F, Nikon) and then merged with the software ImageJ.

II.8 SEM microscopy

To characterize the cellular response to the material, cells were fixed with glutaraldehyde 1.5% (v/v) in PBS at room T for 2h. The samples were washed three times with PBS and,

after that, the samples were immersed in ethanol solutions at different concentrations, 25%, 50%, 75% and 100% for 30 min each at room T. Before the observation of the substrates they were coated with an Au/Pd layer of 30 nm using a Polaron model E5100 coater (Quorum Technologies). Images were obtained using a Field Emission Gun Scanning Electron Microscope (FEG-SEM) (JEOL, JSM-7001F model).

II.9 NSCs culturing

II.9.1 Cell line

ReNcell VM (Millipore®) is an immortalized human neural progenitor cell line that was derived from the ventral mesencephalon region of a human fetal brain tissue and that was immortalized by retroviral transduction with the v-myc oncogene. This cell line has the ability to differentiate into neurons and glial cells [Donato, R. et al. 2007].

II.9.2. NSCs thawing

The cells were thawed from liquid nitrogen and the frozen vials were submerged in a 37ºC water bath, and resuspended in DMEM/F12 (Life Tecnologies). The mixture was centrifuged for 3 min at 1000 rpm, and the supernatant was discarded from the mixture. The cells were resuspended in the expansion medium: DMEM/F12 supplemented with 20 ng/mL EGF (Prepotech), 20 ng/mL FGF-2, 1% N2 supplement (Life Technologies), 20 µl/mL B27 supplement (Life Technologies), 20 µg/mL additional insulin (Sigma), 1.6 g/L additional glucose (Sigma) and 1% penicillin/streptomycin. The Trypan Blue (Gibco®) exclusion method is used to determine cells number and viability. This process was carried out fast to avoid losing cell viability.

II.9.3. NSCs expansion

In order to expand cells, RenCell VM were platted on T-flasks (Falcon®, BD Biosciences) that had been previously incubated with poly-L-Ornithine (Sigma) for 30 minutes, at 37°C and 5% CO2 humidified environment, washed once with PBS and incubated for 4 hours with laminin (20µg/mL, Sigma) diluted in PBS. The T-flasks with cells were incubated at 37ºC and 5% CO2 in a humidified atmosphere using DMEM/F12 medium. The medium was changed every 2 days until cells reached an 80-90% confluence. They were then harvested using Accutase (Gibco) by incubation at 37ºC and 5% CO2-humidified atmosphere for 3-5 min. Then, the cell suspension was diluted with DMEM/F12 and centrifuged at 1000 rpm for 3 min. The pellet was resuspended in an expansion medium and cells number and viability was determined through Trypan Blue exclusion method using a hemocytometer under an optical microscope (Olympus).

II.9.4. NSCs cryopreservation

After expansion, the remaining cells were dissociated using Accutase, centrifuged for 3 minutes at 1300 rpm and resuspended in culture medium with 10% (v/v) dimethyl sulfoxide (DMSO). Then, they were transferred to cryogenic vials for storage at - 80ºC. The freezing in liquid nitrogen at -196 ºC is used to cryopreserve cells for long time.

II.9.5. NSCs differentiation

Differentiation is induced by the withdrawal of growth factors EGF and FGF2 and the culture medium change to a 1:1 mixture of Neurobasal media (Invitrogen, Life Technologies) supplemented with B27 (20µl/mL), 2.5mL L-Glutamin 2mM, 0.5% penicillin streptomycin (Invitrogen), and DMEM/F12+Glutamax supplemented with 1% penicillin streptomycin, 1% N2 Supplement (Invitrogen), 20µg/mL insulin (Sigma), 1.6 g/L glucose (Sigma). The differentiation process was carried out for 7 days, changing the medium every 2 days.

II.10 Electrical stimulation

II.10.1 Set-up

The physiological behaviour of *in vitro* cultured cells could be altered in response to physical stimuli as electric field, mechanical force and topography. In this study, we engineered a substrate (Fig.20) that modulates electrical fields on living cells to investigate the effects of pulsed square DC electric field on fetal NSCs proliferation and differentiation processes.

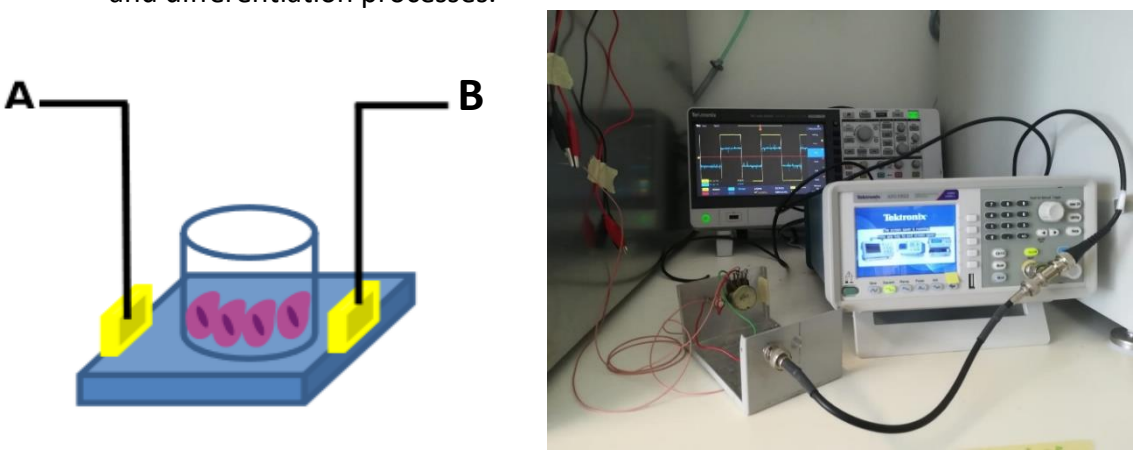

Figure 20 Schematic illustration of the electric field setup used in this experiment to stimulate cells (left) and real electrical set-up pictures (right).

Ten layers of PEDOT:PSS were deposited on glass slide. A hollow cylinder in center of substrate was 3D-printed and glued with silicon in order to stanch the culture system. To enhance the electrical contact, stripes of gold with 40 nm of thickness were deposited on two ends of the sample. Copper wires were glued in these stripes with silver paste (conductive) and an external DC power supply, connected to the electrodes, was used to apply an electric field vector that runs horizontally.

The electrical circuit was designed as illustrated in Fig. 21:

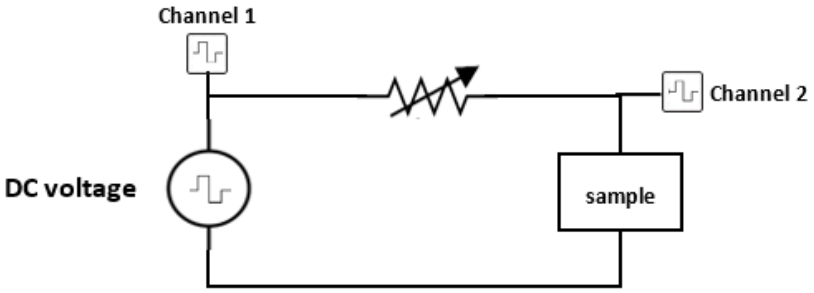

Figure 21. Schematic diagram of the electrical circuit assembled to stimulate the cells

DC voltage source (Tektronix AFG 1022) is injecting a square wave of 4V amplitude; channel 1 of the oscilloscope (Tektronix TBS 200 Digital Oscilloscope) registers the applied voltage. A potentiometer (10kΩ) is used to vary the resistance of the circuit in order to know the current value that reaches the sample; channel 2 of the oscilloscope registers the voltage difference across the sample. In this configuration, another sample can be put in parallel to the previous one, just regulating the potentiometer. In this case, the potentiometer was always regulated in order to apply 1V/cm across the samples. Resistance of the potentiometer was measured with a multimeter (), and the total current circulating in the circuit was calculated with Ohm's law:

$$I = \frac{(V_{channel2} - V_{channel1})}{R_{potentiometer}}$$

II.10.2 NSCs expansion

We exposed the cells to a 100 Hz electrical stimulation with a magnitude of 1V/cm with 10ms pulse duration in a continuous manner according to the culture schedule shown in Fig.22.

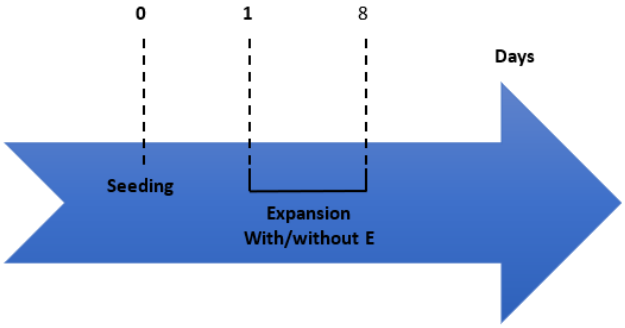

Figure 22. Experimental scheme with the electrical stimulation during the proliferation

II.10.3 NSCs differentiation

NSC differentiation was studied under applied DC electric fields and compared to control experiments with no applied electric field. We exposed the cells to a 100 Hz electrical stimulation with a magnitude of 1V/cm with 10ms pulse durations in a continuous manner during expansion time and over 12h per day during differentiation time, according to the culture schedule shown in Fig.23. Medium was changed every two days.

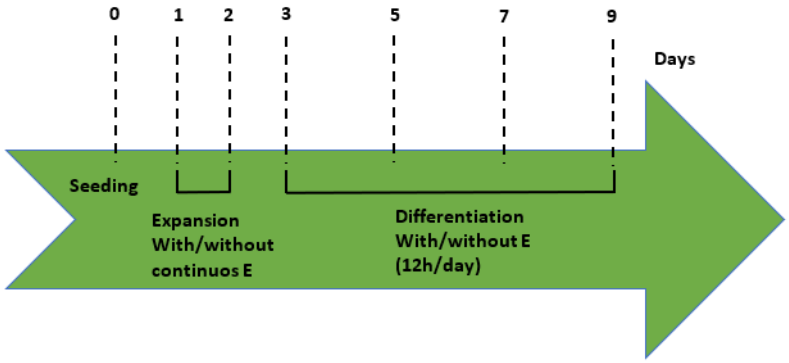

Figure 23 . Experimental scheme with the electrical stimulation during the NSCs proliferation and differentiation

II.10.4 Immunocytochemistry

In order to evaluate the differentiation of cells into different neural phenotypes, the cells can be immunostained for specific markers: nestin, microtubule-associated protein 2 (MAP2) and β-tubulin (Tuj1) for neurons, glial fribrillary acidic protein (GFAP) for astrocytes and NG2 and adenomatous polyposis coli (APC) for oligodendrocytes 21. ReNcell VM line has a normal karyotype and proliferates indefinitely, showing a positive signal for the NSCs marker nestin. When the growth factors are omitted from the medium, these cells undergo differentiation in neuronal and glial direction, showing a strong labeling for the neuronal marker Tuj1 and for the dopaminergic marker tyrosine hydrolase (TH). In this work, only βIII-tubulin (Tuj1) and glial fribrillary acidic protein (GFAP) were used for the immunostaining.

Cells were fixed with PFA 4% (2mL per well of a six well-plate) for 30 minutes at room temperature, and then washed twice with PBS. Cells were incubated for 30 minutes at room temperature with blocking solution (90%PBS, 10% NGS and 0.1% Triton X) and, after this, the primary antibodies diluted in staining solution were incubated at room temperature for 2 hours. After the incubation with the primary antibody, cells were washed three times with PBS and incubated with the appropriate secondary antibody for 45 minutes at room temperature in a dark container. Finally, cells were washed two times with PBS and incubated with DAPI nucleic acid stain for 2 minutes at room temperature and washed twice with PBS. The stained cells were visualized under a fluorescence microscope (Leica DMI 3000B), using the software Nikon-AcT1.

Primary Antibodies	Type	Source	Dilution
Anti-TUJ1	Mouse IgG	Covance	1:4000
GFAP	Rabbit IgG	Abcam	1:100

Table 4. Primary antibodies used in immunocytochemistry

	Type	Source	Dilution
Anti-Alexa 546	goat anti mouse IgG	Life Technologies	1:500
Anti-Alexa 488	goat anti rabbit IgG	Life Technologies	1:500

Table 5. Secondary antibodies used in immunocytochemistry

II.10.6 Single Cell Calcium Imaging (SCCI)

To determine the functional neuronal differentiation of NSCs cells, the variations of intracellular calcium concentration ([Ca2+]i) in single cells following stimulation with 50 mM KCl and 100 mM histamine (Sigma–Aldrich) were analyzed as previously described by [Rui S. Rodrigues, 2017], as showed in Fig.24.

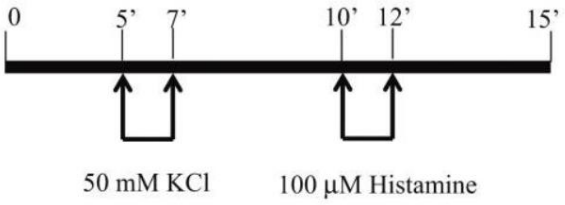

Figure 24 Time points for SCCI experiment. *[Rui S. Rodrigues, Interaction between Cannabinoid Type 1 and Type 2 Receptors in the Modulation of Subventricular Zone and Dentate Gyrus Neurogenesis, frontiers in pharmacology, 2017]*

KCl depolarization causes an increase in [Ca2+]i in neurons, whereas stimulation with histamine leads to an increase in [Ca2+]i in stem/progenitor cells [Agasse, F., 2008],[Xapelli, S., 2013]. For SCCI analysis ReNcells cultured on the material surface after 2 days of expansion and 7 days of differentiation were loaded for 45 min with 5 µM Fura-2/AM (Invitrogen) and 0.02% pluronic acid F-127 (Invitrogen) in Krebs solution (132 mM NaCl, 4 mM KCl, 1.4 mM MgCl2, 1 mM CaCl2, 6 mM glucose, 10 mM HEPES, pH 7.4), in an incubator with 5% CO2 and 95% atmospheric air at 37◦C. After a 5 min postloading period at RT in Krebs solution without Fura-2/AM and pluronic acid, to obtain a complete hydrolysis of the probe, the dish was mounted on

an inverted microscope with epifluorescent optics (Axiovert 135TV, Zeiss) equipped with a xenon lamp and band-pass filters of 340 and 380 nm wavelengths. Cells were continuously perfused with Krebs solution and stimulated at defined periods of time by applying high-potassium Krebs solution (containing 50 mM KCl, isosmotic substitution with NaCl) and 100 µM histamine. Throughout the experiments, the cells were continuously superfused at 1.5 mL/min with physiological solution. KCl and histamine were applied focally through a drug filled micropipette placed under visual guidance. Image pairs obtained every 200 ms by exciting the preparations at 340 and 380 nm were taken to obtain ratio images. Excitation wavelengths were changed through a high-speed wavelength switcher, Lambda DG-4 (Sutter Instrument, Novato, CA, United States), and the emission wavelength was set to 510 nm. Image data was recorded with a cooled CCD camera (Photometrics CoolSNAP fx) and processed and analyzed using the software MetaFluor (Universal Imaging, West Chester, PA, United States). Regions of interest were defined manually over the cell profile. KCl and histamine peaks given by the normalized ratios of fluorescence at 340/380 nm, at the proper time periods, were used to calculate the ratios of the responses. Microscopy Fluorescence images were recorded using an LSM 880 confocal microscope or an Axiovert 200 inverted widefield fluorescence microscope (both from Carl Zeiss Inc., Göttingen, Germany), with a 40x objective. Images were recorded using the softwares ZEN 2.1 (black edition) or AxioVision 4 (both from Carl Zeiss Inc.).

Chapter III: Results

III.1 Research strategy

The aim of this project was to find a suitable conductive substrate for NSCs growth and differentiation. Different materials combinations and shapes (both 2D and 3D) were tested in order to find the best manufacturing process and condition. In this study, 2D structures were prepared by spin coating, while 3D structures referes to electrospun fibrous mesh. Threfore, a 3D structure has a thin thickness, with porosity given by the spaces between the fibers, and the three-dimensionality is provided by different layers of fibers.

First, physical properties of the materials were studied: substrates were assessed to be stable in cell culture conditions, and electrical conductivity was checked for its importance in the stimulation of the cells. For the 3D scaffolds, an examination with SEM was fundamental to determine the microscopic morphology of the samples.

Then, biocompatibility was assessed with fibroblasts L929 cell line: indirect and direct cytotoxicity assays, cells culture on the materials, cells viability assays and staining were performed to characterize the biological response to the materials. Finally, the substrate which obtained the best performances related to biocompatibility and electrical conductivity, was chosen for the culture and the differentiation of NSCs. The effect of the electrical stimulation on the cells was determined through the expression of neural markers, cell morphology and presence of voltage-dependent channels.

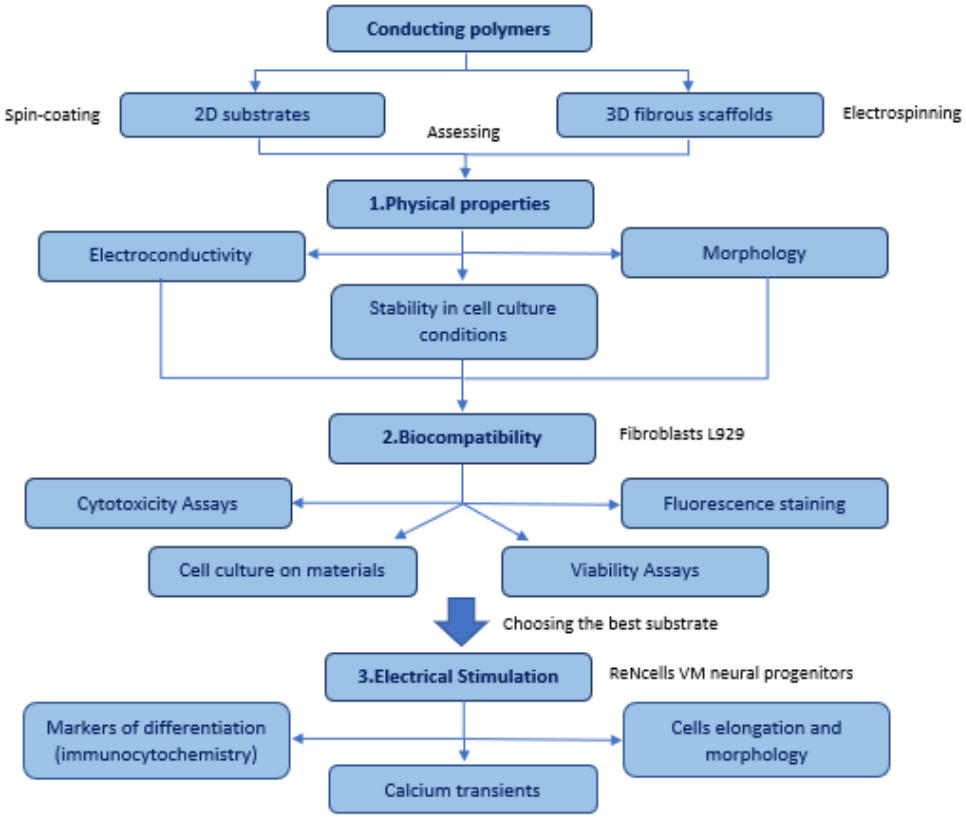

Figure 25. Scheme of the research strategy followed in this project

III.2 2D PEDOT:PSS films

PEDOT:PSS films alone and with both GOPS and DVS crosslinking methods were successfully obtained through spin coating technique. Samples were transparent and with an average thickness of 80 nm.

III.2.1 Conductivity measurements

Conductivity was measured by 4 probe-method. First, samples were coated with four gold stripes in order to have four different channels for the measurements. Then, four probe-setup was connected to the sample with silver glue (conductive), as shown in Fig.26.

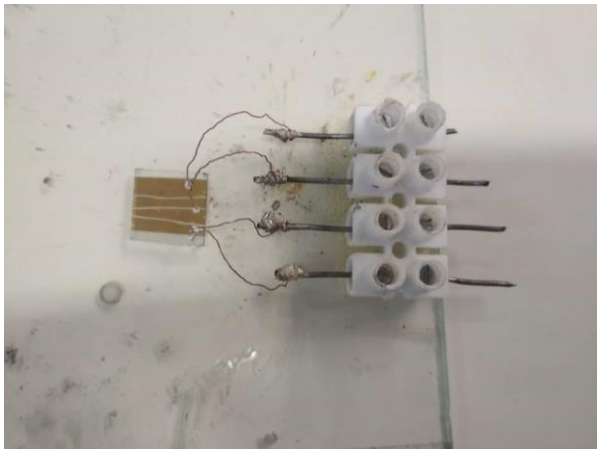

Figure 26. 4-probe set-up assembled in our laboratories.

Currents values ranging from ±0.1 μA to ±50 μA were applied to the external channels, while the corresponding voltage was measured by the internal electrodes. Every couple of values was used to build a straight line and calculate the slope, that corresponds to the electrical resistance R. Calculated values of resistance, resistivity and conductivity are reported in Table 6.

	PEDOT:PSS Clevios	PEDOT:PSS + DBSA + GOPS	PEDOT:PSS + DBSA + DVS	PEDOT:PSS + DBSA + GOPS + DVS
Cross-section [m^2]	4.95×10^{-7}	6.41×10^{-7}	7.2×10^{-7}	6.2×10^{-7}
Resistance [kΩ]	2.8×10^{3}	0.8	0.0031	0.67

Resistivity ρ [Ω*m]	4.1	1.6×10^{-3}	6.5×10^{-6}	1.2×10^{-3}
Conductivity σ [$\Omega^{-1} * m^{-1}$]	2.4×10^{-1}	6.18×10^{2}	9.57×10^{4}	8.03×10^{2}

Table 6. Conductivity measurements on PEDOT:PSS films.

As conductivity values of PEDOT:PSS crosslinked with only GOPS or only DVS were the higher, only these two samples were selected for the subsequent tests. Conductivity measurements were repeated after poly-ornithine and laminin coating, essential for neural stem cells adhesion on the materials; results are shown in Table 7.

Material	Coating		Resistance	Conductivity
Glass coverslip	Poly-ornithine laminin	+	7141.6 kΩ	5.15×10^{-4} S/m
PEDOT:PSS:GOPS film	Poly-ornithine laminin	+	3.06 kΩ	5.84 S/m
PEDOT:PSS:DVS film	Poly-ornithine laminin	+	5.32 kΩ	5.24 S/m

Table 7. Conductivity measurements after poly-ornithine and laminin coating.

III.2.2 Stability test

The morphology of all the films was intact after 2 weeks in MilliQ water: none of the samples was deteriorated or swelled. After two weeks, water from an empty well was compared to the water that stayed in contact with the films by absorbance analysis from 230 nm to 900 nm. Duplicates were considered for each film. Results of the spectrum are in Graph 1.

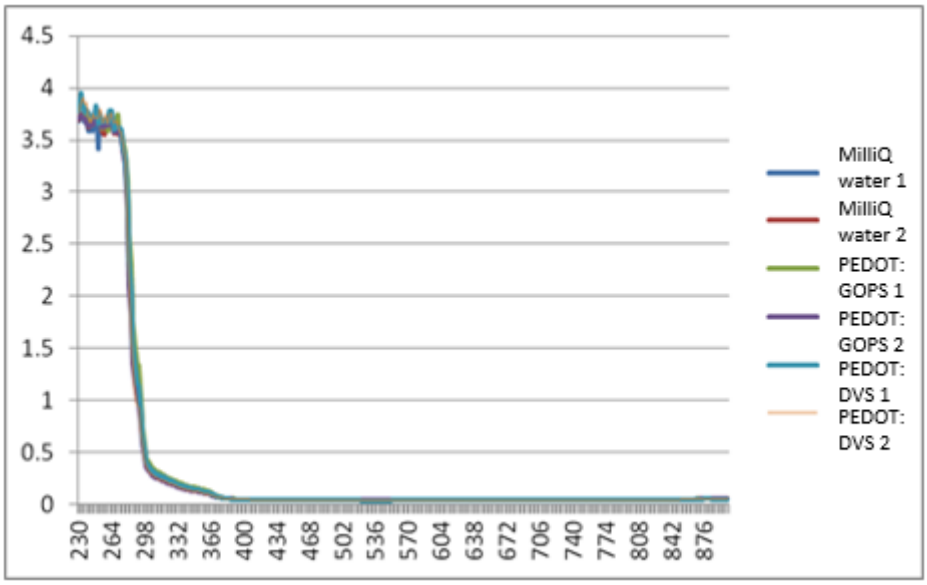

Graph 1. Results of stability test with absorbance analysis. The MilliQ water where samples were immersed for 2 weeks presents the same profile of pure MilliQ.

Samples were also left in culture medium (DMEM + 10% FBS) for 2 weeks to check the possibility of material deterioration or swelling. None of these two fenomena was reported (same thickness of 80±5nm was measured).

III.3 3D scaffolds

III.3.1 PEDOT:PSS:PVP fibers

III.3.1.1 Morphology

Fibers of PEDOT:PSS blended with PVP were successfully electrospun with a flow rate of 0.3mL/h, an applied voltage of 30 kV and a distance spinneret-collector of 14cm. Fibers were obtained with few defects, with a regular morphology and with diameter homogeneity, as shown in Fig.27.

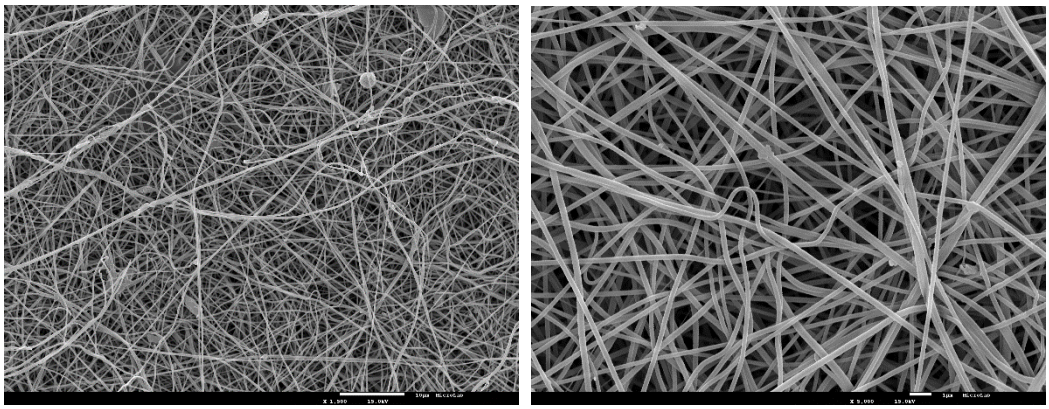

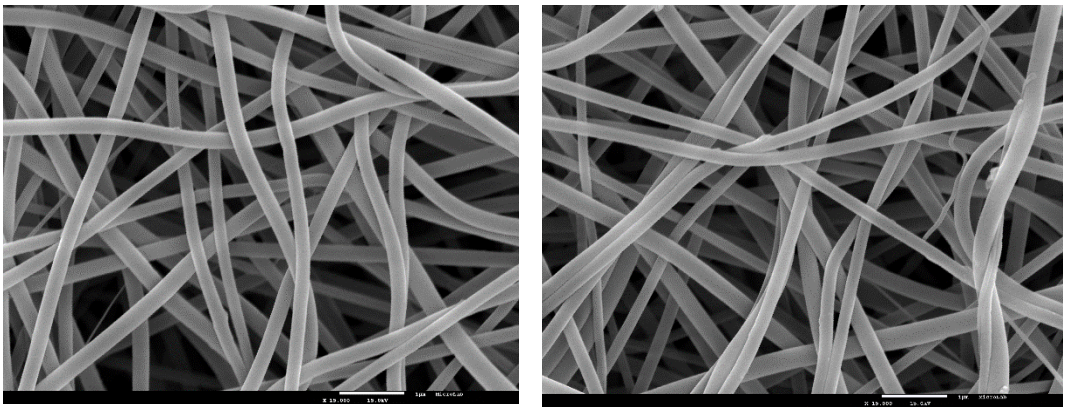

Figure 27 PEDOT:PSS blended with PVP fibers. *Up left: 1500x magnification. Up right: 5000x magnification. Bottom: 15000x magnification.*

Diameter size was calculated with the software ImageJ: average value of 225±0.05 nm was reported for these conditions. Diameter size distribution is shown in Graph 2.

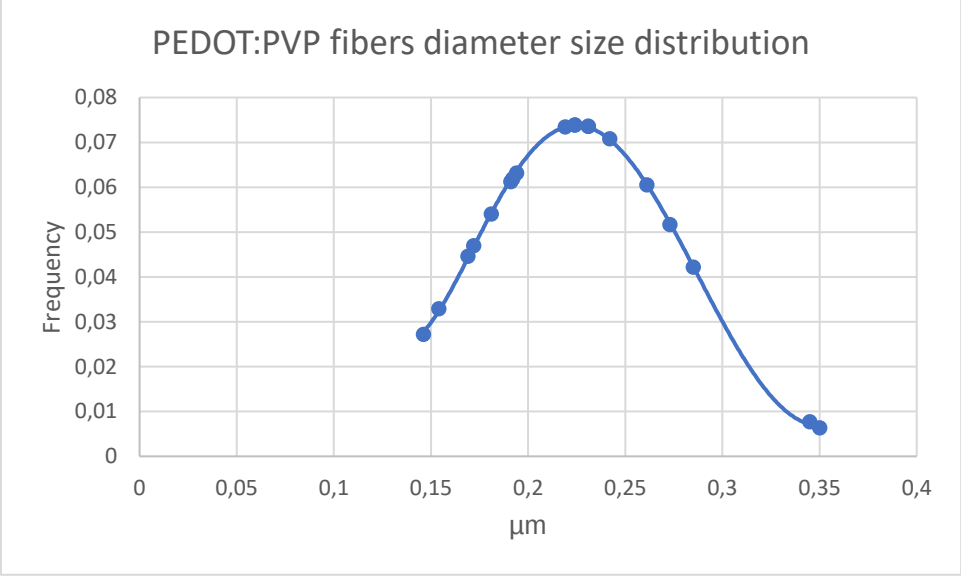

Graph 2. PEDOT:PVP fibers diameter size distribution

III.3.1.2 Stability tests

PEDOT:PSS blended with PVP fibers were immersed in MilliQ water for 2 weeks. After 2 weeks, fibers were completely dissolved. For this reason, the stability test in culture medium was never tried.

III.3.1.3 Conductivity measurements

Samples of fibers were successfully coated with four golden stripes with physical vapor deposition, in order to measure the conductivity. However, the measurement was never obtained through 4 probe-method set-up, as the resistance of the fibers was too high, and was impossible for the instrument to record a potential difference while applying a current.

III.3.2 PEDOT:PSS fibers

Fibers made only with PEDOT:PSS solution were never obtained, because of the low viscosity of the tested solution.
The first tested solutions were the ones obtained with the two crosslinking methods described at section II.1.3. As the crosslinking process decreases the solubility of PEDOT:PSS in water, these two treatments were chosen to obtain fibers stable in water. Viscosity measurements are reported in Table 8.

Solution	Viscosity	Electrospinnability
PCL (reference)	3000 cP	Yes
PEDOT: PSS	7 cP	No
PEDOT:PSS + GOPS	10.2 cP	No
PEDOT:PSS + DVS	11.7 cP	No

***Table 8**. Viscosity measurements on PEDOT:PSS solutions.*

A second test was carried on adding increasing concentrations of sorbitol to solution crosslinked with GOPS. Again, no sufficient viscosity increase was reached.

Solution	Viscosity	Electrospinnability
PEDOT:PSS + GOPS + 1% Sorbitol	8.7 cP	No
PEDOT:PSS + GOPS + 5% Sorbitol	10.8 cP	No
PEDOT:PSS + GOPS + 10% Sorbitol	28.4 cP	No
PEDOT:PSS + GOPS + 20% Sorbitol	82.3 cP	No

Table 9. Viscosity measurements on PEDOT:PSS solution with increasing concentration of Sorbitol.

Then, physical treatments to evaporate water content in PEDOT:PSS commercial solution were carried on in order to check viscosity increase. Trough lyophilization treatment, a powder was not obtained as PEDOT:PSS was retaining some water molecules. Rotavapor treatment only evaporated 1% water content after 24 hours.

Treatment	Viscosity	Electrospinnability
PEDOT:PSS after Rotavapor	10.3 cP	No

Table 10. Viscosity measurements on PEDOT:PSS solution after Rotavapor

With RapidVap technique, a more concentrated solution of PEDOT:PSS was obtained: after 1 hour and 30 minutes of treatment, the concentration of the solution increased from 1.3 % w/w to 2.18%, and after 2 hours and 30 minutes reached 3.9%. PEG300 was also added after the treatment, as viscosity enhancer. Results are in Table 11.

Treatment	Viscosity	Electrospinnability
PEDOT:PSS after RapidVap (1h 30min)	26.7 cP	No
PEDOT:PSS after RapidVap (2h 30min)	?	No
PEDOT:PSS + 25% PEG300	7.7 cP	No
PEDOT:PSS after RapidVap (1h 30min) + 25%PEG300	27.6 cP	No
PEDOT:PSS after RapidVap (2h 30min) + 25%PEG300	335.6 cP	No

Table 11. Viscosity measurements on PEDOT:PSS solutions after RapidVap treatment

III.3.3 PEDOT:PSS coating onto electrospun fibers

III.3.3.1 PBI fibers Morphology

PBI fibers were successfully electrospun. The morphology, observed both with SEM (Fig. 28) and optical microscope (Fig.29), is regular and homogeneous, with an average diameter of 118.5±0.03 nm, calculated with ImageJ; the distribution of the diameter size is reported in Graph 3.

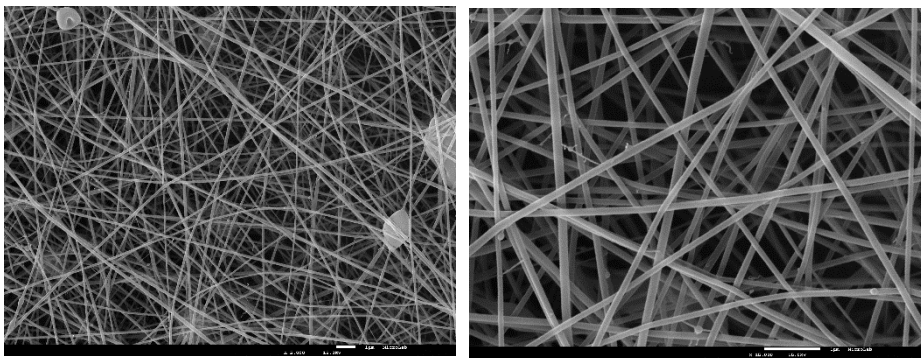

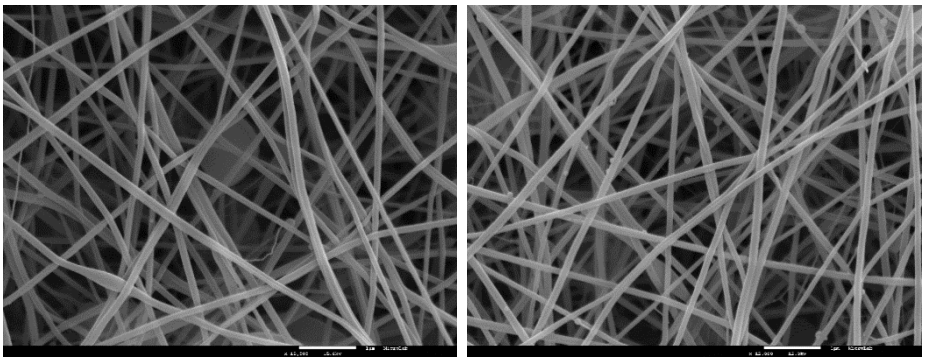

Figure 28. SEM pictures of PBI fibers with a magnification of 5000x (up left) and 15000x (up right, bottom left and right)

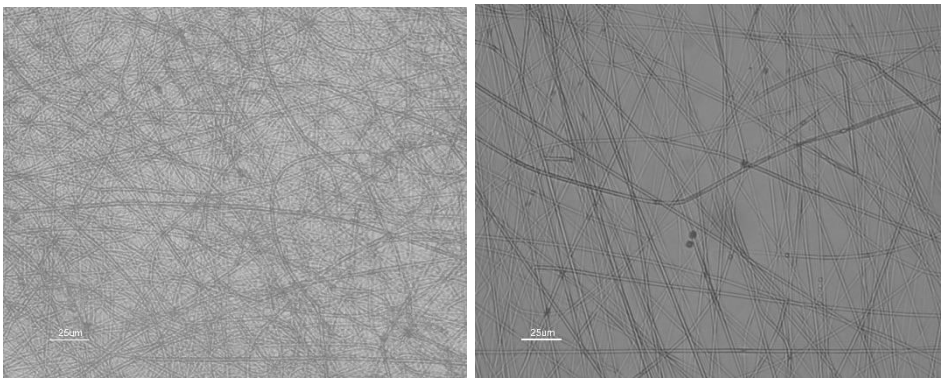

Figure 29 PBI fibers with a magnification of 40x (optical microscope). Left: random fibers obtained with flat collector; Right: aligned fibers obtained with parallel plate collector.

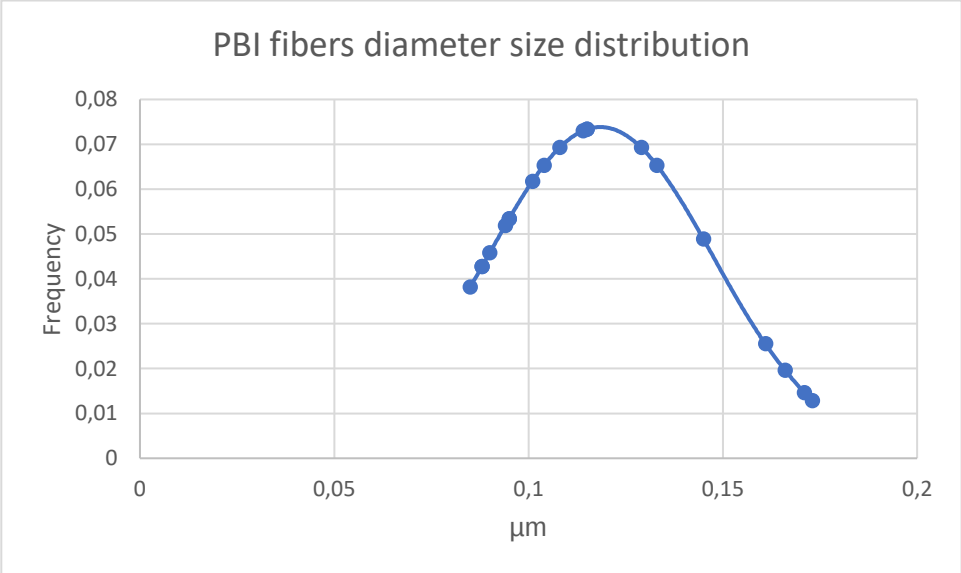

Graph 3. Diameter size distribution of PBI fibers.

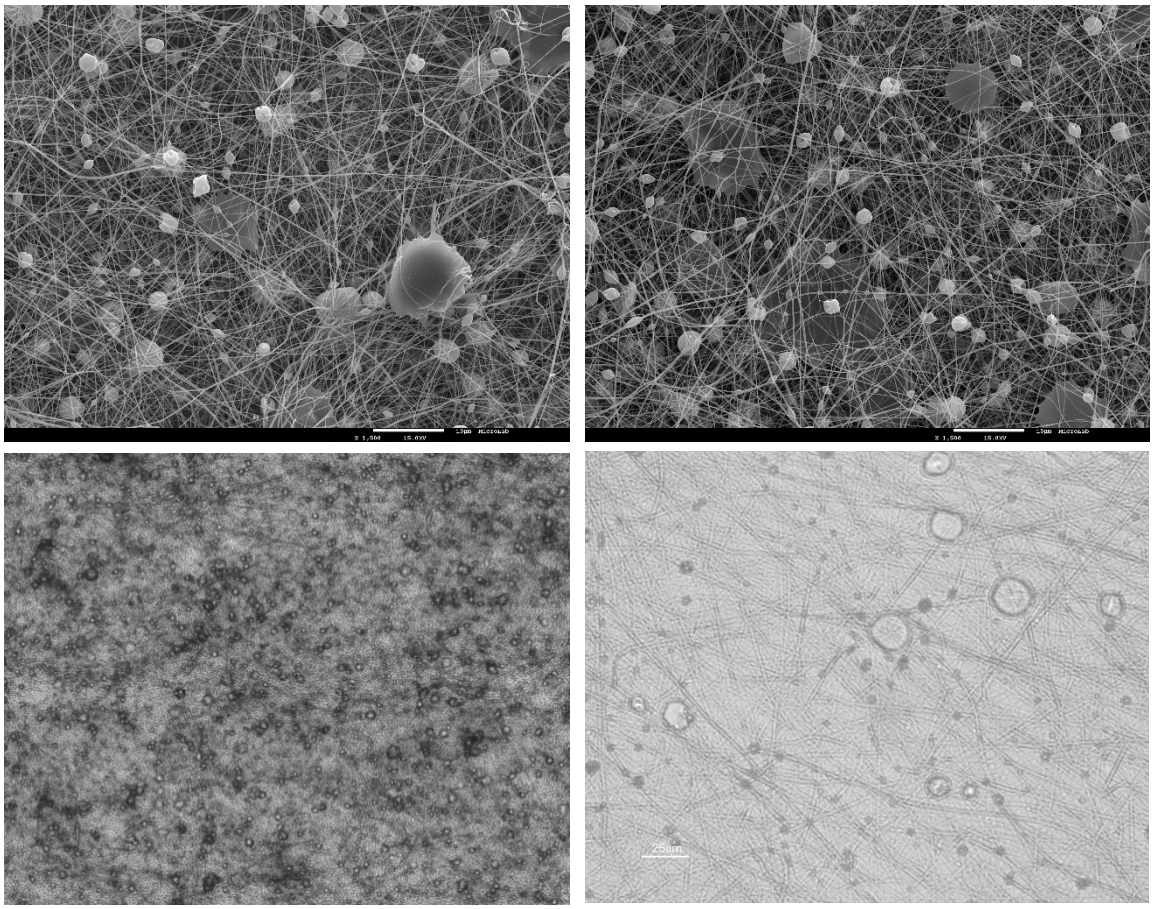

Figure 30. PBI fibers electrospun with humidity lower than 50% (less than 30% for the SEM pictures above, less than 40% for the optical microscope pictures below).

Humidity revealed to be a crucial parameter for the manufacture of PBI fibers, consistently reducing the amount of defects; results of electrospinning performed with a lower humidity are reported in Fig.31.

Additional tests were also performed on PBI fibers to assure the total solvent removal: PBI fibers were put in a desiccator with vacuum for 3 hours, then were washed with MilliQ water; other fibers were instead heated up to 160°C and then washed again with MilliQ water. An absorbance scan was then performed on the water after the two treatments and on fresh MilliQ water, for comparisons: results are in Graph 4.

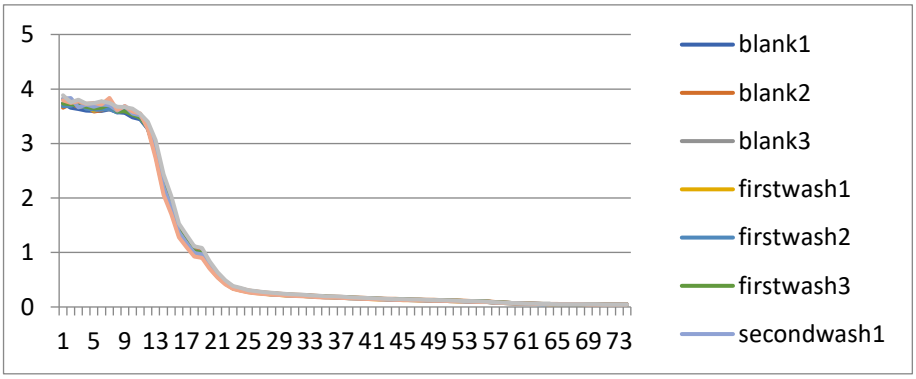

***Graph 4. Absorbance scan on the MilliQ water after the treatments performed onto PBI fibers, compared to normal MilliQ water (blank**). Firstwash = samples that stayed in vacuum for 3 hours and then were washed with water; Secondwash= samples that received also a Ttreatment at 160°C and were then washed again. Results are shown in triplicates.*

Samples after T treatment were also observed with SEM microscope to assess the increase or decrease of defects; pictures are in Fig.31.

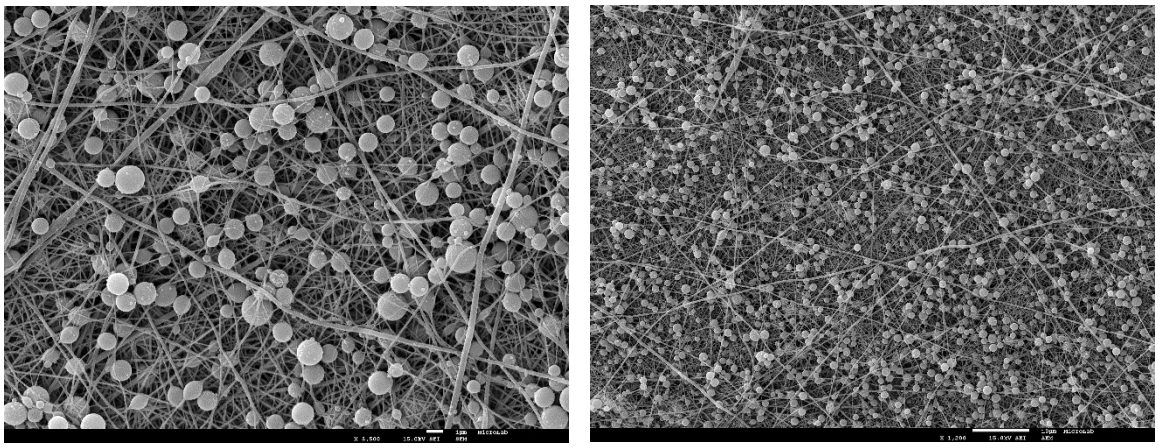

Figure 31 PBI fibers after being heated on hot plate at 160°C.

III.3.3.2 PCL fibers Morphology

Optical and SEM microscope images of electrospun PCL random fibers are reported in Fig.32. Fibers' morphology is homogeneous, with few defects and regular diameter of 1.75±0.32 µm average size; distribution of size diameter is reported in Graph 5.

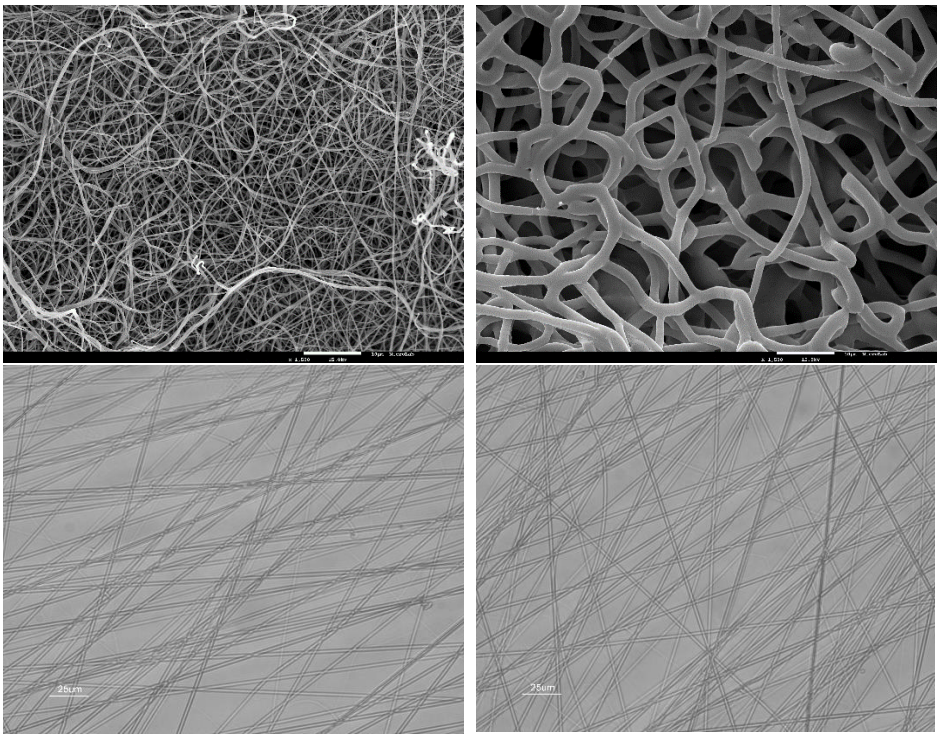

.Figure 32 PCL random fibers with SEM microscope (up left: magnification of 5000x; up right: magnification of 15000x) and optical microscope 8bottom, magnification 40x), obtained with flat collector.

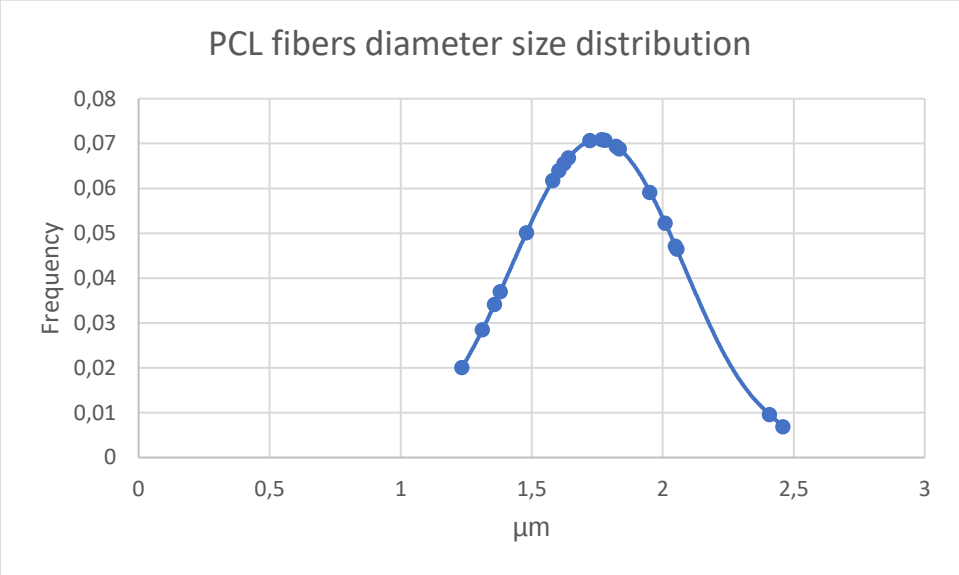

Graph 5. Diameter size distribution of PCL fibers.

High alignment of fibers was also obtained with this material, with parallel plate collector, as reported in Fig.33.

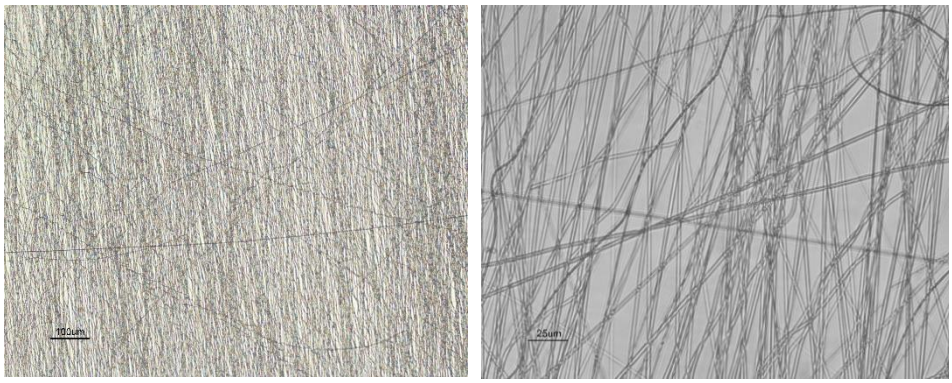

Figure 33 PCL aligned fibers seen with optical microscope (left: 100x; right: 400x).

III.3.3.3 PVA fibers Morphology

The last tested polymer for the manufacture of fibers was PVA. Also PVA fibers showed a regular morphology, as seen with optical microscope, both in random (Fig.34) and in aligned (Fig.35) configuration, with and average diameter of 1.597±0.28 µm, as reported in Graph 6.

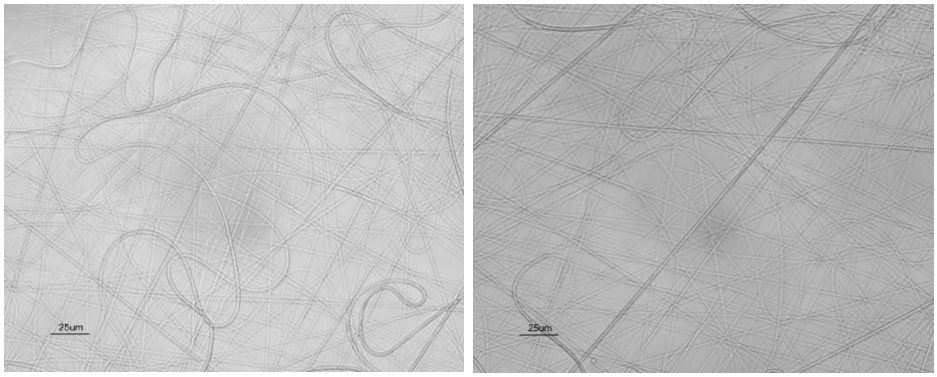

Figure 34. PVA random fibers with optical microscope, magnification of 400x.

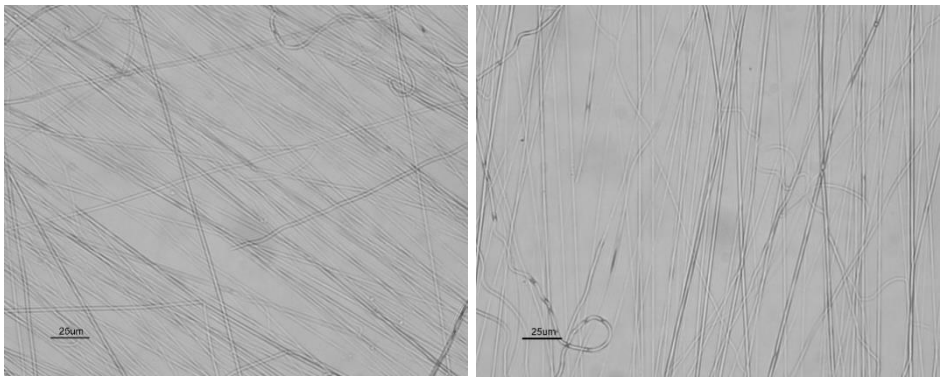

Figure 35 PVA aligned fibers with optical microscope, magnification of 400x.

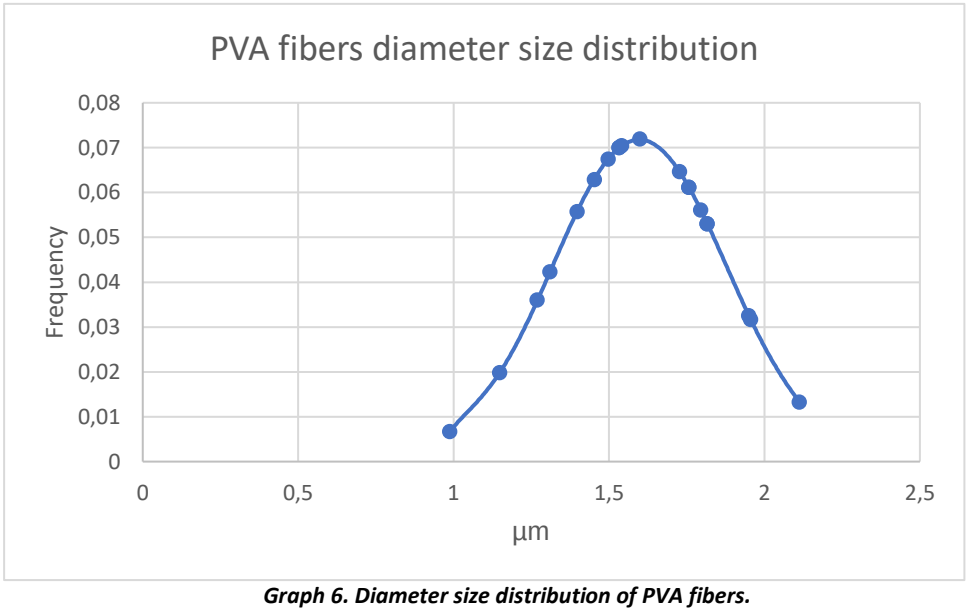

Graph 6. Diameter size distribution of PVA fibers.

A critical parameter for the PVA electrospinning was determined to be the combination of high spinneret-collector distance and low applied voltage: in the opposite case, fibers with many defects were obtained (Fig.36: Distance: 8 cm; V: 20 kV).

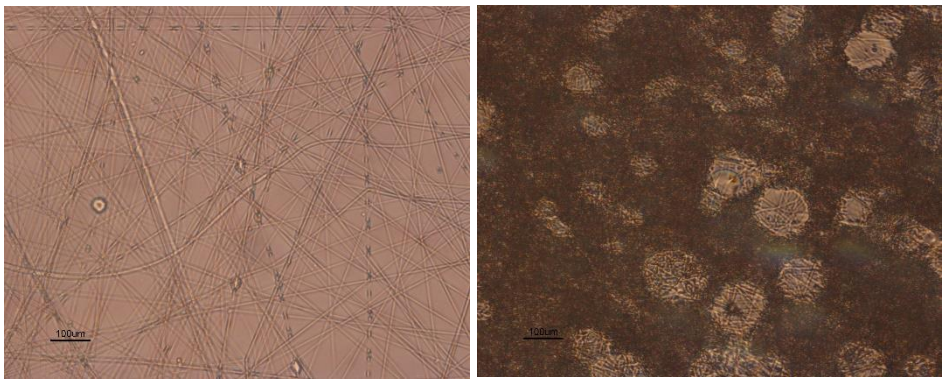

Figure 36. PVA fibers electrospun with a spinneret collector distance of 8 cm, an applied voltage of 20 kV, and a flow rate of 0.8 mL/h)

III.3.3.4 PEDOT:PSS coating

Different coatings were tested in order to optimize the results, both in terms of chemical crosslinkers composition and in terms of coating deposition. Three different coating strategies were tested on the same PBI fibers, to understand which process leads to coating uniformity and stability: a solution of PEDOT:PSS crosslinked with GOPS (see section II.1.3) was prepared to realize the three different treatments. In the first case, the solution was spin coated directly onto the PBI fibers; in the second case the fibers were dip several times into the solution and in the last case, the fibers were left immersed in the solution for 24 hours. All treatments were followed by annealing process after, with the conditions described in section 1.4. EDS analysis, during SEM microscope observation, was used to determine in which case the peak of Sulfur, main element of PEDOT:PSS chemical structure, was higher on the analyzed surface. Results of SEM and EDS are in Fig.37.

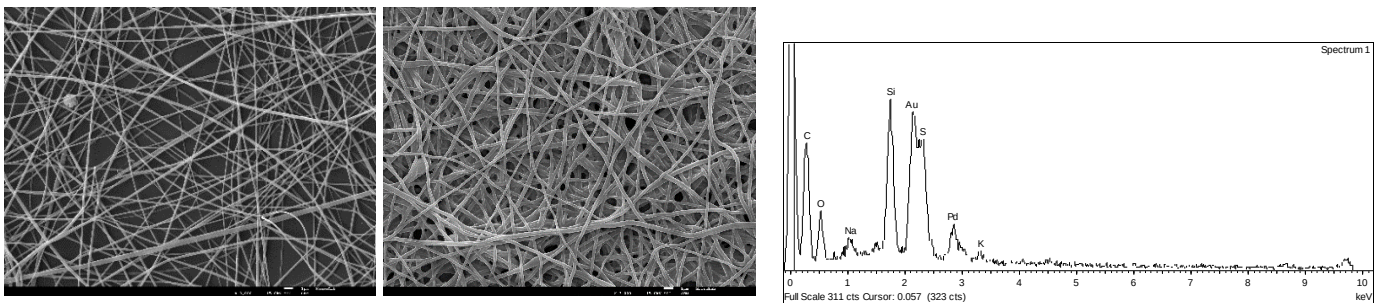

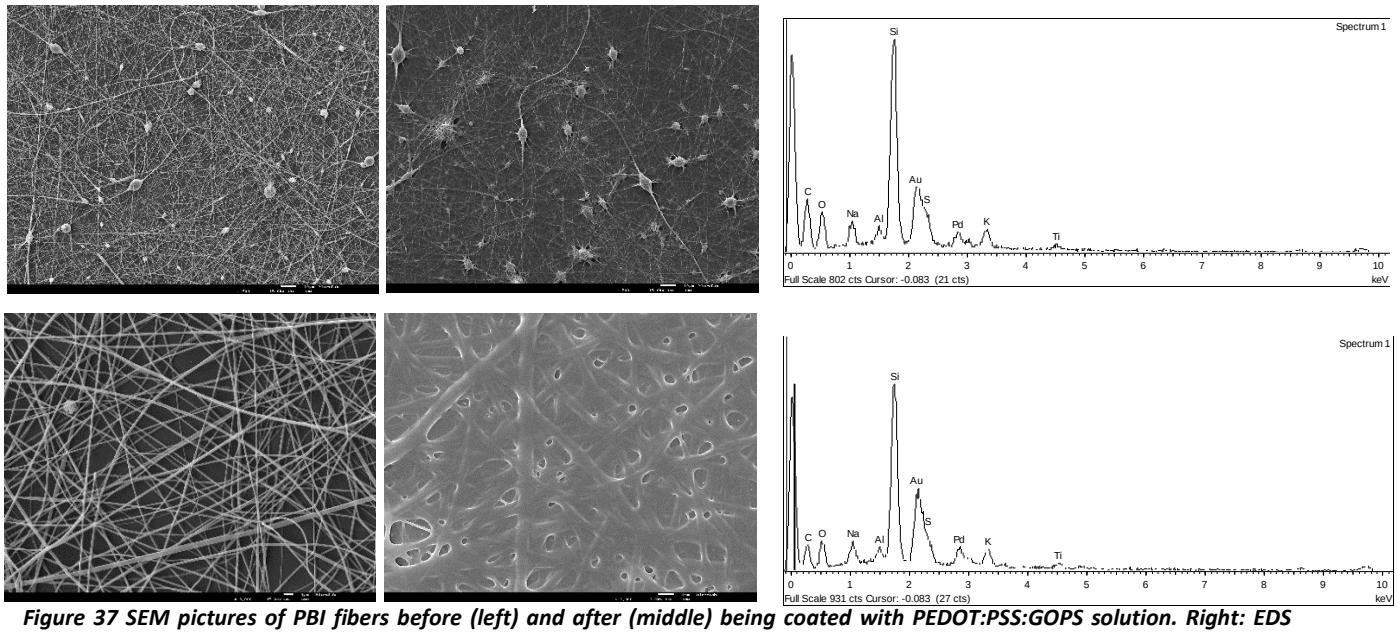

Figure 37 SEM pictures of PBI fibers before (left) and after (middle) being coated with PEDOT:PSS:GOPS solution. Right: EDS analysis on the coated fibers. Up: coating obtained subemerging the fibers in the solution for 24h; Middle: coating obtained dipping the fibers in the solution; Bottom: PEDOT solution has been spin coated onto the fibers

.

In all three cases the diameter of the fibers is increased after coating. The peak of Sulfur was reported for all the three treatments. However, in the case of the spin coating, the process itself caused a loss in the 3D shape of the scaffold, generating a uniform layer of PEDOT:PSS in which few fibers are visible. For this reason, the treatment was discarded as coating procedure.

For the other two treatments, a second EDS analysis was repeated after keeping the coated fibers for two weeks in water, as a stability test on the coating. Results are in Fig.38.

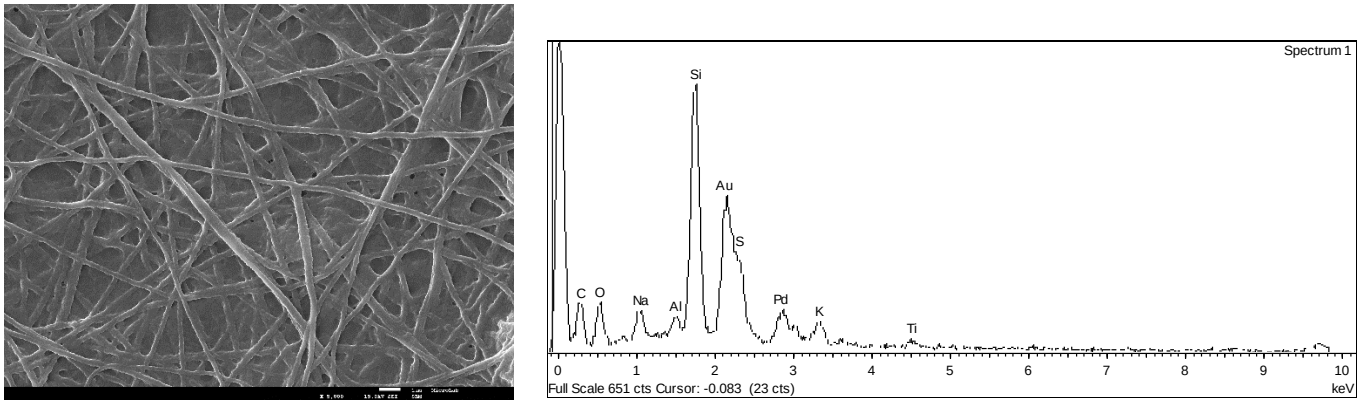

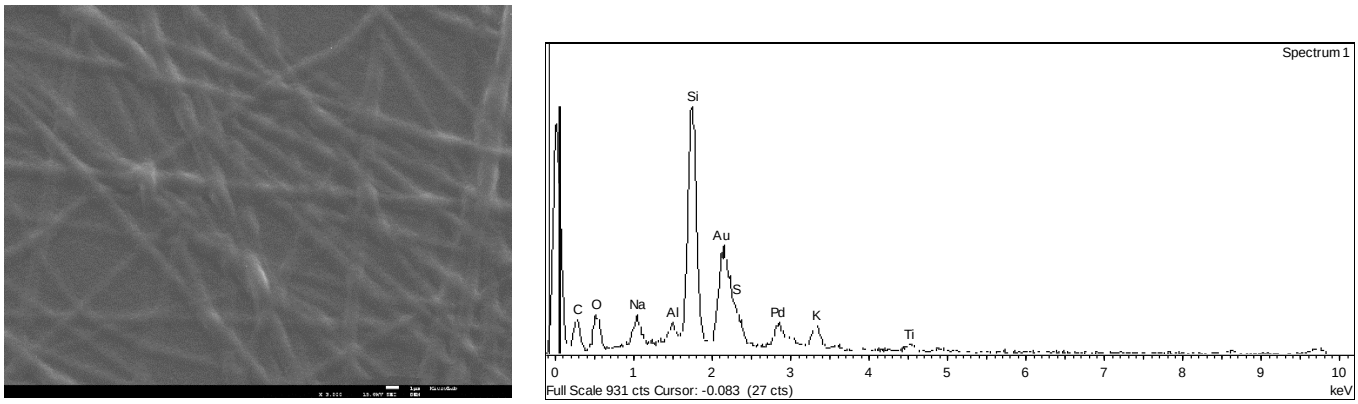

Figure 38. SEM pictures of PBI fibers with PEDOT:PSS:GOPS coating after two weeks in water (left) and subsequent EDS analysis (right). Up: coating obtained subemerging the fibers in PEDOT solution for 24h; bottom: coating obtained dipping the fibers in PEDOT solution.

On the sample where the coating was obtained dipping the fibers for several times in the crosslinked PEDOT:PSS solution, the peak of Sulfur was greatly reduced, in comparison to the one where the fibers were left in contact with the solution for 24 hours. For this reason, also this treatment was discarded.

PBI fibers with PEDOT:PSS crosslinked with GOPS were also imaged with SEM in the cross-section, in order to see the fibers throughout the thickness (Fig.39), to assess if the coating was only superficial or was covering also deeper fibers. Thickness size distribution is reported in Graph 7.

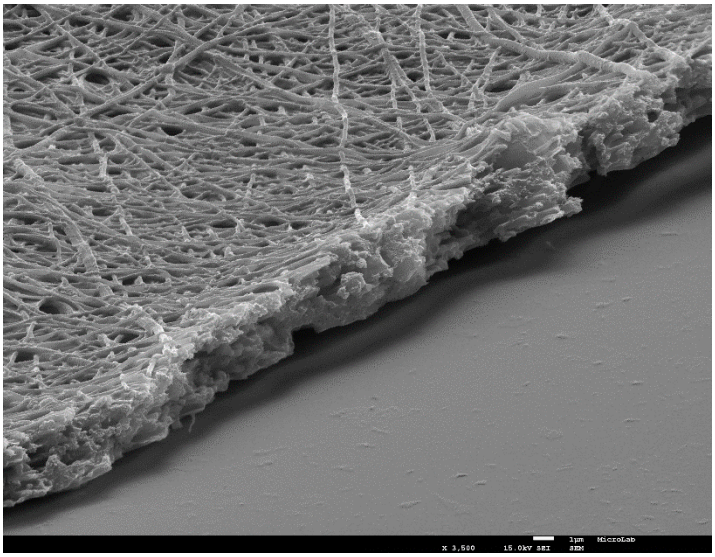

Figure 39 SEM picture of the cross section of PBI fibers coated with PEDOT:PSS + GOPS solution.

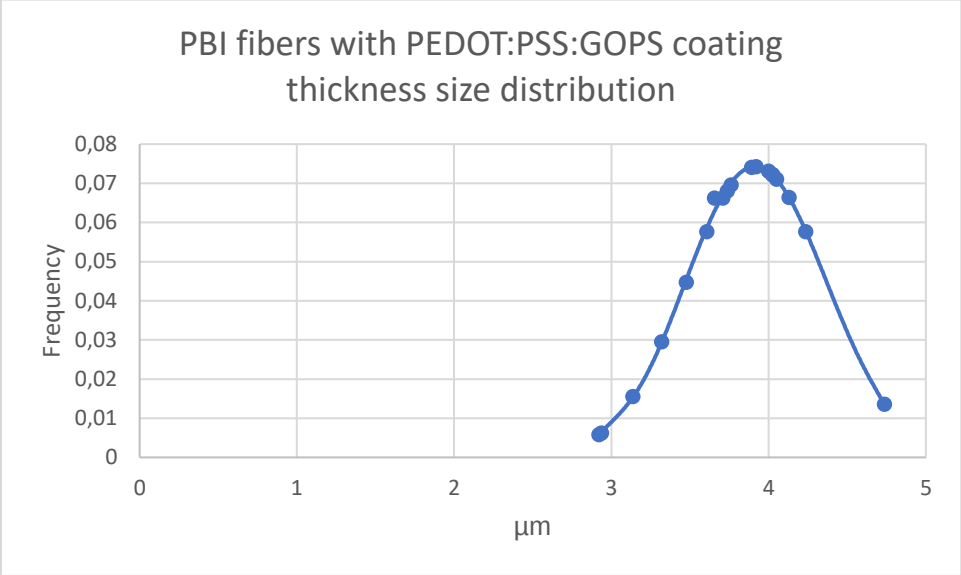

Graph 7. Thickness size distribution of PBI fibers coated with PEDOT:PSS solution crosslinked with GOPS.

The diameter size of the fibers after the coating was calculated with ImageJ and resulted to be 243±0.05 nm average (Graph 8).

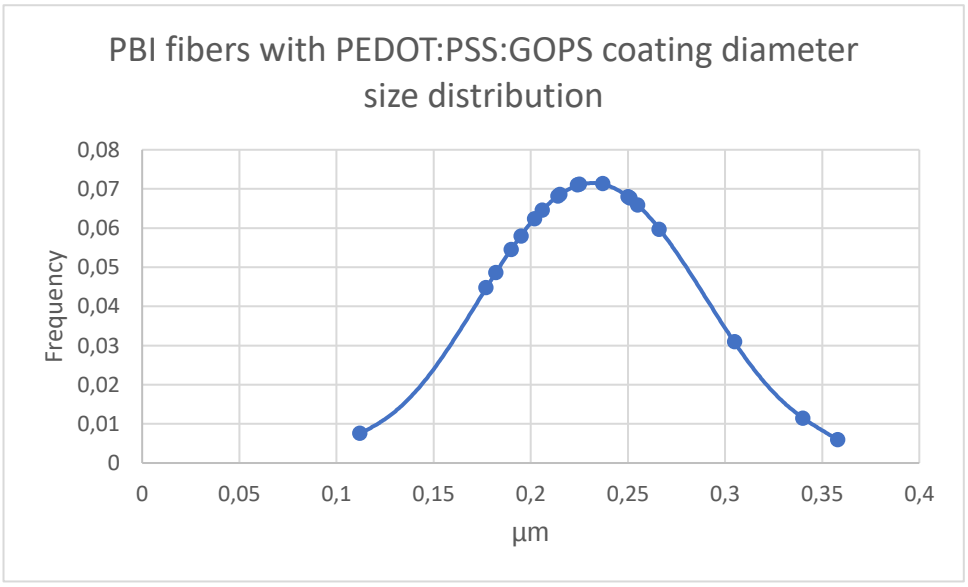

Graph 8. Diameter size distribution of PBI fibers coated with PEDOT:PSS solution crosslinked with GOPS.

The coating obtained after 24 hours immersion in the solution was chosen as the best and tested also on the fibers realized with PVA and PCL. On both type of fibers, the coating failed: PCL fibers didn't survive to the annealing treatment, because of the high temperature that melted the material, while PVA fibers totally dissolved in the PEDOT:PSS crosslinked solution.

III.3.3.5 Conductivity measurements on PEDOT:PSS coated fibers

Conductivity measurements were carried on with 4 probe-method; results are reported in Table 12. Conductivity values were calculated also after a poly-ornithine and laminin coating, essential for the adhesion of neural progenitor cells.

Material	Coating	Conductivity
PBI fibers	No	6.99×10^{-5} S/m
PCL fibers	No	-
PVA fibers	No	-
PBI fibers	PEDOT:PSS + GOPS	9.7 S/m
PBI fibers	PEDOT:PSS + DVS	4.1 S/m
PBI fibers	PEDOT:PSS:GOPS + laminin	0.89 S/m
PBI fibers	PEDOT:PSS:DVS - laminin	0.84 S/m

Table 12. Conductivity values calculated with 4-probe method.

III.3.3.6 Stability in cell culture conditions

Samples of PBI fibers coated with PEDOT:PSS solutions were left in culture medium in the incubator (37°C) for two weeks. Morphology of the samples after two weeks was investigated with optical microscopy (Fig.40).

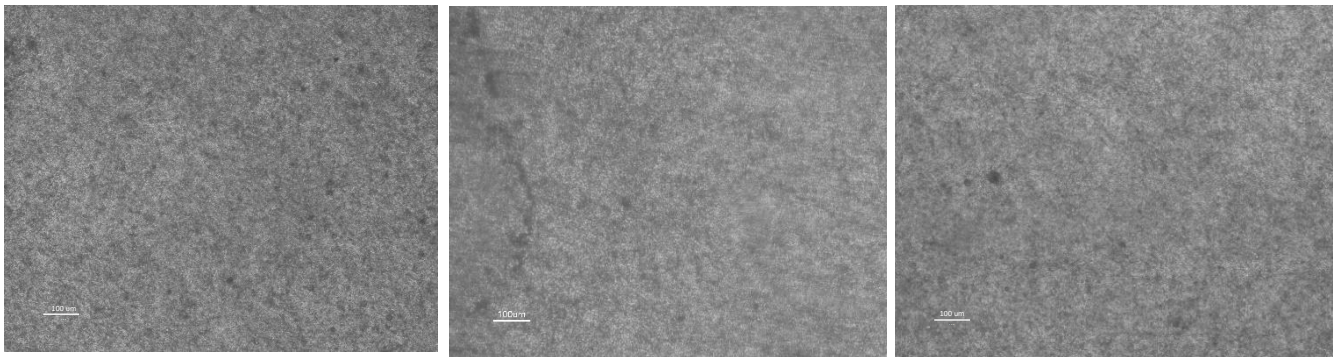

Figure 40 PBI fibers with PEDOT:PSS + GOPS coating. Picture 1: day 0. Picture 2: after 7 days in culture medium at 37°C. Picture 3: after 15 days in culture medium at 37°C.

EDS analysis after 10 days in culture medium, already performed on PEDOT:PSS coating crosslinked with GOPS, was repeated on PEDOT:PSS coating crosslinked with DVS to assess its stability in cell culture conditions (Fig.41).

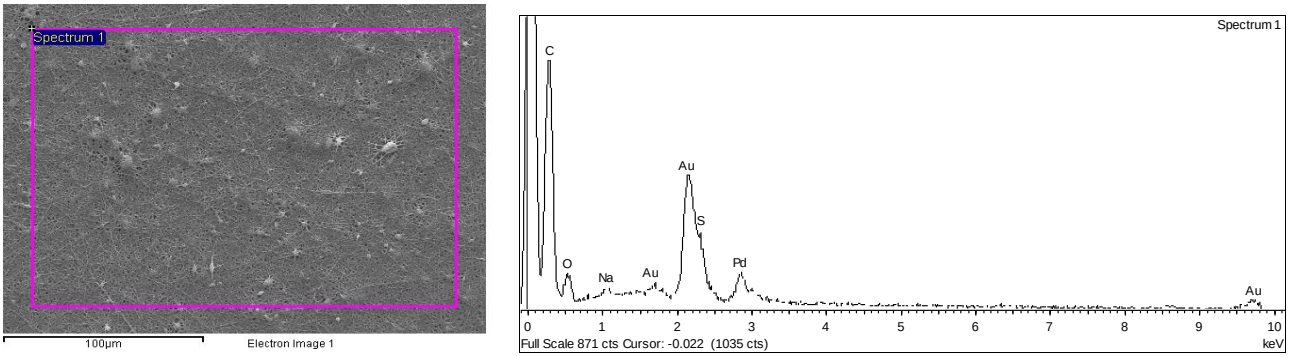

Figure 41 EDS analysis on PBI fibers coated with PEDOT:PSS solutions crosslinked with DVS after 10 days in culture medium.

Samples were also tested for the sterilization: first, a treatment of 1 hour and 30 minutes with UV light was performed, followed by two days immersion in a solution of Antibiotic/Antimicotic 1% in PBS. Results are shown in Fig.42.

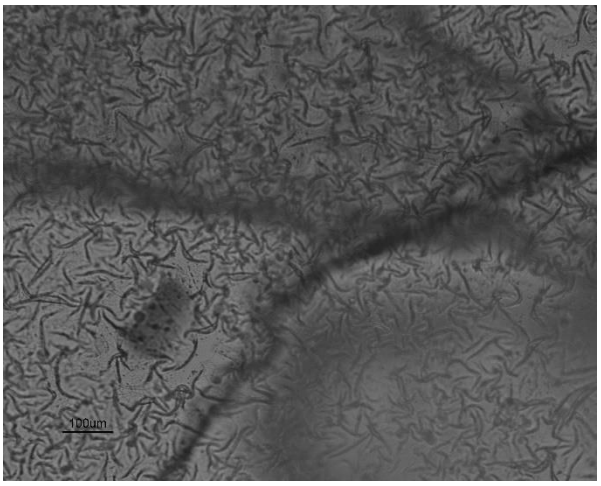

Figure 42 PEDOT:PSS + GOPS coating after sterilization with UV treatment + two days in 1% Anti/Anti solution

The appearance of the coating was different compared with the morphology before the treatment: the coating seemed wrinkled and detached from the fibers. This treatment was so discarded, and the following sterilizations were carried on without UV light treatment.

III.3.3.7 3D-printed frame

SEM pictures of the PBI fibers electrospun on the 3D printed frame and coated with PEDOT:PSS crosslinked with GOPS are shown in Fig.43. Fibers show few defects and diameter homogeneity.

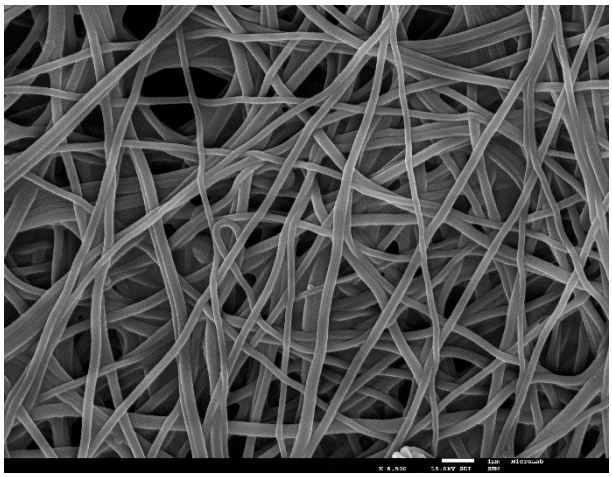

Figure 43 SEM pictures of PBI fibers with PEDOT:PSS crosslinked coating on 3D printed frame.

III.4 Biocompatibility Assessment

III.4.1 Cytotoxicity Assays

Cytotoxicity assays in vitro were performed according to the ISO 10993-5:2009(E) guidelines in order to assess the biocompatibility of materials. Materials were exposed directly and indirectly in contact to the cell culture system (L929 mouse fibroblast cell line), allowing the production of reproducible results. Cytotoxicity assays were carried on 3D scaffolds obtained with PBI fibers alone and PBI fibers coated with PEDOT:PSS crosslinked with GOPS or DVS. PBI fibers alone were tested after receiving 4 different treatments, to better characterize the biocompatibility of the material: staying in vacuum for 3 hours, washing, heating at 160°C and washing again. These tests were performed to assess if the materials were releasing toxic residues in culture medium after 24 hours (indirect assay) or if they were causing cell death by contact (direct assay).

III.4.1.1Indirect cytotoxicity

Fibroblasts L929 were seeded in a 24 well plate with a density of $8x10^4$ cells/cm^2 and left in the incubator for 24 hours, after which they reached confluency. Samples of PBI fibers were put in a 6 well plate and immersed in 2mL of culture medium; a piece of latex glove (positive control) was also left in culture medium. After 24 hours, the culture medium that stayed in contact with the materials was used to culture the cells for other 24 hours; a negative control was prepared with fresh culture medium in contact with cells. Pictures of the cells after the incubation with the liquid extracts of the material are shown in Fig.44.

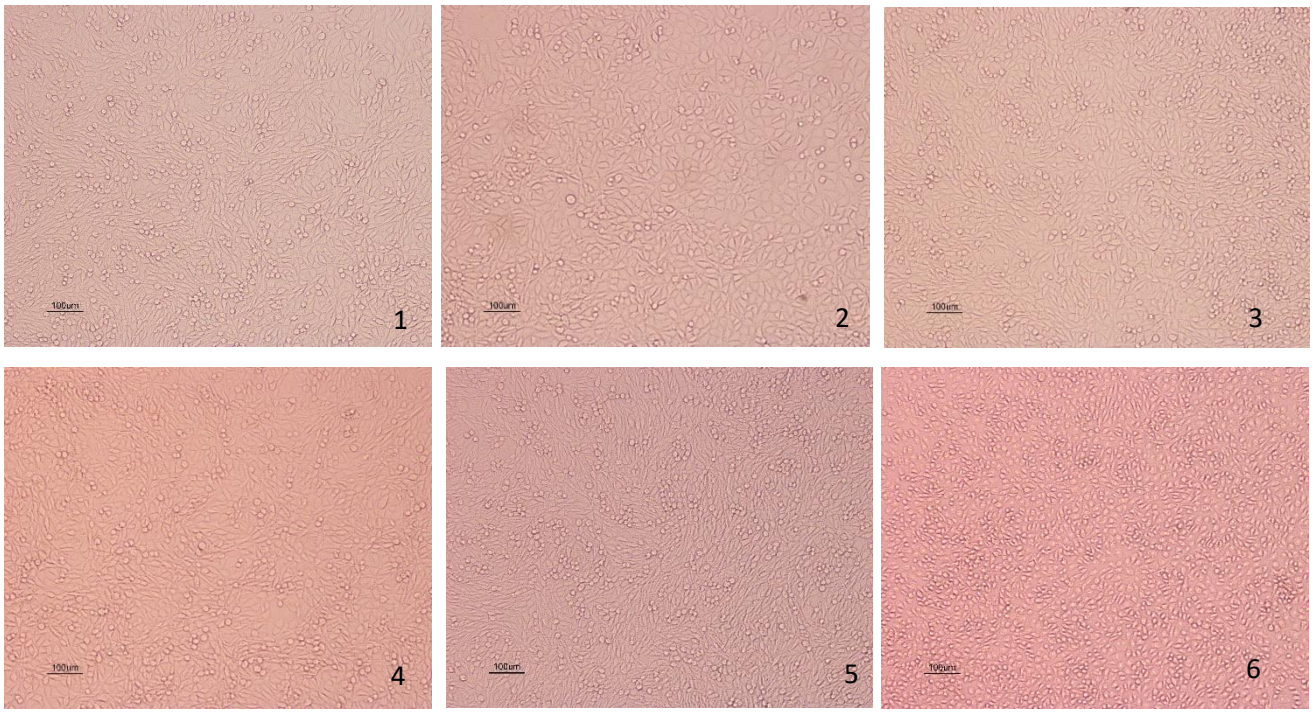

Figure 44 Indirect cytotoxicity assay performed on fibroblasts L929 cell line. Cell were incubated with eluates from PBI fibers after different treatments: vacuum for 3h (1), washing (2), T treatment at 160°C (3), and washing again (4). (5) reports the negative control (cells incubated with fresh culture medium) and (6) is the positive control (cells incubated with toxic latex glove).

At the end, MTT assay was performed on the cells to quantify cells viability. Regarding PBI fibers alone, results of MTT assay are shown in Graph 9.

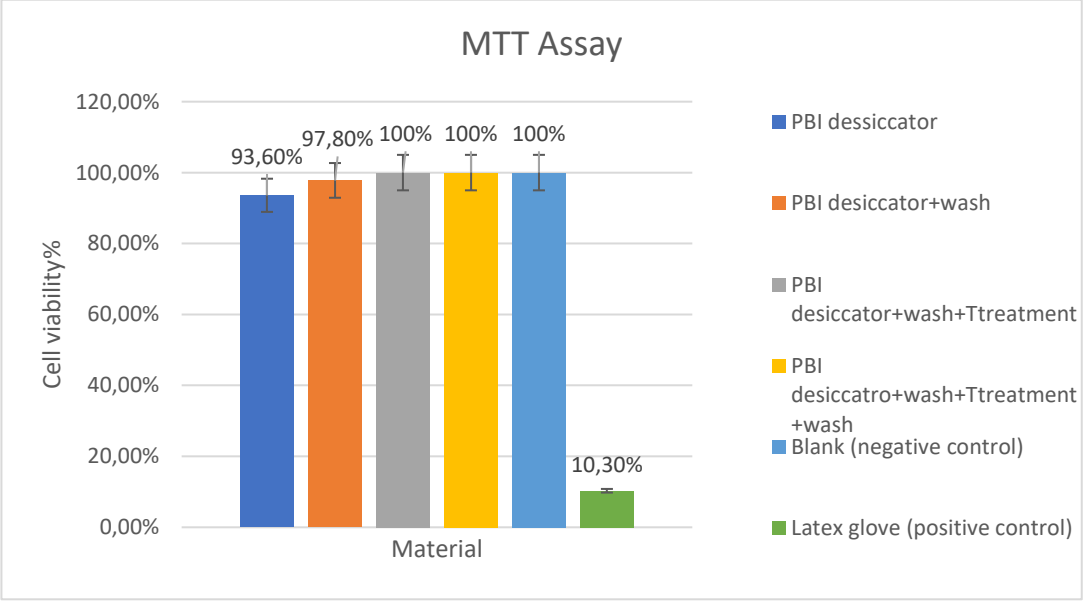

Graph 9. MTT assay on PBI fibers after several treatments to eliminate solvent residues.

Indirect cytotoxicity tests were repeated with PBI fibers and PEDOT:PSS crosslinked coatings. Pictures of the cells and MTT results are shown in Fig.45, Graph 10.

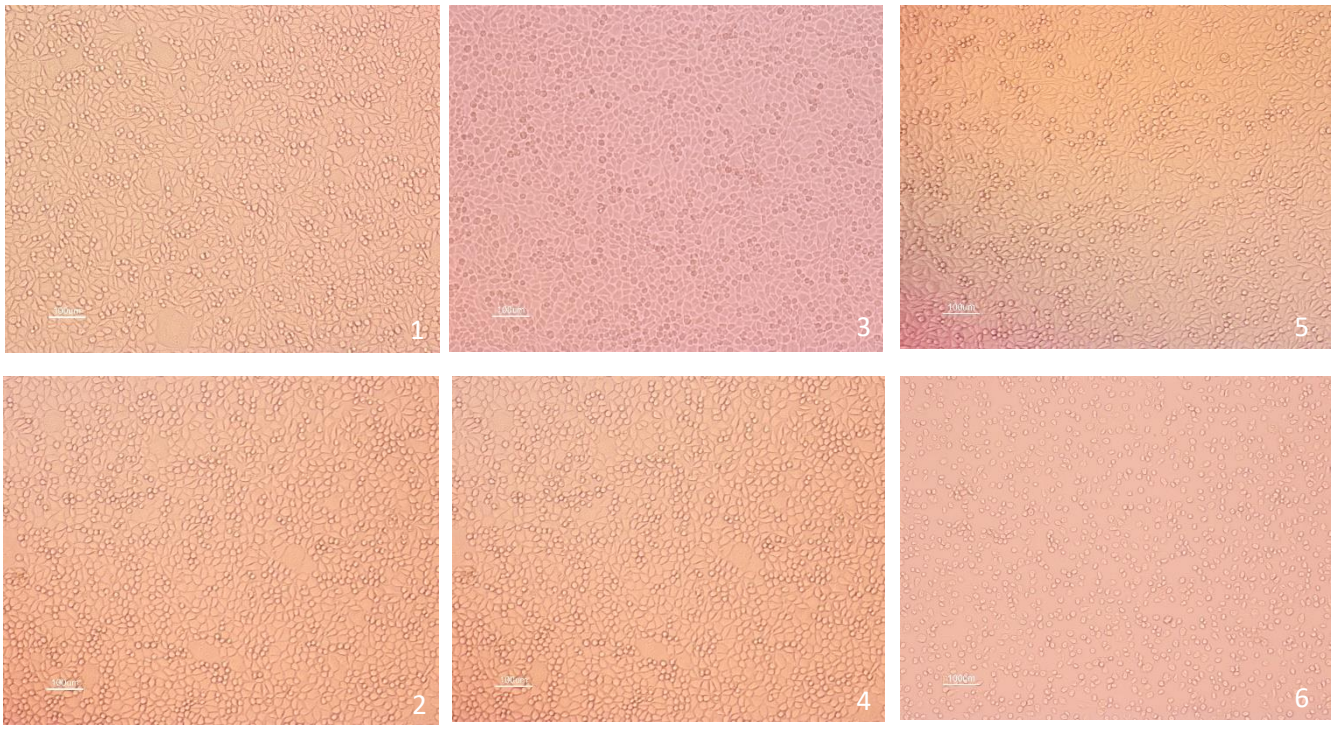

Figure 45 Optical microscope pictures of the L929 cells after 24h culture with the liquid extracts from the materials (Indirect Cytotoxicity Assay). (1) PEDOT:PSS:GOPS film; (2)PEDOT:PSS:DVS film; (3) PEDOT:PSS:GOPS coated PBI fibers; (4) PEDOT:PSS:DVS coated PBI fibers; (5) negative control; (6) positive control.

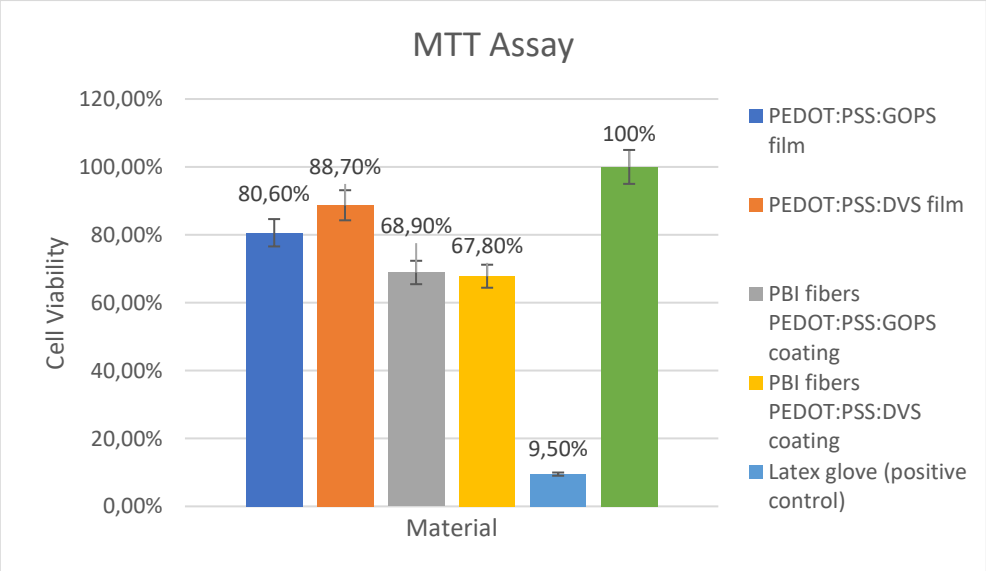

Graph 10. Results of MTT Assay on PEDOT:PSS crosslinked films and on PBI fibers coated with PEDOT:PSS

III.4.1.2 Direct cytotoxicity

Cells were seeded in a 6 well plate with a density of $8x10^4$ cells/cm^2 and left in the incubator for 24 hours. Then, sterilized samples of PBI fibers were put on the top of the cell layer and left in contact for 24 hours. After that, optical microscope was used to see if a halo of inhibition was forming around the samples. A glass coverslip was used as negative control, while a piece of latex glove (toxic) was used as positive control. Results for PBI fibers are shown in Fig.46.

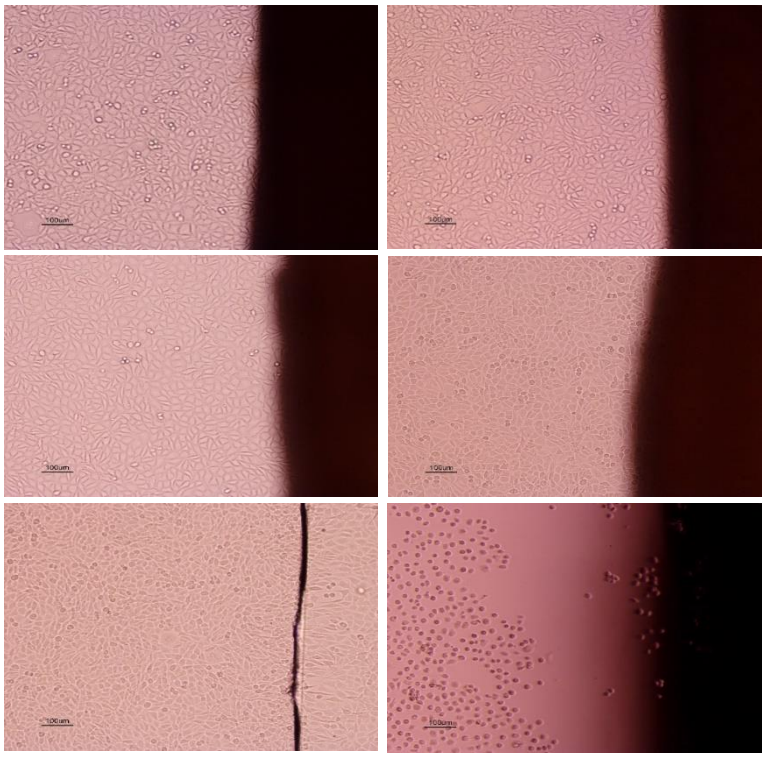

Figure 46 Optical microscope pictures of Direct cytotoxicity assay onto PBI fibers.

Results for PBI fibers with PEDOT:PSS coatings, tested in the same way, are shown in Fig.47. In no one of the samples a halo of inhibition was noticed, but the cells shape in the well with the latex glove appeared roundish compared to the other wells.

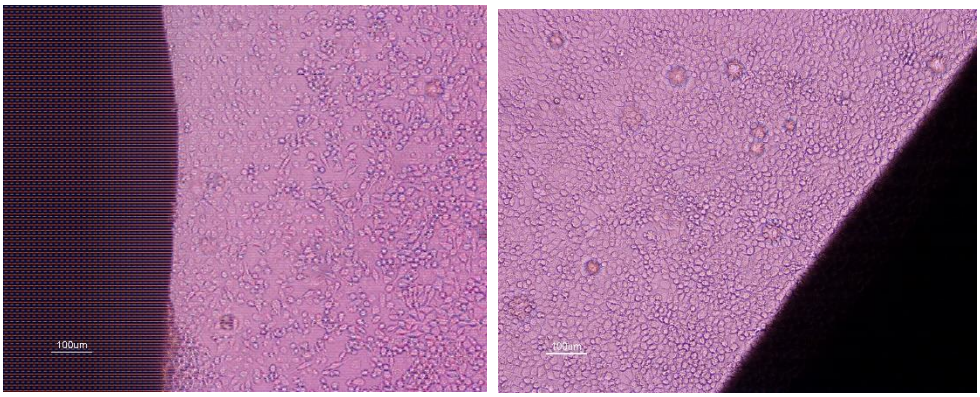

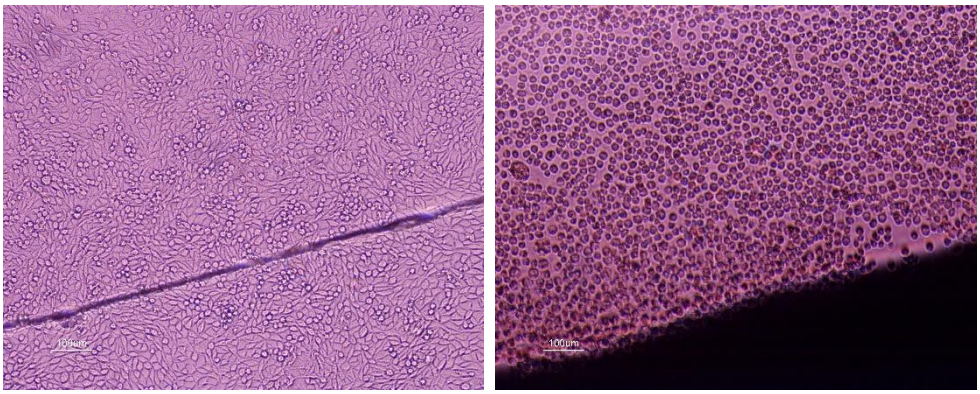

Figure 47 L929 direct cytotoxicity assay. Up left: negative control (glass coverslip); up right: PBI fibers coated with PEDOT:PS crosslinked with GOPS. Bottom left: PBI fibers coated with PEDOT:PSS crosslinked with DVS; bottom right: positive control (latex glove).

III.4.2 Adhesion tests

Fibroblasts L929 were seeded with a density of $1.5x10^5$ cells/cm^2 onto the surface of different samples and left in culture for 10 days. Chosen samples were 2D films of PEDOT:PSS crosslinked with GOPS or DVS, and 3D scaffolds made of PBI fibers alone or coated with PEDOT:PSS crosslinked with GOPS or DVS. Cells were also seeded in the central part of the 3D printed frame with electrospun PBI fibers coated with PEDOT:PSS + GOPS. Cells were imaged first with fluorescence (optical and confocal microscopy) and then with SEM microscopy.

III.4.2.1 Calcein staining

Calcein staining was performed for two reasons: first, because the observation of the cells on the fiber scaffolds was very hard with optical microscope, due to the high fiber density. Second reason is that calcein can be considered as a qualitative viability assay, because the fluorescent dye stains only viable cells: cells were stained with calcein and imaged with fluorescence while still alive. Regarding PBI fibers alone, this material was discovered to be fluorescent for UV, blue and green light (Fig.48); fluorescence as an imaging technique was so abandoned.

Figure 48 PBI fibers observed with fluorescent UV light (left), blue light (middle) and green light (left), without any fluorescent dye.

PBI fibers with PEDOT:PSS coatings were tested instead, checking if the PEDOT:PSS on top was masking the autofluorescence of the fibers. Pictures were acquired at day 4, 7 and 10 (Fig.49,50,51). As showed in pictures, cells appear alive and confluent on the surface of the films at every time point; instead, the staining failed at every time point for the 3D substrates, as the images are too blurry to distinguish anything.

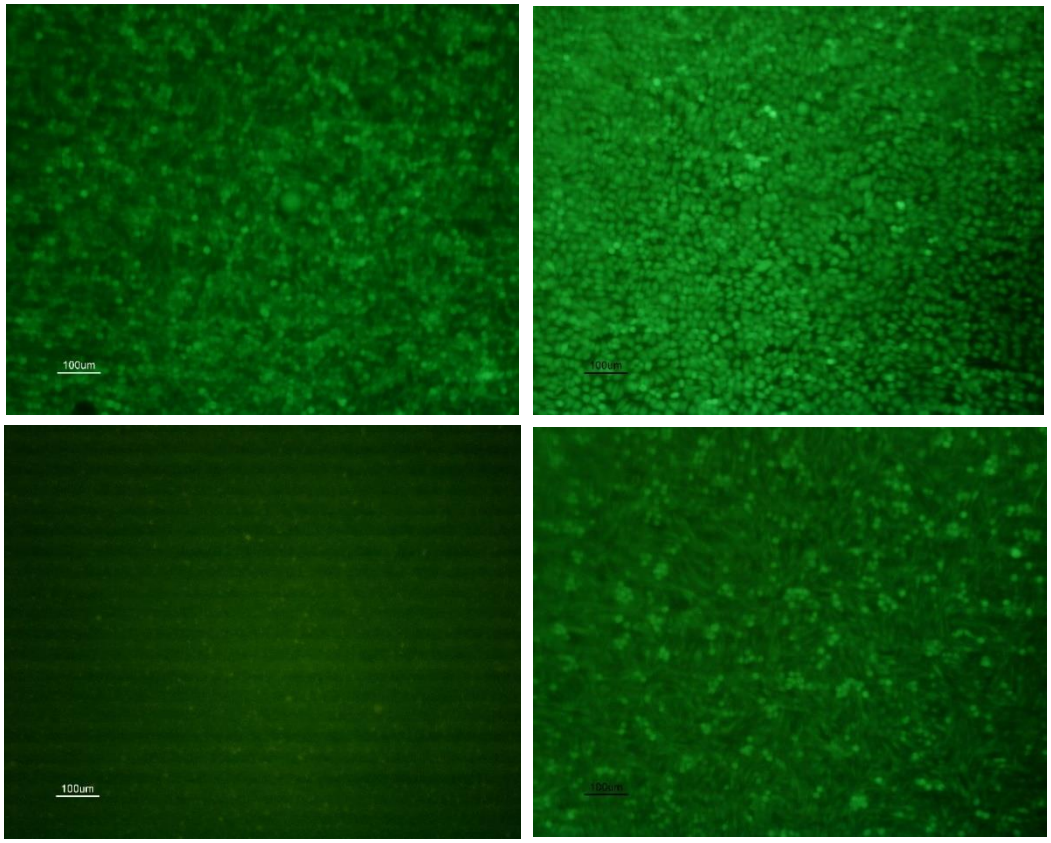

Figure 49 Calcein fluorescence staining on L2929 fibroblast seeded onto the samples at day 4. Up left: PEDOT:PSS+DVS film; up right: PEDOT:PSS+GOPS film. Bottom left: PBI fibers coated with PEDOT:PSS+DVS; bottom right: PBI fibers coated with PEDOT:PSS+GOPS.

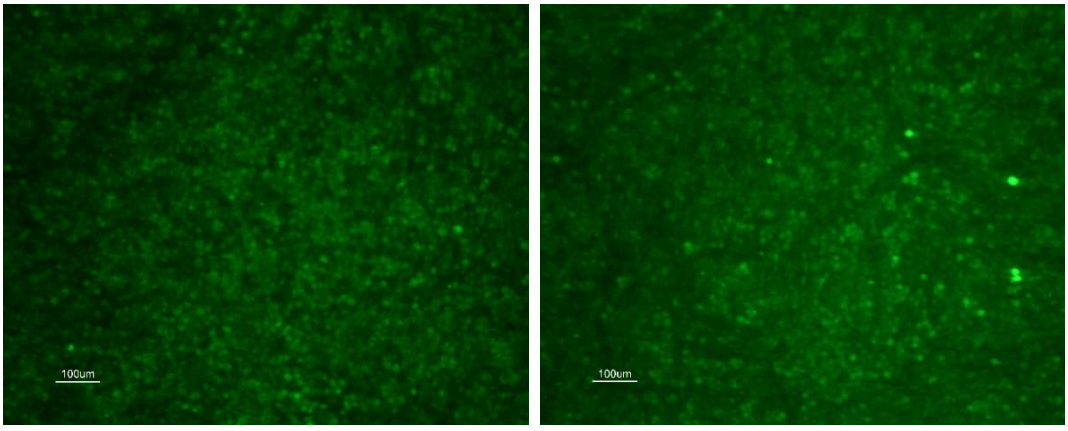

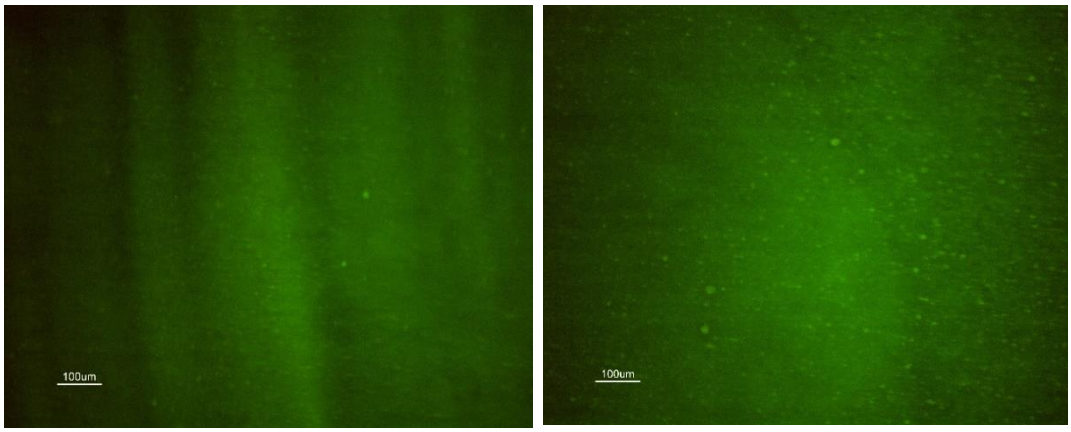

Figure 50 Calcein fluorescence staining on L2929 fibroblast seeded onto the samples at day 7. Up left: PEDOT:PSS+DVS film; up right: PEDOT:PSS+GOPS film. Bottom left: PBI fibers coated with PEDOT:PSS+DVS; bottom right: PBI fibers coated with PEDOT:PSS+GOPS.

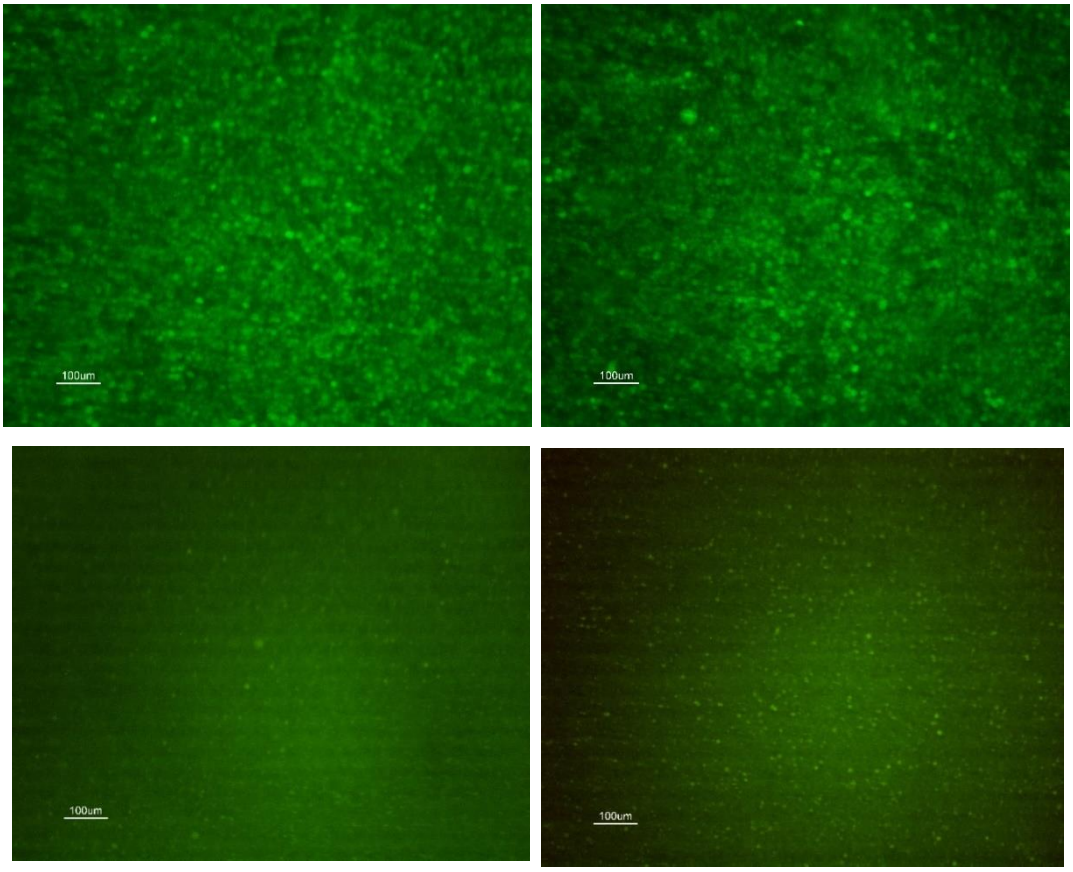

Figure 51 Calcein fluorescence staining on L2929 fibroblast seeded onto the samples at day 10. Up left: PEDOT:PSS+DVS film; up right: PEDOT:PSS+GOPS film. Bottom left: PBI fibers coated with PEDOT:PSS+DVS; bottom right: PBI fibers coated with PEDOT:PSS+GOPS.

III.4.2.2 DAPI and Phalloidin staining

DAPI and Phalloidin staining was also used to stain the cells onto the surface of the samples after 10 days of culture. Images of the two fluorescent staining were acquired separately with optical microscope and then merged with the software ImageJ; DAPI blue dye is used to stain the nuclei of the cells, while Phalloidin is a fluorescent red dye for the cytoskeleton. In the case of the two PEDOT:PSS films, the staining was successful, as showed in Fig.52.

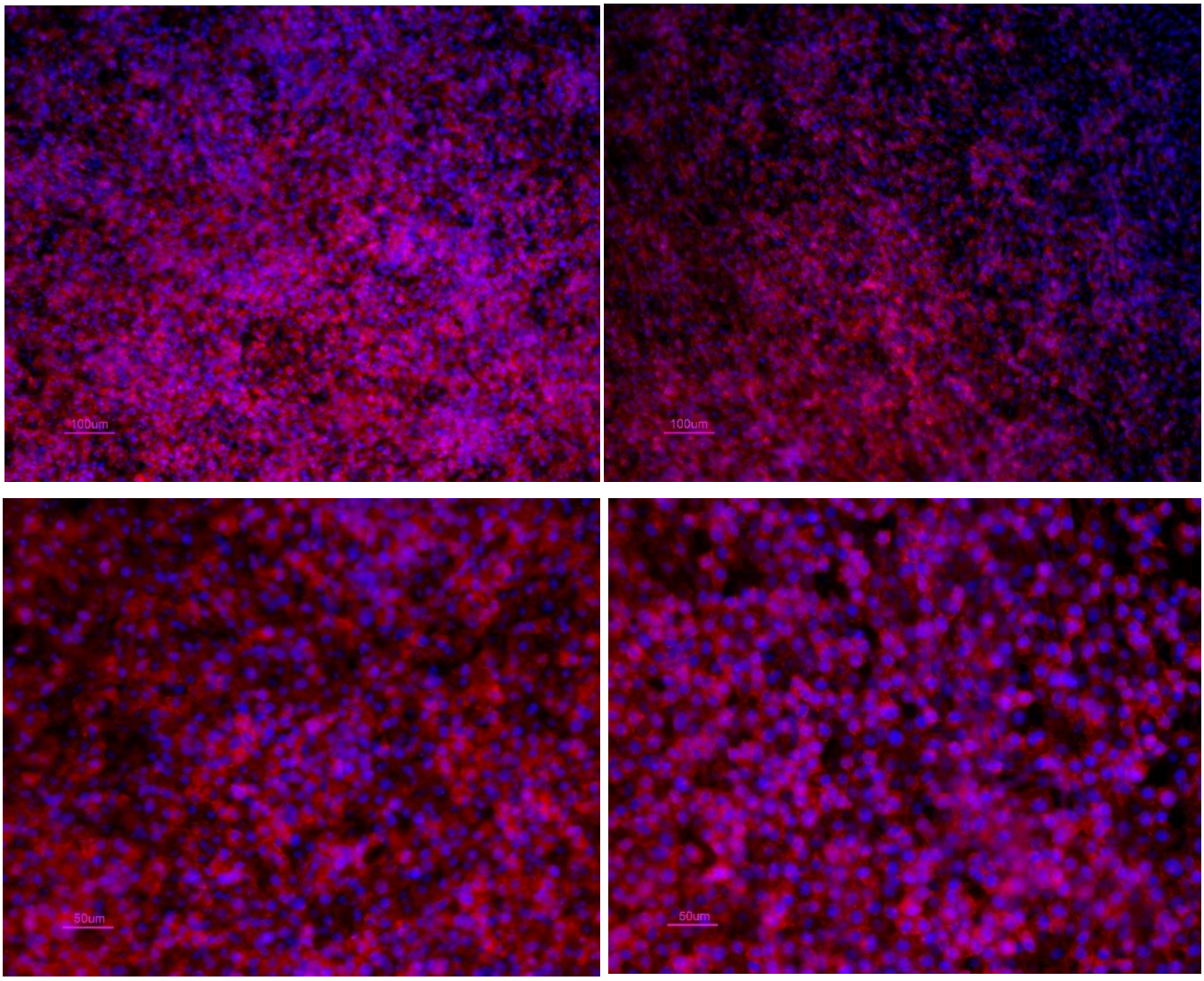

Figure 52 DAPI + Phalloidin staining onto PEDOT:PSS films crosslinked with DVS (left) and GOPS (right). Up: magnification of 100x. Bottom: magnification of 200x.

In the case of fibers, instead, the staining was again not successful, as the reported fluorescence was the one from the fibers and not by the cells (Fig.53).

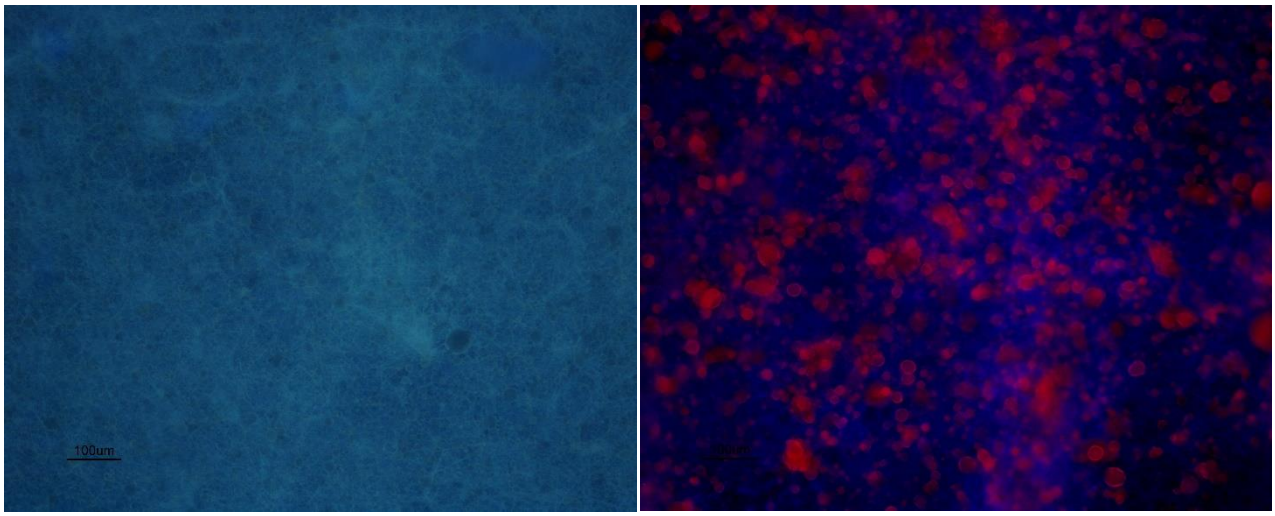

Figure 53 Left: DAPI staining onto PBI fibers coated with PEDOT:PSS + GOPS. Right: DAPI + Phalloidin staining onto PBI fibers coated with PEDOT:PSS + DVS.

The same interaction was observed also on the 3D printed frame with electrospun PBI fibers coated with PEDOT:PSS crosslinked with GOPS. L929 were seeded also in the central hole of the 3D printed frame, not to have any interaction with the glass coverslip or with the glue, and were stained with DAPI and Phalloidin to see their structure; again, the dyes and fibers interaction made impossible to see the cells.

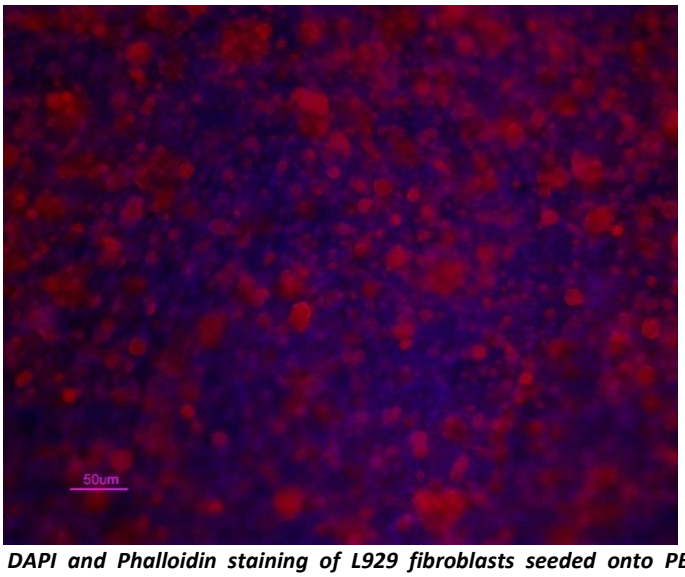

Figure 54 DAPI and Phalloidin staining of L929 fibroblasts seeded onto PBI fibers coated with PEDOT:PSS + GOPS and electrospun on 3D printed frame. Magnification of 200x.

DAPI and Phalloidin staining was used also to see the cells with confocal microscope (Zeiss LSM 710). Again, the observation of the cells was possible only on the 2D films (Fig.55), while on the fibers the images were blurry (Fig.56).

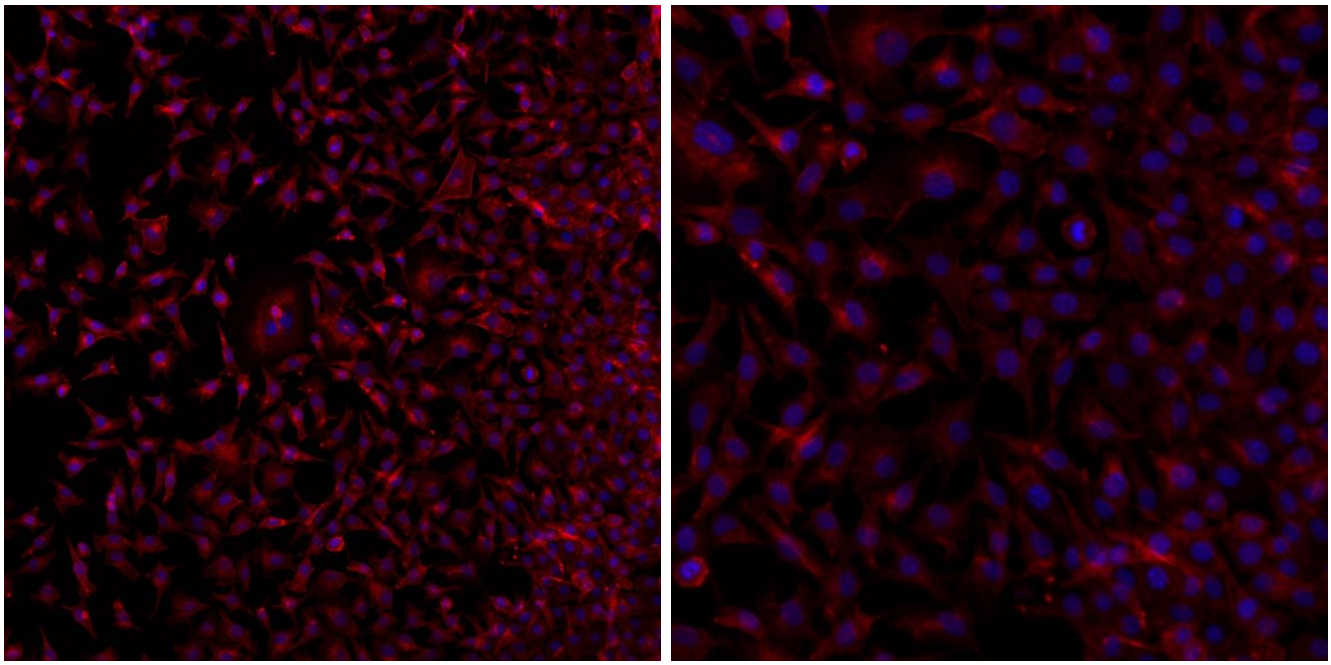

Figure 55. Fibroblasts L929 on 2D films made of PEDOT:PPS + DVS (left) or PEDOT:PSS + GOPS (right); images obtained with confocal microscope. Left: magnification of 100x. Right: magnification of 200x

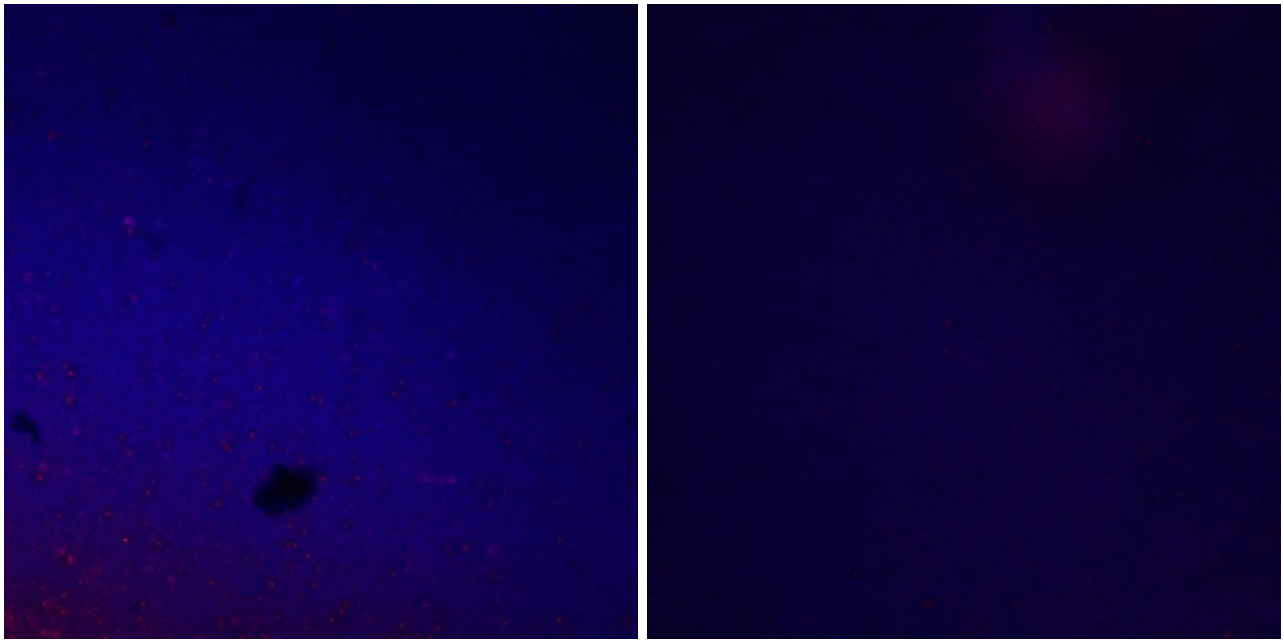

Figure 56. DAPI and Phalloidin staining onto PBI fibers crosslinked with PEDOT:PSS + DVS (left) or PEDOT:PSS + GOPS (right). Magnification of 100x.

Due to this interference of the material with the fluorescent staining, another fluorophore was tested in order to image the cells: Alexafluor 488 Phalloidin (Termofisher scientific) green staining, showed in Fig.57.

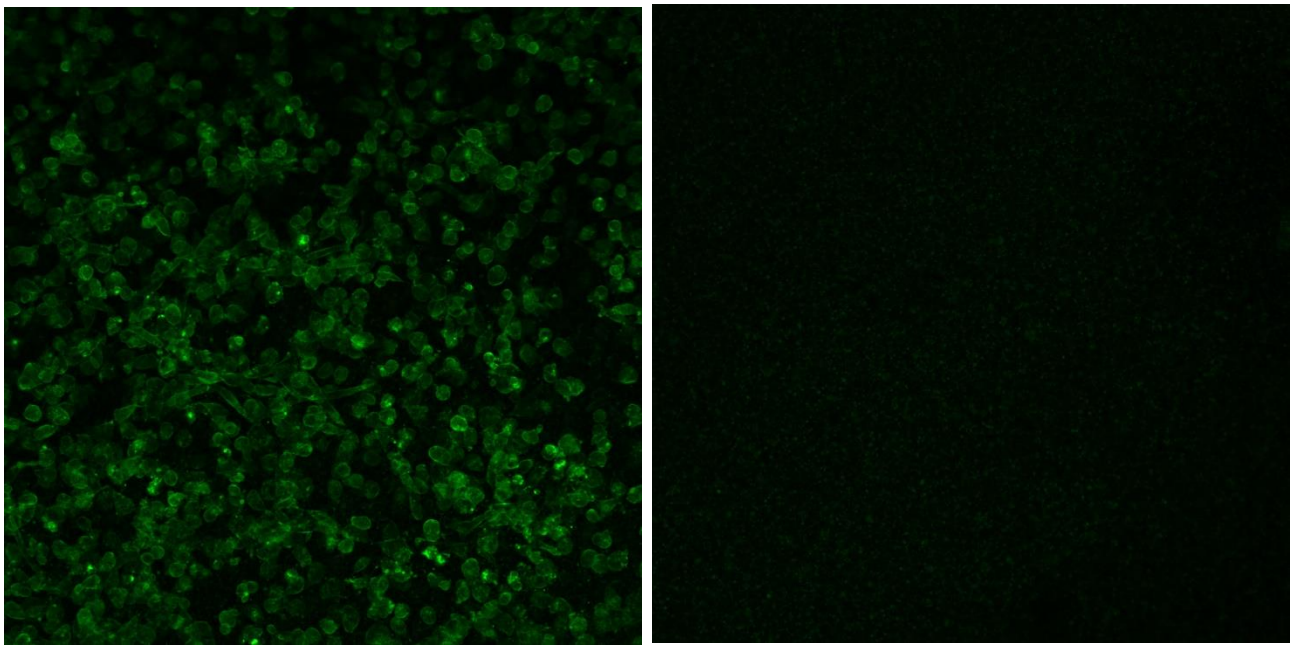

Figure 57 Confocal microscope pictures of PBI fibers wih fibroblasts L929 stained with Alexafluor 488 Phalloidin (left) and fibers without cells and without fluorescent staining (right).

This dye was finally able to image the fibroblasts seeded onto the cells. They show high confluence and fibroblastic typical elongated cytoskeleton.

III.4.2.3 SEM microscopy

SEM pictures of fibroblasts L929 seeded onto PEDOT:PSS crosslinked films are shown in Fig.58.

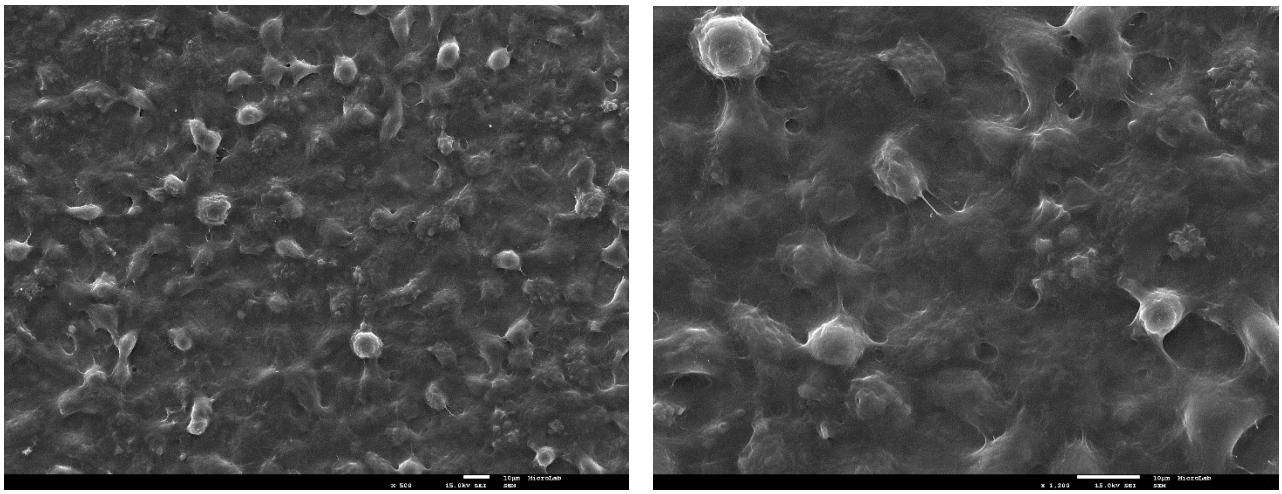

Figure 58 SEM images of fibroblasts cultured for 7 days on PEDOT:PSS crosslinked films (left: crosslinking with GOPS; right: crosslinking with DVS).

Cells appear elongated and very confluent, as already assessed by fluorescence staining; extracellular matrix has been deposited all over the surface of the film.

Fibroblasts seeded onto PBI fibers alone are shown in Fig.59; images were acquired after 7 days of culture. Again, evidence of extracellular matrix deposit and cells spreading is present.

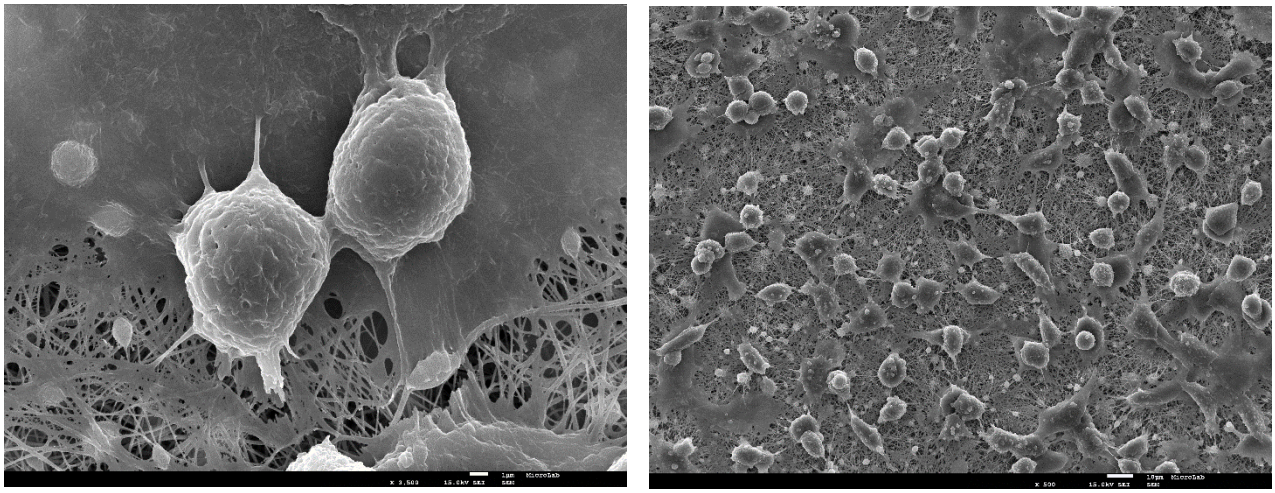

Figure 59 SEM pictures of fibroblasts L929 after 7 days of culture on PBI fibers.

Finally, pictures of fibroblasts seeded onto PBI fibers with PEDOT:PSS coatings and cultured for 7 days are shown in Fig.60.

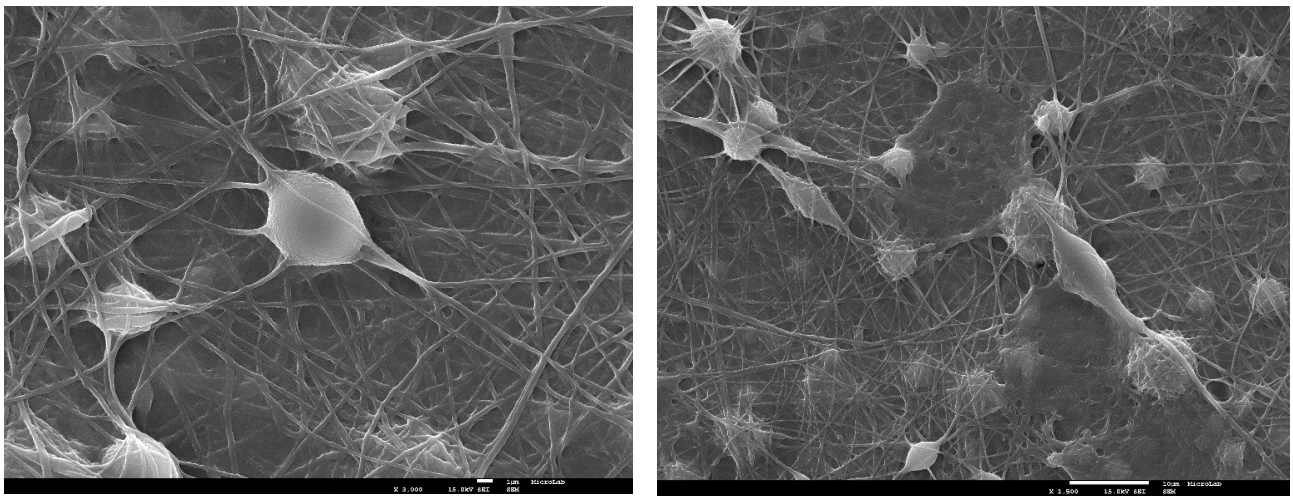

Figure 60 SEM pictures of fibroblasts cultured for 7 days onto PBI fibers with PEDOT:PSS crosslinked coatings (left: GOPS crosslinker; right: DVS crosslinker).

Fibroblasts appear attached to the fibers and spread onto the surface of the sample.

III.5 NSCs culturing

ReNcells VM cell line was used to determine the response of neural progenitor cells to the electrically conductive substrates. NSCs were seeded with a density of 100.000 cells/cm^2 on the 2D films of PEDOT:PSS and on the 3D fibrous scaffolds made of PBI and coated with PEDOT:PSS, crosslinked with GOPS or DVS; materials were previously sterilized with a solution of PBS + 1% Antibiotic/Antimicotic by incubation overnight and then coated with poly-ornithine and laminin to help NSCs adhesion. ReNcells were then cultured for 2 days with growth factors (FGF and EGF) to induce expansion, and then for 7 days with N2-B27 neural differentiation medium to induce differentiation into neurons.

After two days of expansion, ReNcells were already 100% confluent and covered the whole surface of the materials, so the differentiation was started. As reported by R. Corteling [R. Corteling, 2008], ReNcell VM cell line is demonstrated to differentiate in 4 days after induction, showing extensive processes and mature neuronal morphologies.

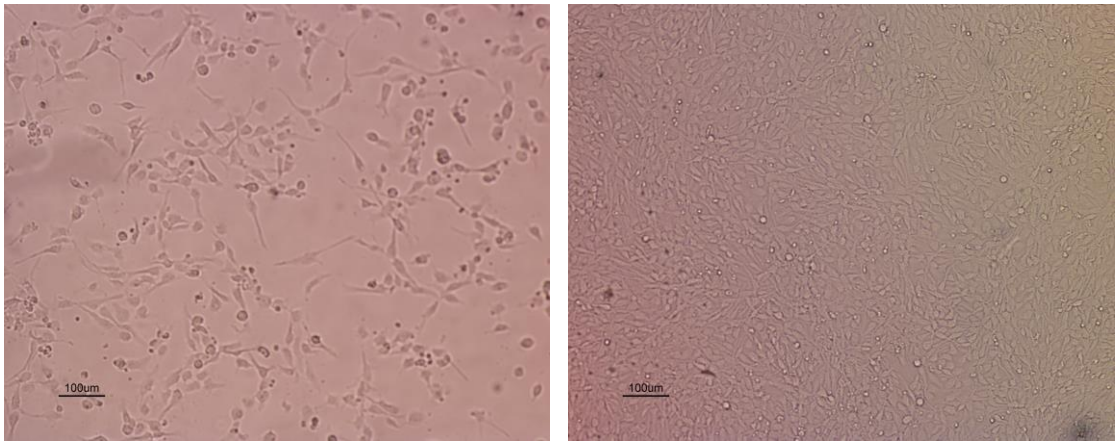

Figure 61 ReNcells optical microscope pictures during expansion: day 0 (left) and day 2 (right). After two days of culture with growth factors, cells were already 100% confluent

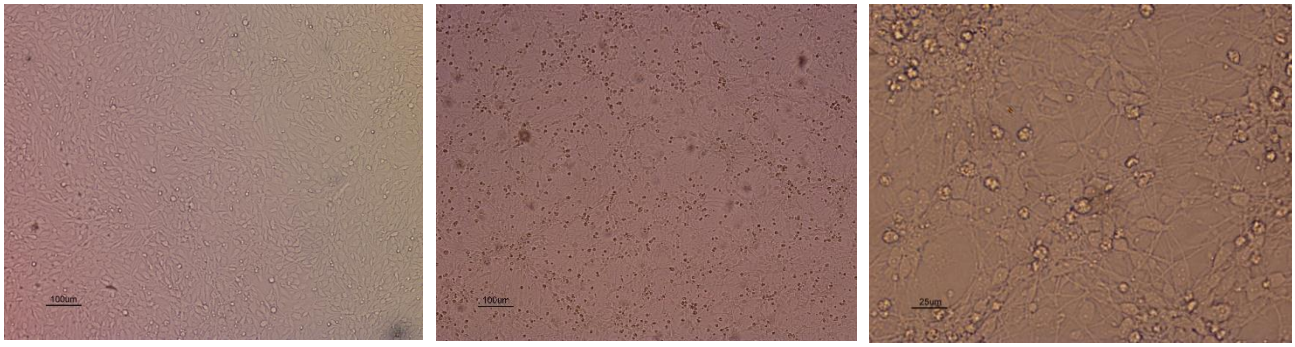

.***Figure 62 ReNcells before differentiation (left) and at day 7 of differentiation (middle:100x, right:400x).***

III.6 Electrical stimulation

III.6.1 Set-up

Copper wires were glued with silver paste on the edges of 2D PEDOT:PSS films, in correspondence of the gold stripes previously deposited. Wires were then connected to the electrical set-up in order to apply an electrical stimulation on the cells. To avoid the contact of electrodes for electrical stimulation with the culture medium, a 3D printed container was used to isolate the cell culture environment; PDMS was used to glue the containers on the films surface, to avoid leakages. Then, the materials surface inside the container was sterilized with PBS + 1% Antibiotic/ Antimicotic solution and coated with poly-ornithine and laminin by incubation for 30 minutes and 4 hours, respectively, before cell seeding.

With the voltage power source, a square wave of 4V amplitude was applied to the circuit. The potentiometer was regulated in order to have 1V/cm voltage difference across the samples; as the difference between the electrodes in the films was 2cm, 2V stimulation was required (Fig.63).

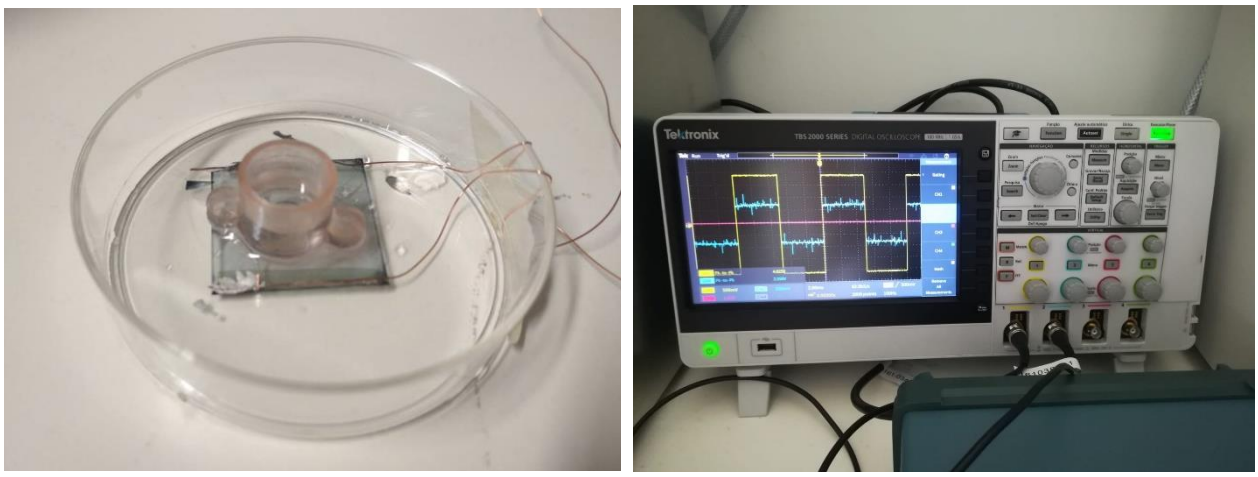

Figure 63 Assembled set-up used for cell stimulation (left) and Voltage recorded by oscilloscope in the electrical set-up used to stimulate the cells (right).

Samples with same material resistance were then put in parallel in the circuit. The resistance across the potentiometer was measured with a multimeter and reported the value of 5160Ω. Knowing the value of the resistance, it was possible to calculate the total current flowing in the system trough Ohm's law:

$$I = \frac{V_2 - V_1}{R} = \frac{4V - 2V}{5160\Omega} = 387.5\ \mu A$$

As two samples were put in parallel, but they had the same resistance, the value of the current flowing in the samples was exactly half of the total one, corresponding to 193.75µA. In this way it was possible to evaluate the resistance of every sample:

$$R = \frac{\Delta V}{I} = \frac{2V}{193.75\mu A} = 10k\Omega$$

III.6.2 NSCs expansion

ReNcells were seeded with a density of 100.000 cells/cm^2 onto 2D films of PEDOT:PSS crosslinked with GOPS and DVS. Unfortunately, samples crosslinked with DVS showed some leakages from the glued container and were so eliminated from the experiment. DMEM/F12 supplemented with grow factors (FGF and EGF) was used to expand the cells. Cells were exposed to a 100 Hz electrical stimulation with a magnitude of 1V/cm with 10ms pulse duration in a continuous manner for 2 days. After 48 hours, ReNcells were already 100% confluent (Fig.64).

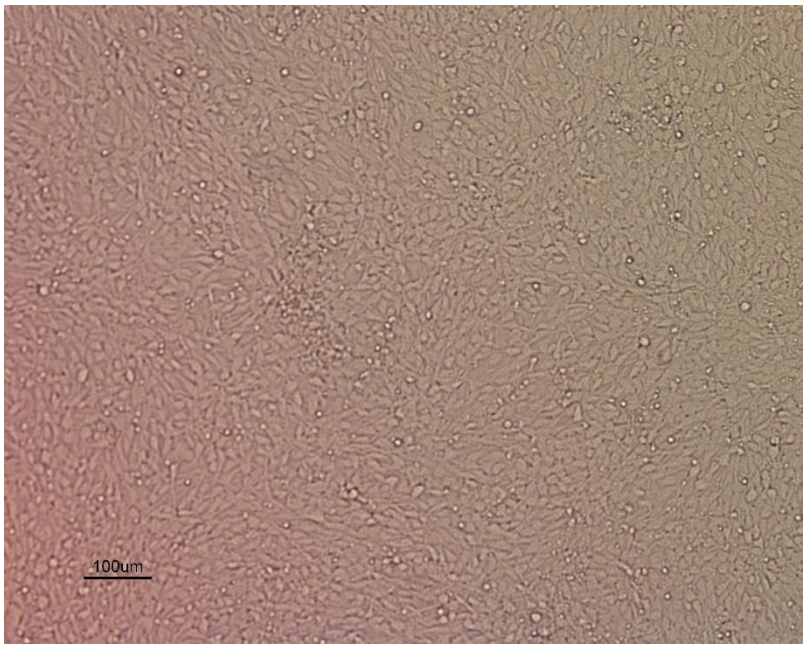

Figure 64 ReNcells after 2 days expansion with electricity

.

III.6.3 NSCs differentiation

NSC differentiation was studied under applied AC electric fields and compared to control experiments with no applied electric field. Cells were exposed to a 100 Hz electrical stimulation with a magnitude of 1V/cm with 10ms pulse durations over 12h per day during differentiation time. Neural differentiation medium, supplemented with B27 and N2, was used to culture the cells in this phase.

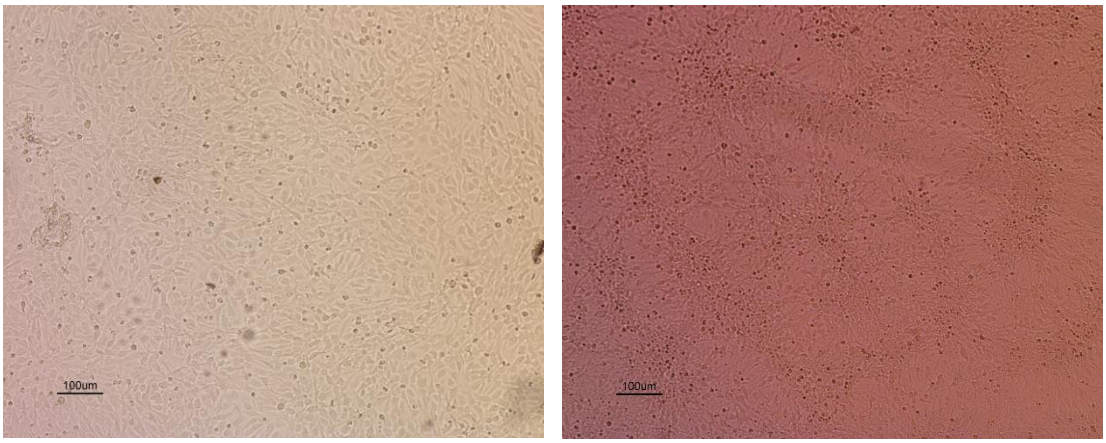

Figure 65 ReNcells at day 0 of differentiation (left) and at day 7 (right) with electricity.

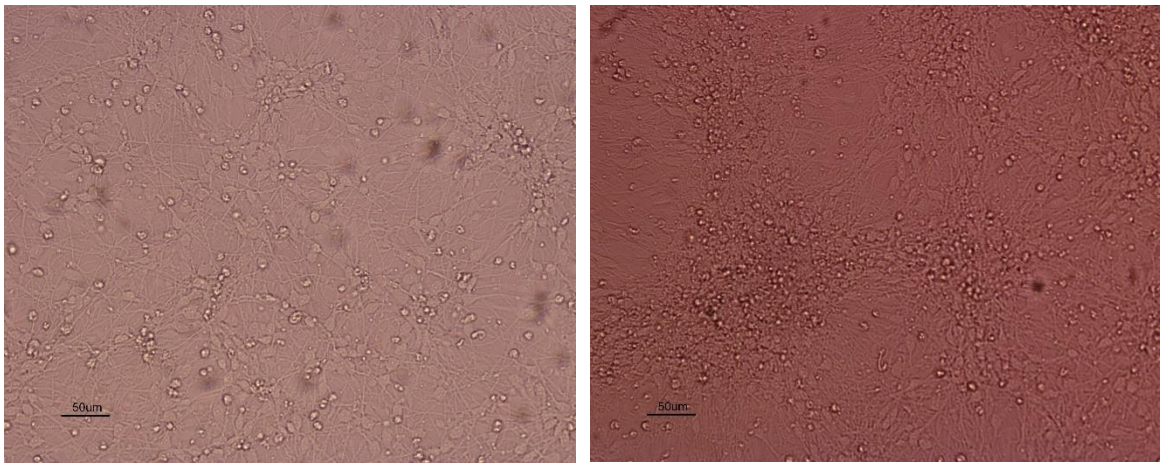

F***igure 66 ReNcells differentiation at day 7 without electricity (left) and with electricity (right). 200x Magnification***

III.6.4 Immunocytochemistry

Cells were fixed with 4% PFA after 7 days of differentiation with and without exposure to AC electric field for 12h/day in the absence of growth factors. Immunofluorescence study was performed using specific antibodies against Tuj1, which labels neurons in early development as well as mature neurons and GFAP to identify the differentiated level of astrocytic populations. Pictures are shown in Fig.67.

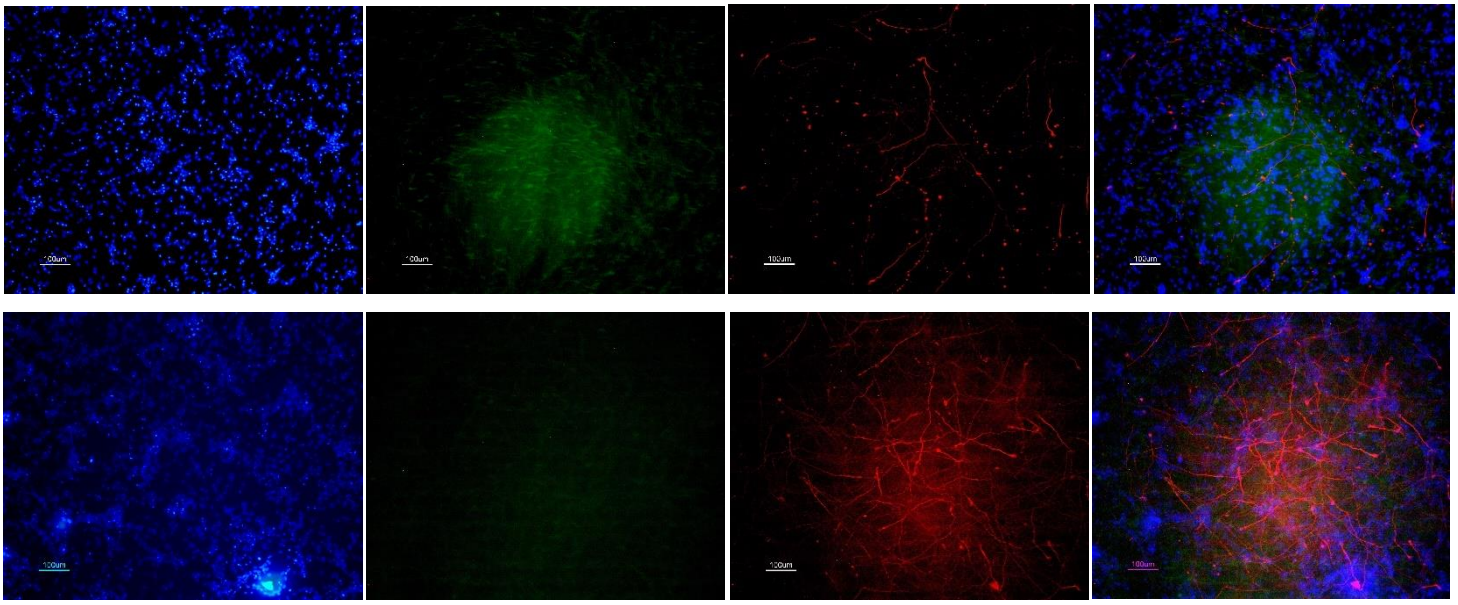

Figure 67 Immunostaining on ReNcells cultured on PEDOT:PSS:GOPS films after 2 days expansion and 7 days of differentiation without electricity (up) and with electricity (down).

Graph 11 is showing the percentage of cells positive for Tuj1, indicating a higher number of neural differentiated cells, calculated with ImageJ.

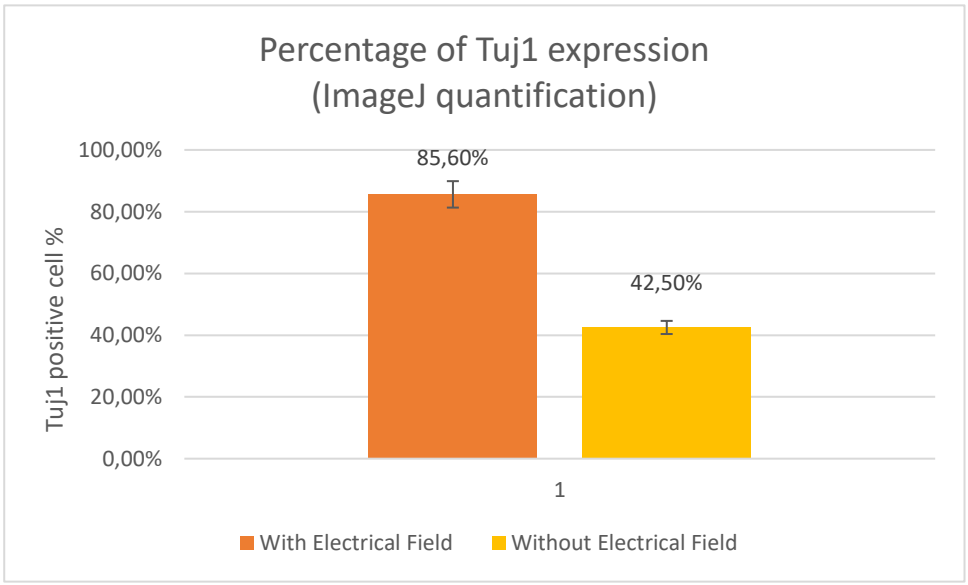

Graph 11. ImageJ software quantification of cells showing positive immunostaining for Tuj1 in NSCs at day 7 of differentiation.

III.6.6 Single Cell Calcium Imaging (SCCI)

The profile of [Ca2]i variations was characterized in single ReNcells upon KCl and histamine stimulation, on samples where cells were stimulated with electricity. The cells were loaded with the Fura-2 AM calcium probe, perfused continuously for 15 min with Krebs solution, and shortly (2 min) stimulated with 50 mM KCl or with 100 M histamine.

Changes in 340/380 nm ratios of fluorescence were monitored constantly during all the experiment. Fig.68 provides an example of [Ca2]i variations in ReNcells upon KCl and histamine stimulation. Cells displaying a rise in the [Ca2]i following KCl stimulation but not following histamine perfusion, show a behavior consistent with a neuronal-like profile. An immature-like profile, instead, is characterized by an absence of response to KCl but a rise in [Ca2]i following histamine stimulation. Astrocytic populations should not respond to both stimulations, even if some cases were found in literature [O'Connor ER, 1993].

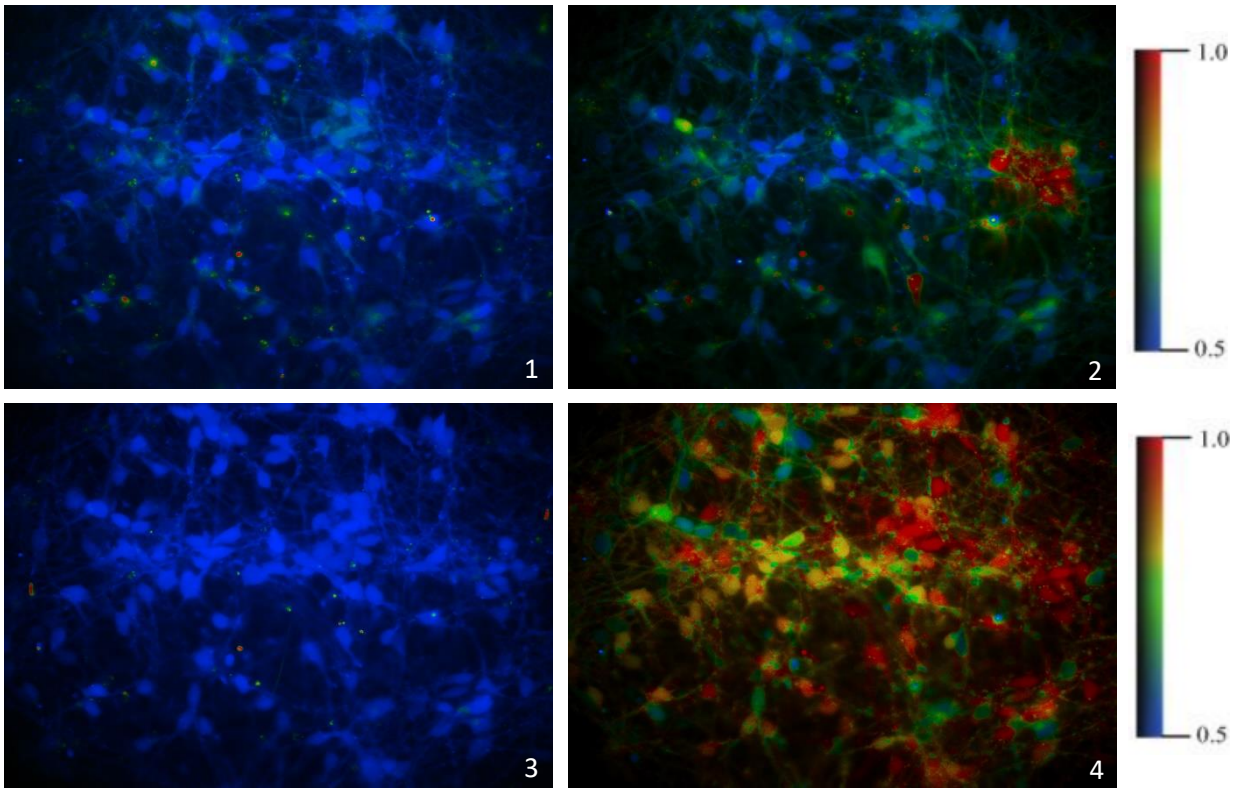

Figure 68 Pictures of ReNcells during SCCI. 1: Cells at the beginning of the experiment; 2: cells after the injection of KCl solution; 3: cells after recovery; 4: cells after histamine solution injection.

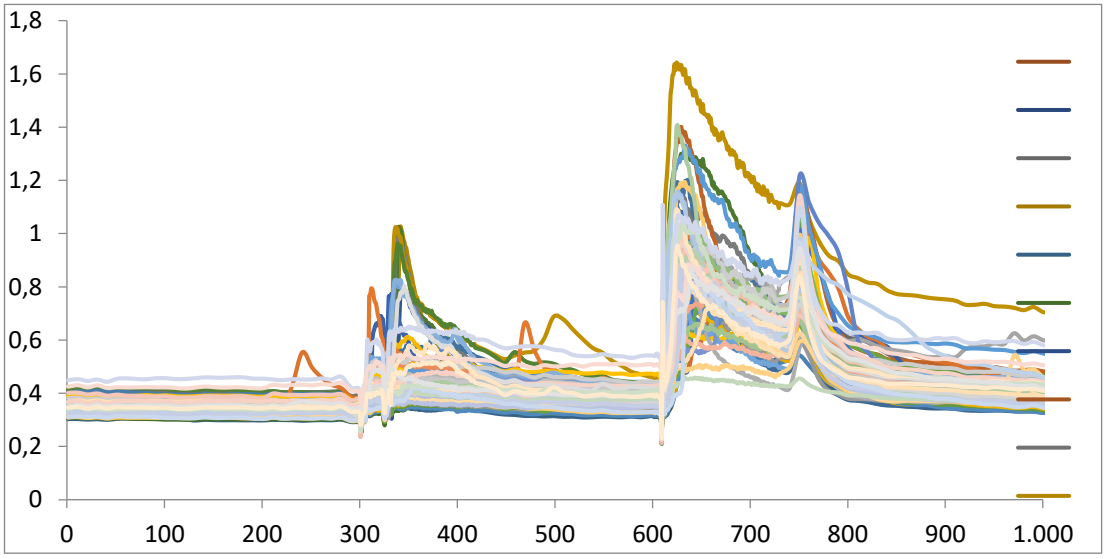

Figure 69 Cells response profiles of [Ca2]i variations to KCl and histamine stimulations.

For the ratio histamine/KCl analysis, data were first normalized: peak of KCl was normalized to the profile at the beginning of the experiment, while peak of histamine was normalized to the profile after KCl solution wash. Results are shown in Table 13.

Cell population	Ratio	Number of cells	Percentage
-	<50	0	0%
neurons	50-80	2	2%

immature	80-90	3	3%
astrocytes	90-100	1	1%
immature	>100	94	94%

Table 13. Ratio of Histamine/KCl peaks for NSCs during SCCI

Chapter IV: Discussion

IV.1 2D PEDOT:PSS films

Conductivity measurements on PEDOT:PSS films confirmed what reported in literature by Soares et al. and Mantione et al.. DBSA and PEG molecules are increasing the conductivity of the commercial material; GOPS crosslinking agent increases PEDOT:PSS stability but greatly reduces its conductivity. While samples with DVS have a very high conductivity, the addition of GOPS immediately drops this value by two orders of magnitude. Even if values of conductivity of PEDOT:PSS crosslinked with DVS were higher, both crosslinking method were tested in order to understand in which case the values were closer to the *in vivo* ones, and so could lead to a better cell electrical stimulation.
After the coating with poly-ornithine and laminin, values of conductivity were consistently reduced for both crosslinking methods, approaching the same values; however, polymer conductivities are not limited by LN, which is instead very insulating.
Regarding the stability of the films in water and culture medium, both crosslinking methods were able to reduce the natural PEDOT:PSS solubility in water, resisting up to two weeks without dissolving.

IV.2 3D scaffolds

IV.2.1 PEDOT:PSS blend PVP fibers

Fibers with PVP blend were successfully obtained because PVP content in weight (12.2%) was much higher than the one of PEDOT:PSS (1.3%). In this way, the viscosity of the solution was increasing sufficiently to perform electrospinning process, but the amount of conductive polymer was not enough to obtain conductive fibers, as demonstrated by the conductivity measurements, even if PVP was proven to be slightly conductive by the literature [B. Chaudhuri, 2016]. PVP removal was possible to obtain with a heating treatment up to 150°C; however, due to the high amount of PVP in respect to PEDOT:PSS, this will lead to the possibility to obtain totally different fibers shape or holes in the structure. Moreover, the problem of the solubility in water made this strategy unsatisfactory.

IV.2.2 PEDOT:PSS fibers

PEDOT:PSS Clevios commercial solution has a very low viscosity. Many trials were performed adding to the material other chemical compounds or polymers, always in a quantity lower than 20% w/w; this percentage is the threshold of discrimination between additives and blends. To try to obtain fibers made mainly of PEDOT:PSS, it was decided not to exceed this value, in order to leave PEDOT:PSS conductive polymer as main component and avoid the blends that can lead to non conductive fibers, as demonstrated by previous results with PVP. With these experiments was proven that tested additives

are not sufficient to increase the viscosity of the solution. A strategy to improve the viscosity can be to polymerize EDOT monomers in the laboratory without purchasing a commercial solution and deciding the quantity of solvent (water) to add, as performed by [J. Wo, 2013]. However, this process was not considered in the development of this thesis.

Physical treatments on the commercial solution were contradictory: even if with RapidVap a considerable amount of water was evaporated, it is impossible to understand if some molecules of PEDOT:PSS were evaporated as well, leading to a different concentration than the one calculated in the labs. For its incompleteness, and for the impossibility to obtain sufficiently high viscosity values, this strategy was abandoned. Lyophilization process was also incomplete: a dry sponge was obtained, but no powder, seeming that some water molecules were still bound to the PEDOT:PSS structure and that the treatment was not working in the proper way. Rotavapor process was discarded as too slow.

IV.2.3 PEDOT:PSS coating onto polymeric fibers

The idea of a coating development came from the high conductivity values obtained for the 2D films, and the impossibility to realize a 3D scaffold only with PEDOT:PSS. It is already demonstrated that 3D substrates can have a more positive influence on the cells behavior *in vitro*, as the environment reproduces more closely the conditions *in vivo* [S. Han, 2016]. In order to achieve both goals, high conductivity and three-dimensional structure, fibers were realized trough electrospinning technique with other materials different from PEDOT:PSS, and then coated with the same solutions that gave good results for the bidimensional films. The chosen materials were:

- PBI
- PCL
- PVA

PBI was chosen because it has an intrinsic electrical conductivity; moreover, membranes made of PBI fibers are currently used to remove sulfur atoms from a solution [Ogunlaja AS, 2014], as the polymer reacts with it. PEDOT:PSS polymer is characterized by the presence of sulfur; even if the type of chemical bond between PEDOT:PSS and PBI was not investigated trough FTIR spectroscopy, the PEDOT:PSS crosslinked coating was demonstrated to remain attached to the PBI fibers. Moreover, PBI is a polymer with very high glass transition temperature (400°C), so was expected not to suffer the annealing treatment necessary to obtain PEDOT:PSS coating. Finally, PBI was already successfully electrospun in form of nanometric fibers: good random fibers were obtained, but never aligned, which could have been useful instead to give the cells a preferential direction of elongation, introducing another topographical stimulus. The solvent used to prepare the solution, DMAc, is soluble in water, so can be removed by washing, while the polymer instead is insoluble. However, as the PBI biocompatibility is not deeply investigated yet, many treatments were applied to the fibers in order to check the total solvent removal. PBI fibers were so washed with water, put into a desiccator with vacuum for 24 hours, or

received a thermal treatment at 160°C (evaporation temperature of DMAc). Combinations of the treatments were also tested, with repeated washes with MilliQ water; the water was then analyzed with absorbance scan and compared to normal MilliQ water to check the presence of solvent residues. No residues were found, as shown by the full absorbance spectrum, so the results of the biocompatibility tests can be attributed totally to the PBI itself (results of biocompatibility assessment are discussed in a later section).

PCL, instead, is a very common material used for biomedical applications. Easiness of fibers obtainment trough electrospinning technique, assured biocompatibility and water stability for short periods were the main characteristics why this polymer was chosen. To obtain electrospun PCL fibers was easier than with PBI. Few defects were found, and high alignment was achieved with parallel plate. However, the melting temperature of this polymer is only 60°C, but glass transition temperature is much lower (-60°C): for this reason, both coating treatments failed during annealing process.

PVA has a very high chemical versatility, biocompatibility, water solubility and excellent physical properties [Paradossi G.,], so it was already deeply studied for biomedical applications. Fibers of PVA were easier to electrospin in comparison to PBI but harder than PCL; fibers were successfully obtained in both random and aligned configuration, even if the percentage of alignment was lower than the one of PCL. PVA polymer was chosen for its hydrophilicity and thus possibility to react with PEDOT:PSS during the coating procedure. Unfortunately, the affinity between these two materials is so high that the PVA fibers totally dissolved in the coating solutions, showing the impossibility to use this material for this application.

If it was possible to realize a viscous solution of crosslinked PEDOT:PSS, a coaxial electrospinning strategy should have been the best way to achieve a perfect and uniform coating. As this was not possible to realize, three others different coating strategies were tested: spin-coating, dip in the solution, immersion in the solution for 24 hours. All the strategies were followed by an annealing treatment (with proper conditions for the two solutions, as described in section 1.3).

SEM observation of the fibers after the coating consented to discard the spin-coating process, because it caused a loss of three-dimensionality of the substrate.

EDS analysis consented to discard the dip treatment: as PCL is not reacting with PEDOT:PSS, the coating detaches after two weeks in water, leading to a loss of PEDOT:PSS on the surface of PCL fibers, as demonstrated by the drop of the sulfur peak.

Conductivity measurements were useful to determine which type of fibers was better not to reduce the high electrical conductivity of the PEDOT:PSS solution used as coating. The results demonstrates that only PBI was able to maintain the conductivity at the same order of magnitude as the crosslinked PEDOT:PSS film itself. This is due probably to the conductive nature of the polymer, that is intrinsically able to conduce electricity; even if the conductivity of the fibers alone is low, the PBI is not an electrical insulator.

After this selection, the only scaffold that was satisfying all the requisites for neural stem cells stimulation, was the one made of PBI fibers with PEDOT:PSS coating crosslinked with both GOPS or DVS. For this reason, it was the only one that was tested for the stability in cell culture conditions and for the biocompatibility.

Regarding the stability in cell culture conditions, that means culture medium (DMEM + 10% FBS) and incubator at 37°C, the substrates made of PBI and PEDOT:PSS crosslinked coating perfectly maintained the characteristics for two weeks, that is the minimum useful period for neural stem cells growing and differentiation. This can be mainly due to the insolubility of PBI in water, and to the chemical bonds between the fibers and the coating, that avoid it to detach, and additionally to the crosslinkers present in the coating, that make it stable and resistant in water environment. To be used with cells, samples need also to be sterilized. A treatment with UV light was tried on the fibers with coating, but the results were not positive: UV light can act as a second annealing treatment making the coating more rigid and shrunk, giving the wrinkled aspect that is possible to see with SEM microscope. Successive sterilization was carried on only with several washing in a solution of 1% Antibiotic/Antimicotic in PBS.

IV.3 Biocompatibility assessment

IV.3.1 Indirect Cytotoxicity Assay

Indirect biocompatibility of PBI fibers after 24 hours in culture medium was confirmed by this assay; cells demonstrated a viability of 100%, as the control, during MTT assay.

IV.3.2 Direct Cytotoxicity Assay

Direct biocompatibility was also confirmed for PBI fibers after 24 hours: no halo of inhibition was noticed, and the cells appearance was still elongated, indicating a fibroblastic phenotype. Also for PBI fibers coated with PEDOT:PSS, no halo of inhibition was observed.

IV.3.3 Adhesion tests

This experiment was carried on in order to understand the response of the cells to the substrates, in terms of adhesion and colonization. While 2D films were already tested, with good results in terms of cell culture [Soares et al.], [Mantione et al.], for the 3D scaffolds was the first time, as no one ever tried this combination of materials in literature; a deep study was needed in this case to characterize these scaffolds. The main problem of this study was that the direct observation of the cells seeded on the fibers was impossible, due to the high density of fibers in the scaffolds that impedes the light to penetrate. Fluorescence was so used as a strategy for cells visualization, starting with Calcein green dye, which stains alive cells: the results of this observation, repeated at different time points during the culture, were not satisfactory for both the scaffolds. The pictures were always blurry: at the beginning, this effect was thought to be due to the

biological glue above the fibers. Other factors that could have contributed to this blurring were the difficulty of the optical microscope to image cells on a substrate with three-dimensional shape, and maybe the absorption of the fluorescent dyes by the fibers. But as this effect was also present on the 3D frame, where there was no glue, this main theory was discarded; also, the difficulties in cell imaging with optical microscope were not sufficient to explain this phenomenon, because the confocal microscope also was not able to image anything. After seeing the PBI fibers alone with fluorescent light, it was clear that the material itself was interacting with the staining. Calcein fluorescent dye is excited at wavelengths of 495 nm (blue light) and emits at 515 nm (green light). PBI in DMAc has an excitation spectrum with a peak of 405 nm and a shoulder at 460 nm, with emission monitored at 524 nm (UV light), as reported by Kojima T., 1980 (Fig.70). This study explains the interaction with DAPI staining: excited at 380 nm, PBI has a fluorescence spectrum with peaks around 400 nm, thus perfectly covering the emission of DAPI at 461 nm while excited at 358 nm. These studies were performed in air with dry samples: is it possible that the PBS or culture medium are shifting the spectrum of emission, thus interacting also with calcein and Phalloidin staining and explaining the blurry effect in the acquired pictures. Also the PEDOT:PSS coating on the fibers can be responsible for the shift in the spectrum of emission.

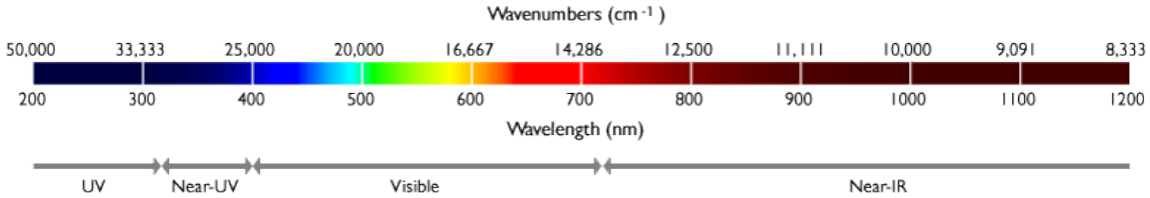

Figure 70 Spectrum of light waves

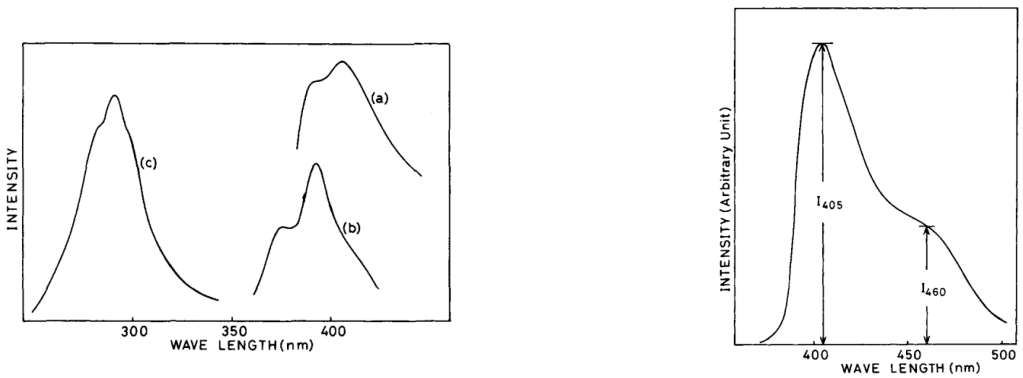

Figure 71 Right: Fluorescence spectra of PBI (a), MBI (b), and benzimidazole (c) in DMA. Excitation wavelengths: (a) 380; (b) 360 Left: Excitation spectrum monitored at 524 nm for PBI-DMA. [Kojima T. Studies of Molecular Aggregation of a Polybenzimidazole in Solution by Fluorescence Spectroscopy , Journal of Polymer Science, 1980]

Results of SEM observation of the cells are comparable to the ones found in literature by Li et al., 2002, for fibroblasts growing on an artificial fibrous scaffold (Fig.72), meaning that the material is suitable for fibroblasts adhesion and proliferation.

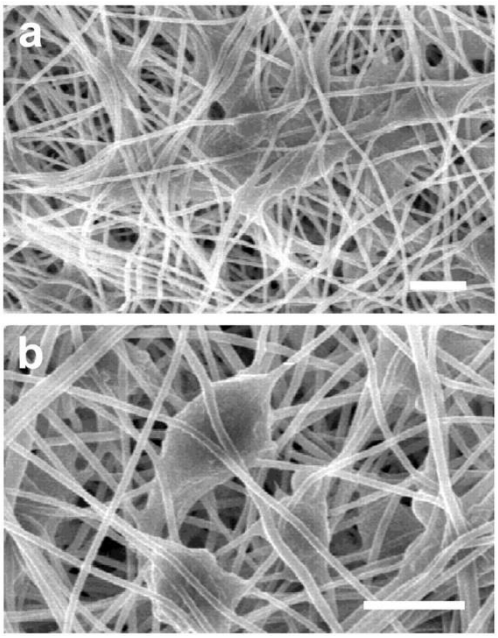

Figure 72 Cells growing on engineered scaffolds. (a,b) Scanning electron microscopy (SEM) images of mouse fibroblasts grown on PLGA nanofibers for 7 days, as described previously (Li et al., 2002). Images are displayed at: (a) original magnification ×1500 and (b) original magnification ×2500. Scale bar: 10 µm. Images printed with permission from Li et al. (Li et al., 2002). Scale bar: 50 µm

IV.4 NSCs culturing

ReNcells successfully grew on 2D PEDOT:PSS films during expansion phase in culture medium with growth factors. After 7 days of differentiation, their morphology is consistently changed into a more neuronal-like phenotype, showing interconnected dendrites. Due to the difficulties in live imaging the cells onto PBI fibers coated with PEDOT:PSS, it was impossible to evaluate their response to 3D environment through microscopy technique. Cell behaviour could thus be tested with PCR analysis or with flow cytometry.

IV.5 Electrical stimulation

Besides chemotactic signals and topography, electric fields can be a source of directional cues in vitro to control cellular processes including microfilament reorganization, proliferation, differentiation and migration of NSCs towards specific targets. When cells are exposed to electric fields there is a redistribution of charged cell-surface receptors and a charge movement is generated on the outer surface of the cells. Cations such as Na+ will drag along water, generating an electro-osmotic flow, which asymmetrically redistribute membrane proteins to the cathode-facing side of cells. The ability of electric fields to control cell shape, the release of signaling molecules and cell migration, could have potential clinical applications. However, the response to electric fields is diverse depending on cell type, developmental stage, and species. Electric fields of 12V/cm occur during morphogenesis and

wound healing and have been shown to orient the movements of a wide variety of cells in vitro [Li, X. & Kolega, J. 2002]. Taking this into account and also in order to avoid the electrolysis of water (occurs at 1,2V) that would change pH of medium due to the ions produced or consumed, the 1V/cm was the magnitude chosen to be applied. The purpose of this study was to determine whether 1 V/cm vertical alternating current electric field, applied at 100 Hz using the substrates previously illustrated, influences survival and proliferation of NSCs.

IV.5.1 Set-up

Evaluating the resistance of the samples in the circuit, it is immediate to notice that the reported value is slightly higher than the one measured by four-probes method. This can be a consequence of the cells presence, increasing the resistance of the material on the surface, or the presence of culture medium.

IV.5.2 NSCs expansion

ReNcells successfully expanded onto PEDOT:PSS films with applied electrical field and culture medium containing growth factors. After two days, the confluence was already 100%. No differences were reported between cells with and without electrical stimulation.

IV.5.3 NSCs differentiation

ReNcells morphology on PEDOT:PSS films after seven days differentiation was showing a neuronal-like phenotype, with interconnected dendrites and more elongated shape. No differences in morphology were shown between cells on samples with and without electrical stimulation.

IV.5.4 Immunocytochemistry

Several studies suggest that conductivity of substrate can be an essential factor for differentiation and determination of cell fate [Ostrakhovitch, E., 2012]. The electrical stimulation influences the neuronal differentiation, so, when the electrically PEDOT:PSS:glass substrate was placed into an electrolyte solution, it was able to sustain local electrochemical currents between the substrate and cell monolayer. These redox reactions between the conductive surface and cell monolayer may have changed the intracellular distribution of redox couples and, consequently, the intracellular redox potential, regulating in this way the cell differentiation. Changes in the effective redox potential may alter the conformation of proteins or may stimulate signaling molecules that make cells more oxidized, which is a prerequisite for neural differentiation. However, deeper investigation is needed to understand the effects of electrically conducting polymers on cell differentiation. Results of immunocytochemistry demonstrated a higher staining for anti-Tuj1, marker for neurons in early development

as well as for mature neurons, for substrates with applied electrical field, suggesting that the electrical stimulation is positively influencing the neural differentiation.

IV.5.6 Single Cell Calcium Imaging (SCCI)

In 2008, Agasse et al. developed a method to functionally evaluate neuronal differentiation in SVZ cell cultures. This method is based on the profiles of [Ca2]i variations according to cell type, following KCl depolarization and stimulation with histamine. KCl depolarization was used as a feature of neuronal differentiation, since voltage sensitive calcium channels (VSCC) are absent or expressed at very low levels in neural precursors, whereas during neuronal differentiation and in differentiated neurons there is expression of high levels of these channels [Maric D, 2000].

In agreement, they observed that following KCl perfusion, there is an increase in [Ca2]i in neuronal cells due to the opening of VSCC, whereas in immature cells or glial cells the bulk cytoplasmic [Ca2]i remained unchanged. In the study, they monitored [Ca2]i rise using SCCI and correlated these data with subsequent immunocytochemical characterization of the same imaged cells: [Ca2]i increase following KCl perfusion but not following histamine stimulation was associated with MAP-2-positive neurons, whereas cells responding to KCl and with minor response to histamine are DCX-positive immature neuronal precursors. Cells where [Ca2]i was not significantly affected by either KCl or histamine were positive for GFAP. The analysis of the ratio of responses following histamine and KCl perfusion (Hist/KCl) supported the conclusion that cells presenting a Hist/KCl ratio value below 0.80 are mature neurons, phenotypically identifiable by MAP-2 expression. Cells responding only to histamine and thus displaying a high Hist/KCl ratio (higher than 1) were identified as immature nestin-positive cells. GFAP expression was found in cells responding to neither KCl nor histamine, as well as in a subpopulation of cells responding to histamine and co-expressing nestin, consistent with the wide expression of nestin among cells of the
SVZ, including a subpopulation of astrocytes.

In this experiment, some cells were found to respond to both stimulations: it is possible that a subset of cells, mainly neuronal progenitors, still respond to histamine and start to respond to KCl and eventually show a net ratio of calcium transients close to 1. However, these cells can be distinguished from GFAP-positive cells on the basis of their different profile of response. This may indicate that cells are successfully differentiating into neural phenotypes, but this can be verified only prolonging the differentiation phase for more than 7 days.

Chapter 5: Conclusions

The development of new scaffolds that can support NSCs growth and differentiation, represents a promising strategy, for instance to test drugs targeted against neurodegenerative disorders such as Alzheimer´s and Parkinson´s diseases. In their in vivo microenvironment, cells grow in a complex 3D environment and are exposed to various endogenous electric fields, different stiffnesses and biomolecules that modulate their behavior. In this thesis work, several substrates were tested in order to achieve this goal.

First, 2D films of conjugated polymer PEDOT:PSS crosslinked with two different crosslinkers, GOPS and DVS, were realized. Crosslinker GOPS showed a conductivity of 618 S/m, two orders of magnitude lower in comparison to DVS, which conductivity was $9.57x10^4$ S/m; after coating the substrates with laminin and poly-ornithine, the conductivity approached the same value of 5 S/m. Both substrates showed biocompatibility for L929 fibroblasts cell line, and they were demonstrated to be stable in culture medium at 37°C for 15 days.

Then, a 3D scaffold was made by electrospinning technique using PEDOT:PSS blended with PVP. Fibers were successfully obtained, with few defects and sharp diameter size distribution, but they showed no conductivity. Electrospun fibers made of only PEDOT:PSS were never obtained, due to low viscosity of the solution.

Another 3D scaffold was realized using the conductive polymer PBI. Nanofibers with a sharp diameter size distribution were obtained, and they showed biocompatibility to L929 fibroblasts cell line, but the conductivity of the fibers was measured to be low. In order to increase the conductivity, a coating with PEDOT:PSS solution, crosslinked with both GOPS and DVS crosslinking agents, was applied submerging the fibers in the solution for 24 hours. The coated fibers were demonstrated to be stable in culture medium at 37°C for 15 days. Conductivity values for PEDOT:PSS:GOPS coated PBI fibers were measured to be 9.7 S/m, while PEDOT:PSS:DVS coated fibers showed a conductivity of 4.1 S/m; conductivity values drop to 0.8 S/m after poly-ornithine and laminin coating. Both coated fibers showed biocompatibility for L929 fibroblasts cell line.

ReNcells VM neural progenitor cell line was seeded onto both 2D films, and on both PBI coated fibers. 2D substrates demonstrated to be suitable for cells expansion for 2 days with growth factors and differentiation for 7 days with N2/B27 Neural differentiation medium. Difficulties of cell imaging with electrospun fibers made hard to understand cells behavior on 3D scaffolds.

ReNcells were also tested on 2D films of PEDOT:PSS:GOPS while applying an AC electrical stimulation of 1V/cm continuously during expansion phase (2 days) and for 12h/day during differentiation phase (7 days), and compared with same substrates without electricity. Cells with applied electrical field showed a stronger staining for Tuj1, marker for neural development. Single cell calcium imaging on live cells showed a high percentage of immature neurons also responding to KCl solution, indicating the development of voltage sensitive calcium channels, typical of neural populations. These studies demonstrated that laminin-fuctionalized PEDOT:PSS:GOPS substrates may be used to control complicated cellular functions of fetal NSCs such as cell morphology, proliferation and differentiation.

Chapter 6: Future trends

Recent advances in conjugated polymers and in nanotechnology have been found to cover a broad range of applications in regenerative medicine and offer new possibilities to repair neural defects. The work developed in this thesis may serve as a basis for the design of constructs capable of delivering AC electric fields to cell culture in order to guide NSCs adhesion, proliferation, migration and differentiation. Several challenges have been identified and should be the starting focus point for the progress of future research.

Methods to reduce the intrinsic fluorescence of PBI can be investigated, in order to image live cells during the culture on 3D proposed scaffolds. PBI fibers should also be elecrospun in an aligned configuration, in order to give the cells another topographical stimulus to improve elongation in one direction. PEDOT:PSS coatings can be realized also on other fibers, as they showed high stability and conductivity.

AC electrical stimulation should be carried on for more than 7 days, to better understand the suitability of the substrates for long term culture and ReNcells differentiation into mature neurons.

DVS crosslinking method should also be tried for neural stem cell culture with applied EF.

Several studies suggest the relevant physiological role of the electrical stimulation for control and adjustment of the cellular and tissue homeostasis. The application of electrical stimulation to cells is complicated because cells are highly conductive, allowing for large current flow, which generates heat and changes in pH, significantly increasing the detrimental effects in stimulated cell culture. A study to optimize parameters such as intensity, frequency, direction and duration of the applied electric field must be performed. In addition, quantitative studies, such as Alamar blue assay, PCR, flow cytometry and LDH assays, must be done to correlate the alterations on signaling pathways and gene expression with electrical stimulation.

A cellular study with primary cells, not immortalized ones, would be useful to understand if the proposed substrates are really capable to differentiate cells for clinical applications.

Biocompatibility of PEDOT:PSS and PBI should be studied for *in vivo* implantation, also at long term, to understand if it is possible to use the proposed substrates and scaffolds as grafts capable to be implanted and support neural growth. This can be particularly interesting for spinal cord lesions applications.

Chapter 7: References

1. Chan, B. & Leong, K. *Scaffolding in tissue engineering: general approaches and tissue specific considerations.* European spine journal 17, 467-479 (2008).

2. A. Birgersdotter, *Gene expression perturbation in vitro—a growing case for three-dimensional (3D) culture systems.* Semin Cancer Biol 2005;15:405–412
3. A. Birgersdotter, *Gene expression perturbation* in vitro*—a growing case for three-dimensional (3D) culture systems.* Semin Cancer Biol 2005;15:405–412
4. A. Frenot, *Polymer nanofibers assembled by electrospinning*. Curr. Opin. Colloid. In. 8, 64, 2003
5. A. Reininger-Mack, *3D-biohybrid systems: applications in drug screening*. Trends Biotechnol 2002;20:56–61
6. A.M. Hopkins, *3D in vitro modeling of the central nervous system.* Prog Neurobiol. 2015;125:1–25
7. Aboody, K., Capela, A., Niazi, N., Stern, J.H. & Temple, S. *Translating stem cell studies to the clinic for CNS repair: current state of the art and the need for a Rosetta Stone*. Neuron 70, 597-613 (2011)
8. Agasse, F*., Response to histamine allows the functional identification of neuronal progenitors, neurons, astrocytes, and immature cells in subventricular zone cell cultures.* Rejuvenation Res. 11, 2008, 187–200
9. Ariza, C.A. et al. *The influence of electric fields on hippocampal neural progenitor cells.* Stem Cell Reviews and Reports 6, 585-600 (2010)
10. B. A. Justice, *3D cell culture opens new dimensions in cell-based assays.* Drug Discov Today 2009;14:102–107
11. B. Chaudhuri, *A novel biocompatible conducting polyvinyl alcohol (PVA)-polyvinylpyrrolidone (PVP)-hydroxyapatite (HAP) composite scaffolds for probable biological application*, Colloids and Surfaces B: Biointerfaces 143 (2016) 71–80, 2016
12. Bian, S. Cell *Adhesion Molecules in Neural Stem Cell and Stem Cell-Based Therapy for Neural Disorders.* (2013)
13. C.M. Nelson, *Modeling dynamic reciprocity: engineering three-dimensional culture models of breast architecture, function, and neoplastic transformation*. Semin Cancer Bio. 2005;15:342–352
14. Casarosa, S., Zasso, J. & Conti, L. *Systems for ex-vivo Isolation and Culturing of Neural Stem Cells.* (2013)
15. Chang, K.-A. et al. *Biphasic electrical currents stimulation promotes both proliferation and differentiation of fetal neural stem cells.* PloS one 6, e18738 (2011)
16. Chang, Y.-J., Hsu, C.-M., Lin, C.-H., Lu, M.S.-C. & Chen, L. *Electrical stimulation promotes nerve growth factor-induced neurite outgrowth and signaling.* Biochimica et Biophysica Acta (BBA)-General Subjects (2013)
17. Cherry, J.F. et al. *Oriented, multimeric biointerfaces of the L1 cell adhesion molecule: an approach to enhance neuronal and neural stem cell functions on 2-D and 3-D polymer substrates*. Biointerphases 7, 1-16 (2012).
18. Conover, J.C. & Notti, R.Q. *The neural stem cell niche.* Cell and tissue research 331, 211-224 (2008)]
19. Conti, L. & Cattaneo, E. *Neural stem cell systems: physiological players or in vitro entities?* Nature Reviews Neuroscience 11, 176-187 (2010)
20. Cui, F.-Z., Deng, H., Fang, C.-F., Wei, Y.-T. & Shen, X.-C. *A mini review on interactions between neural stem cells and biomaterials.* Recent Patents Regenerative Medicine 1, 19-29 (2011)
21. D. E. Discher, *Growth factors, matrices, and forces combine and control stem cells*. Science 324, 1673-1677 (2009)
22. D. Mantione, *Low temperature cross-linking of PEDOT:PSS films using divinylsulfone,* Applied materials and interfaces, 2017
23. Dantuma, E., Merchant, S. & Sugaya, K. *Stem cells for the treatment of neurodegenerative diseases.* Stem Cell Res Ther 1, 37 (2010)
24. Dhara, S.K. & Stice, S.L., *Neural differentiation of human embryonic stem cells.* Journal of cellular biochemistry 105, 633-640 (2008)

25. Donato, R. et al. *Differential development of neuronal physiological responsiveness in two human neural stem cell lines*. BMC neuroscience 8, 36 (2007)
26. E. Smela, *Conjugated Polymer Actuators for Biomedical Applications,* Advanced Materials, 20 March 2003
27. E. W. Fischer, *Effect of annealing and temperature on the morphological structure of polymers, Pure and Applied Chemistry,* vol.31, Issue 1-2. 2009.
28. Eduarda G Z Centeno, *2D versus 3D human induced pluripotent stem cell-derived cultures for neurodegenerative disease modelling,* Mol Neurodegener. 2018; 13: 27
29. F. Greco, *Ultra-thin conductive free-standing PEDOT/PSS nanofilms,* Royal Society of chemistry, Soft Matter, 2011, 7, 10642-10650
30. F.Soares, *Neural stem cell differentiation by electrical stimulation using a cross-linked PEDOT substrate: Expanding the use of biocompatible conjugated conductive polymers for neural tissue engineering*, Biochimica et Biophysica Acta (BBA) - General Subjects, Volume 1850, Issue 6, June 2015, Pages 1158-1168
31. Feng, Z. & Gao, F. *Stem cell challenges in the treatment of neurodegenerative disease.* CNS neuroscience & therapeutics 18, 142-148 (2012).
32. Fujigaya T., *Fuel cell electrocatalyst using polybenzimidazole-modified carbon nanotubes as support materials*, Adv Mater. 2013 Mar 25;25(12)
33. Garzón-Muvdi, T. & Quiñones-Hinojosa, A. *Neural stem cell niches and homing: recruitment and integration into functional tissues.* ILAR Journal 51, 3-23 (2010)]
34. Guimard, N.K., Gomez, N. & Schmidt, C.E. *Conducting polymers in biomedical engineering.* Progress in Polymer Science 32, 876-921 (2007)
35. H. Baharvand H*, Differentiation of human embryonic stem cells into hepatocytes in 2D and 3D culture systems* in vitro*.* Int J Dev Biol 2006;50:645–652
36. Harris AR , *Optical and electrochemical methods for determining the effective area and charge density of conducting polymer modified electrodes for neural stimulation*, Anal Chem. 2015 Jan 6;87(1):738-46
37. Harun, M.H., Saion, E., Kassim, A., Yahya, N. & Mahmud, E. *Conjugated conducting polymers: A brief overview.* UCSI Academic Journal: Journal for the Advancement of Science & Arts 2, 63-68 (2007)
38. Hinkle, L., McCaig, C. & Robinson, K. *The direction of growth of differentiating neurones and myoblasts from frog embryos in an applied electric field.* The Journal of physiology 314, 121135 (1981)
39. J. Doshi, *Electrospinning process and applications of electrospun fibers*. J. Electrostat. 35, 151, 1995
40. J. Lee, *Three-dimensional cell culture matrices: state of the art*. Tissue Eng Part B Rev 2008;14:61–86].
41. J. Wo*, Highly Aligned Poly(3,4-ethylene dioxythiophene) (PEDOT) Nano- and Microscale Fibers and Tubes,* Polymer (Guildf). 2013 Jan 24;54(2):702-708, 2012
42. Jaffe, L.F. & Poo, M.M. *Neurites grow faster towards the cathode than the anode in a steady field.* Journal of Experimental Zoology 209, 115-127 (1979)
43. Johe, K.K., Hazel, T.G., Muller, T., Dugich-Djordjevic, M.M. & McKay, R. *Single factors direct the differentiation of stem cells from the fetal and adult central nervous system.* Genes & development 10, 3129-3140 (1996)
44. K. Bhadriraju, *Engineering cellular microenvironments to improve cell-based drug testing.* Drug Discov Today 2002;7:612–620
45. K. Shield, *Multicellular spheroids in ovarian cancer metastases: biology and pathology*. Gynecol Oncol 2009;113:143–148
46. K. Sun, *Review on application of PEDOTs and PEDOT:PSS in energy conversion and storage devices,* Journal of Materials Science: Materials in Electronics July 2015, Volume 26, Issue 7, pp 4438–4462
47. K. Svennersten, *Electrochemical modulation of epithelia formation using conducting polymers*, Biomaterials Volume 30, Issue 31, October 2009, Pages 6257-6264].
48. K. Venstrom, *Extracellular matrix. 2: Role of extracellular matrix molecules and their receptors in the nervous system*. The FASEB journal 7, 996-1003 (1993)
49. Kazanis, I. *Extracellular matrix and the neural stem cell niche.* Developmental Neurobiology 71, 1006-1017 (2011)
50. Keirstead, H.S. et al. *Human embryonic stem cell-derived oligodendrocyte progenitor cell transplants remyelinate and restore locomotion after spinal cord injury.* The Journal of Neuroscience 25, 4694-4705 (2005)
51. Kim, S.U., Lee, H.J. & Kim, Y.B. *Neural stem cell-based treatment for neurodegenerative diseases.* Neuropathology (2013).

52. Kimura, K., Yanagida, Y., Haruyama, T., Kobatake, E. & Aizawa, M. *Gene expression in the electrically stimulated differentiation of PC12 cells*. Journal of biotechnology 63, 55-65 (1998)
53. Kojima T., *Studies of Molecular Aggregation of a Polybenzimidazole in Solution by Fluorescence Spectroscopy* , Journal of Polymer Science, 1980
54. Kokaia, Z., Martino, G., Schwartz, M. & Lindvall, O. *Cross-talk between neural stem cells and immune cells: the key to better brain repair* [quest]. Nature neuroscience 15, 1078-1087 (2012)
55. L. A. Flanagan, *Regulation of human neural precursor cells by laminin and integrins.* Journal of neuroscience research 83, 845-856 (2006)
56. L. Luckenbill-Edds, *Laminin and the mechanism of neuronal outgrowth*. Brain Research Reviews 23, 1-27 (1997)]
57. L. S. Campos, *ß1 integrins activate a MAPK signalling pathway in neural stem cells that contributes to their maintenance.* Development 131, 3433-3444 (2004)]
58. Li, S., Li, H. & Wang, Z. *Orientation of spiral ganglion neurite extension in electrical fields of charge-balanced biphasic pulses and direct current< i> in vitro</i>.* Hearing research 267, 111-118 (2010)
59. Li, X. & Kolega, J. *Effects of direct current electric fields on cell migration and actin filament distribution in bovine vascular endothelial cells.* Journal of vascular research 39, 391-404 (2002)
60. Lim, T.C., Toh, W.S., Wang, L.-S., Kurisawa, M. & Spector, M. *The effect of injectable gelatinhydroxyphenylpropionic acid hydrogel matrices on the proliferation, migration, differentiation and oxidative stress resistance of adult neural stem cells.* Biomaterials 33, 3446-3455 (2012)
61. Little, L., Healy, K.E. & Schaffer, D. *Engineering biomaterials for synthetic neural stem cell microenvironments*. Chemical reviews 108, 1787-1796 (2008)
62. Lu, H.F. et al. *Efficient neuronal differentiation and maturation of human pluripotent stem cells encapsulated in 3D microfibrous scaffolds*. Biomaterials (2012).
63. M. Blain, *Isolation and culture of primary human CNS neural cells*. Protocols for neural cell culture, 2010, pp. 87–104
64. M. Leber, *Long term performance of porous platinum coated neural electrodes*, Biomed Microdevices, 2017
65. M. Zietarska, *Molecular description of a 3D* in vitro *model for the study of epithelial ovarian cancer (EOC).* Mol Carcinog 2007;46:872–885
66. M.V. Carroll, R.B. Sim, *Complement in health and disease*, Adv. Drug Del. Rev. 63 (2011) 965–975
67. Maria H.Bolin, *Nano-fiber scaffold electrodes based on PEDOT for cell stimulation,* Sensors and Actuators B: Chemical Volume 142, Issue 2, 5 November 2009, Pages 451-456
68. Maric D, *Developmental changes in cell calcium homeostasis during neurogenesis of the embryonic rat cerebral cortex*. Cereb Cortex 2000; 10:561–573
69. Marklein, R.A. & Burdick, J.A. *Controlling stem cell fate with material design.* Advanced Materials 22, 175-189 (2010)
70. McKay, R. Stem cells in the central nervous system. Science 276, 66-71 (1997)
71. Ning Li , *Three-dimensional graphene foam as a biocompatible and conductive scaffold for neural stem cells,* Scientific Reports, 2013
72. O. Berezhetska, *A simple approach for protein covalent grafting on conducting polymer films,* Journal of Materials Chemistry B, Issue 25, 2015
73. O'Connor ER, *Role of calcium in astrocyte volume regulation and in the release of ions and amino acids*, J Neurosci 1993;13:2638–2650.
74. Odorico, J.S., Kaufman, D.S. & Thomson, J.A. *Multilineage differentiation from human embryonic stem cell lines.* Stem cells 19, 193-204 (2001)
75. Ogunlaja AS, *Design, fabrication and evaluation of intelligent sulfone-selective polybenzimidazole nanofibers*, Talanta. 2014 Aug;126:61-72.
76. Ostrakhovitch, E., Byers, J., O'Neil, K. & Semenikhin, O. *Directed differentiation of embryonic P19 cells and neural stem cells into neural lineage on conducting PEDOT-PEG and ITO glass substrates*. Archives of Biochemistry and Biophysics (2012)
77. P. Hall, *Laminin enhances the growth of human neural stem cells in defined culture media.* BMC neuroscience 9, 71 (2008)
78. P. P. Quynh, *Electrospinning of Polymeric Nanofibers for Tissue Engineering Applications: A Review*, Tissue Engineering Volume 12, Number 5, 2006

79. P.D. Benya, *Dedifferentiated chondrocytes reexpress the differentiated collagen phenotype when cultured in agarose gels.* Cell 1982;30:215–224
80. Palchesko, R.N., Zhang, L., Sun, Y. & Feinberg, A.W. *Development of polydimethylsiloxane substrates with tunable elastic modulus to study cell mechanobiology in muscle and nerve.* PloS one 7, e51499 (2012)
81. Park, J.S. et al. *Electrical pulsed stimulation of surfaces homogeneously coated with gold nanoparticles to induce neurite outgrowth of PC12 cells.* Langmuir 25, 451-457 (2008)
82. Patel, N. & Poo, M.-m. *Orientation of neurite growth by extracellular electric fields.* The Journal of Neuroscience 2, 483-496 (1982)
83. Prabhakaran, M.P., Ghasemi-Mobarakeh, L., Jin, G. & Ramakrishna, S. *Electrospun conducting polymer nanofibers and electrical stimulation of nerve stem cells.* Journal of bioscience and bioengineering 112, 501-507 (2011)
84. Q. Li, *PBI-Based Polymer Membranes for High Temperature Fuel Cells - Preparation, Characterization and Fuel Cell Demonstration,* Fuel cells 2004, 4, No. 3
85. R. Corteling, *ReNcell VM cell line – a model of human neural development and differentiation*, Millipore, 2008
86. Rodrigues, C.A., Diogo, M.M., da Silva, C.L. & Cabral, J. *Microcarrier expansion of mouse embryonic stem cell-derived neural stem cells in stirred bioreactors*. Biotechnology and applied biochemistry 58, 231-242 (2011).
87. Rui S. Rodrigues*, Interaction between Cannabinoid Type 1 and Type 2 Receptors in the Modulation of Subventricular Zone and Dentate Gyrus Neurogenesis,* frontiers in pharmacology, 2017
88. Rylie A. Green *Conducting polymers for neural interfaces: Challenges in developing an effective long-term implant*, Biomaterials, 2008
89. S. Han, *Bone marrow-derived mesenchymal stem cells in three-dimensional culture promote neuronal regeneration by neurotrophic protection and immunomodulation*, J Biomed Mater Res A. 2016 Jul;104(7):1759-69.
90. Subramanian, A., Krishnan, U.M. & Sethuraman, S. *Development of biomaterial scaffold for nerve tissue engineering: Biomaterial mediated neural regeneration*. J Biomed Sci 16, 108 (2009)
91. T. Subbiah, *Electrospinning of nanofibers.* J. Appl. Polym. Sci. 96, 557, 2005
92. T. Sun, *Culture of skin cells in 3D rather than 2D improves their ability to survive exposure to cytotoxic agents.* J Biotechnol 2006;122:372–381
93. Tai Shung Chung, *A Critical Review of Polybenzimidazoles: Historical Development and Future R&D* J. Macromole. Sci. 1997, C37,277
94. Tarasenko, Y.I., Yu, Y., Jordan, P.M., Bottenstein, J. & Wu, P. *Effect of growth factors on proliferation and phenotypic differentiation of human fetal neural stem cells.* Journal of neuroscience research 78, 625-636 (2004)
95. Théry, M. *Micropatterning as a tool to decipher cell morphogenesis and functions*. Journal of Cell Science 123, 4201-4213 (2010)
96. V.M. Weaver, *Reversion of the malignant phenotype of human breast cells in three-dimensional culture and in vivo by integrin blocking antibodies*. J Cell Biol 1997;137:231–245
97. Valentini, R.F., Vargo, T.G., Gardella Jr, J.A. & Aebischer, P. *Electrically charged polymeric substrates enhance nerve fibre outgrowth< i> In vitro</i>.* Biomaterials 13, 183-190 (1992)
98. Wang, Y. et al. *Interactions between neural stem cells and biomaterials combined with biomolecules.* Frontiers of Materials Science in China 4, 325-331 (2010)].
99. Willerth, S.M. & Sakiyama-Elbert, S.E. *Combining stem cells and biomaterial scaffolds for constructing tissues and cell delivery.* (2008)
100. Winslow, T. & Kibluk, L. *Stem Cells. Scientific Progress and Future Research Directions.* Can Stem Cells Repair a Damaged Heart, 87-91 (2001)
101. Wood, M. & Willits, R.K. *Short-duration, DC electrical stimulation increases chick embryo DRG neurite outgrowth*. Bioelectromagnetics 27, 328-331 (2006)
102. Xapelli, S., *Activation of type 1 cannabinoid receptor (CB1R) promotes neurogenesis in murine subventricular zone cell cultures,* PLoS ONE 8:e63529, 2013
103. Yamada, M. et al. *Electrical stimulation modulates fate determination of differentiating embryonic stem cells*. Stem Cells 25, 562-570 (2007)

104. Yang, K. et al. *Polydopamine-mediated surface modification of scaffold materials for human neural stem cell engineering.* Biomaterials (2012)
105. Yao, L., Pandit, A., Yao, S. & McCaig, C.D. *Electric field-guided neuron migration: a novel approach in neurogenesis.* Tissue Engineering Part B: Reviews 17, 143-153 (2011)
106. Yong Hyun Kim *, Highly Conductive PEDOT:PSS Electrode with Optimized Solvent and Thermal Post-Treatment for ITO-Free Organic Solar Cells,* Advanced functional materials, 15 February 2011
107. Z. M. Huang, *A review on polymer nanofibers by electrospinning and their applications in nanocomposites.* Compos. Sci. Technol. 63, 2223, 2003